PART VIII:

GHRS

■ GHRS

GHRS Instrument Overview

The Goddard High Resolution Spectrograph (GHRS) was designed by the GHRS Investigation Definition Team (IDT) consisting of J. Brandt (Principal Investigator), E. Beaver, A. Boggess, K. Carpenter, D. Ebbets, S. Heap, J. Hutchings, M. Jura, D. Leckrone, J. Linsky, S. Maran, B. Savage, A. Smith, L. Trafton, F. Walter, and R. Weymann. The instrument was built by Goddard Space Flight Center and prime subcontractor Ball Aerospace. The instrument is described in Brandt, J.C., et al., 1994, "The Goddard High Resolution Spectrograph: Instrument, Goals, and Science Results," *PASP*, 106, 890.

You are probably someone who wishes to study archival data from the GHRS since most General Observers (GOs) have completed their data analysis by now. Archival Researchers (ARs) face several problems—only some of which the original observer experienced:

- Determining if any GHRS observations in the archive are likely to be useful for your purposes. To understand the basic properties of the GHRS, you may wish to refer to the *GHRS Instrument Handbook* version 6 because that document was written to guide people writing the detailed proposals that led to the observations that are in the archive. This *HST Data Handbook* includes many portions of the instrument handbook that are useful for archival research.

- Retrieving appropriate observations and other data files needed to calibrate them. Data retrieval and the use of StarView are discussed in Chapter 1 (Volume 1).

- Understanding how those observations were planned and obtained, and assessing overall data quality. Again, the *GHRS Instrument Handbook* best explains how and why observations were taken, although most archival users will find this handbook sufficient. Data assessment for the GHRS is discussed in Chapter 35.

- Recalibrating those observations using the best available knowledge of the instrument. This is the major focus of this handbook.

- Analyzing the observations to extract useful observational quantities. Most of the discussion here is on data reduction, but some aspects of analysis are covered as well.

Of course data reduction is what you must do before you get to the interesting work, which is extracting useful astrophysical information from your data. Reading manuals about the data reduction process is seldom more entertaining than the reduction itself. Our goal in this handbook is to save you a lot of wasted time and effort by helping you to do the reduction job right the first time.

This section follows the basic outline of all of the chapters of this handbook. This first GHRS chapter (Chapter 34) describes the instrument, its general use, and important sources of additional information. Chapter 35 describes the data formats and data assessment—methods for determining whether the target was successfully acquired and the overall quality of the data. Chapter 36 describes the calibration process and how results can be improved. Chapter 37 describes error sources and uncertainty—topics intertwined with calibration. Chapter 38 concludes the GHRS part of this manual and describes various topics related to data analysis.

Although the GHRS was retired as an active instrument, STScI continues to provide analysis support for GHRS data. GHRS questions should be sent via E-mail to: help@stsci.edu. Any updates to GHRS documentation and calibration will be summarized in the HST Spectrographs Space Telescope Analysis Newsletter (STAN).

34.1 GHRS History

Critical events in the operational history of the GHRS include:

1. The GHRS was launched inside HST in April 1990.

2. The Side 1 low-voltage power supply (LVPS) had repeated problems in the summer of 1991, eliminating access to both low- and high-dispersion modes in the far-UV (G140L and Ech-A). Prior to this loss, Ech-A was the most-requested GHRS grating, but deconvolution techniques allowed G160M observations to approach Ech-A resolution. Hence some of this science was done with Side 2 during Cycles 2 and 3.

3. The LVPS problem was fixed during the first servicing mission, restoring important capabilities and leading to greater GHRS usage.

4. The failure of the SC1 calibration lamp eliminated redundancy for wavelength calibration. Fortunately, the specifications for lamps were very conservative and SC2 had ample lifetime to meet observer needs.

5. Acquisitions during the early years had to specify BRIGHT and FAINT limits, leading to failed acquisitions and wasted telescope time. Implementation of BRIGHT=RETURN eliminated this problem. Also, BRIGHT=RETURN used 32 bits, preventing register overflow.

6. Corrective Optics Space Telescope Axial Replacement (COSTAR), installed during the first servicing mission of December 1993, changed the net throughput of the large science aperture (LSA) by very little (two extra reflections offset the better PSF), but the contrast of the PSF changed enormously, resulting in reliable fluxes. Small science aperture (SSA) throughput improved too, by about a factor of two.

7. Before COSTAR, HST's spherical aberration was sometimes a "feature" for acquisitions in the sense that the algorithm could find the wings of the PSF even when centering was poor.

8. A catastrophic failure occurred one week before the second servicing mission, resulting in the complete shutdown of the GHRS. The most important loss was some special observations that were to be made with the COSTAR mirrors withdrawn to try to determine the origin of far-UV sensitivity losses.

GHRS / 34

34.2 Instrument Description

The GHRS was one of the first-generation science instruments aboard HST. The spectrograph was designed to provide a variety of spectral resolutions, high photometric precision, and excellent sensitivity in the wavelength range 1100 to 3200 Å. The GHRS was a modified Czerny-Turner spectrograph with two science apertures (large: LSA, and small: SSA), two detectors (D1 and D2), several dispersers, and camera mirrors. There were also a wavelength calibration lamp, flatfield lamps, and mirrors to acquire and center objects in the observing apertures.

Schematics of the mechanical and optical layout are shown below and can be found in the *GHRS Instrument Handbook*. 6.0, Figures 6-1 to 6-9. The GHRS was installed as one of the axial scientific instruments, with the entrance aperture adjacent to FGS 2 and FGS 3. With the installation of COSTAR, the entrance apertures were at the former position of the High Speed Photometer. The GHRS had two science apertures, designated Large Science Aperture (LSA or 2.0) and Small Science Aperture (SSA or 0.25). The 2.0 and 0.25 designations were the pre-COSTAR size of the apertures in arcseconds. The post-COSTAR size of the LSA was 1.74 arcsec square and the SSA was 0.22 arcsec square. The separation of the two apertures was approximately 3.7 arcsec on the sky and 1.05 mm on the

slit plate. The LSA had a shutter to block light from entering the spectrograph when the SSA was being used, while the SSA was always open. Because of this, scattered light from a bright target in the SSA could contaminate a wavelength calibration exposure (*wavecal*). The locations of the GHRS apertures relative to the spacecraft axes are displayed in Figure 34.1.

Figure 34.1: Aperture Locations Relative to Spacecraft Axes
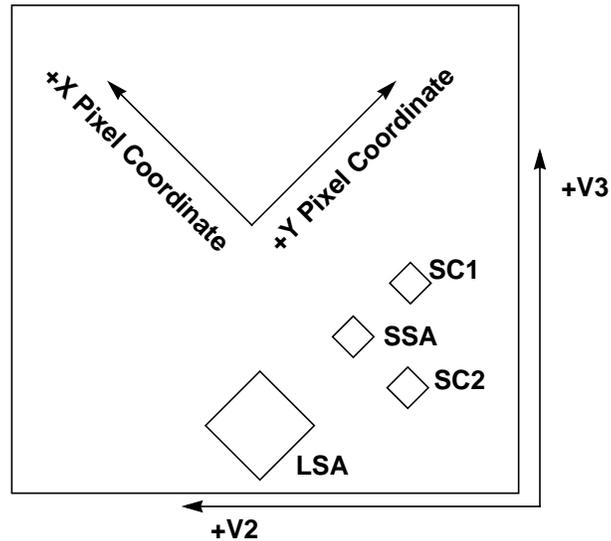
Light from a target was collected by HST and focused onto one of the two GHRS apertures. After passing through an aperture, the light struck the collimating mirror and was directed toward the grating carrousel. The collimated beam illuminates one of the gratings or a flat mirror; selection of a grating or mirror was performed by rotating the carrousel. Camera mirrors focused the dispersed light onto one of the Digicon photocathodes. Photoelectrons from the Digicons were focused onto a linear silicon diode array.
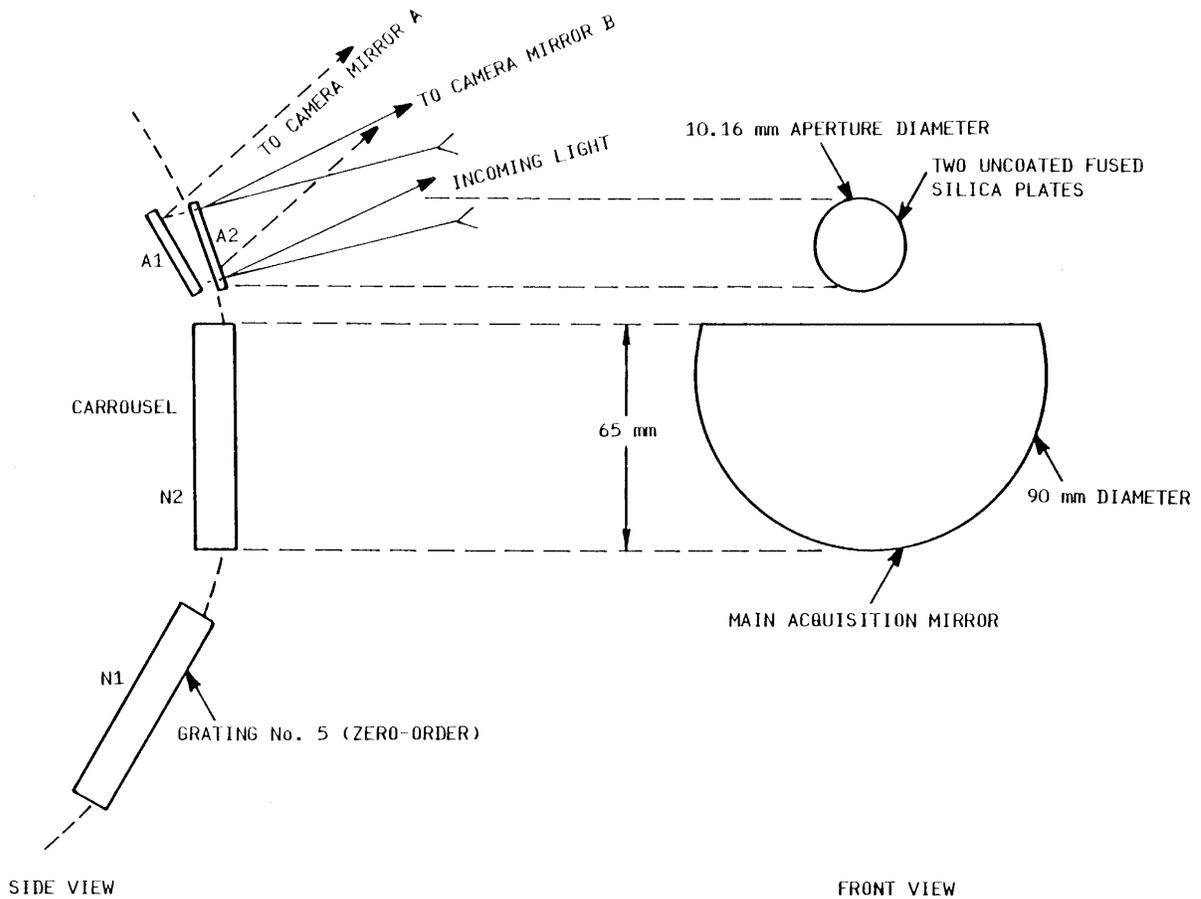
Figure 34.2: GHRS Optics

34.2.1 Dispersers

The dispersers were mounted on a rotating carrousel, together with several plane mirrors used for acquisition. The first-order gratings were designated as G140L, G140M, G160M, G200M, and G270M, where "G" indicates a grating, the number indicates the blaze wavelength (in nm), and the "L" or "M" suffix denotes a "low" or "medium" resolution grating, respectively. The GHRS medium resolution first-order gratings were holographic in order to achieve very high efficiency within a limited wavelength region. G140L is a ruled grating.

Side 1 first-order gratings, G140L and G140M, had their spectra imaged by mirror Cam-A onto detector D1, which had a cesium iodide photocathode and was best for the shortest wavelengths (about 1050 to 1700 Å.). The other three (Side 2) gratings had their spectra imaged by Cam-B onto detector D2, which had a cesium telluride photocathode and worked best at wavelengths from about 1700 to 3200 Å, but which was also useful down to 1200 Å. Also note that detector D2 had a MgF_2 front plate, which attenuated severely below Lyman-α, but that detector D1 had a LiF faceplate for better throughput at the shortest wavelengths. Note that little or no flux below 1150 Å was reflected by the COSTAR mirrors because of their magnesium fluoride coatings. Figure 34.3 shows the GHRS acquisition optics; the main acquisition mirror is N2. The useful spectral wavelength ranges of the first order gratings are listed in Table 34.1.

Figure 34.3: GHRS Acquisition Optics

Table 34.1: Useful Wavelength Ranges for First-Order and Echelle Gratings

Grating	Useful Range (Å)	Å per diode	Bandpass (Å)	Comment
G140L	1100–1900	0.572–0.573	286–287	
G140M	1100–1900	0.056–0.052	28–26	
G160M	1150–2300	0.072–0.066	36–33	2nd order overlap above 2300 Å
G200M	1600–2300	0.081–0.075	41–38	2nd order overlap above 2300 Å
G270M	2000–3300	0.096–0.087	48–44	2nd order overlap above 3300 Å
Echelle A	1100–1700	0.011–0.018	5.5–9	
Echelle B	1700–3200	0.017–0.034	8.5–17	

The carrousel also had an echelle grating. The higher orders were designated as mode Ech-A, and they were imaged onto D1 by the cross-disperser CD1. The lower orders were designated as mode Ech-B, and they were directed to D2 by

CD2. The useful spectral range of the echelle gratings are provided in Table 34.1. Only a single order was recorded in a single observation.

Finally, mirrors N1 and A1 imaged the apertures onto detector D1, and mirrors N2 and A2 imaged onto D2. The "N" mirrors are "normal," i.e., unattenuated, while the "A" mirrors ("attenuated") reflect a smaller fraction of the light to the detectors, so as to enable the acquisition of bright stars. (The mode designated as N1 actually used the zero-order image produced by grating G140L.)

Bright targets were acquired with one of the attenuated mirrors, A1 or A2. These acquisitions took substantially longer than if the N1 or N2 mirrors were used. SSA acquisitions (ACQ/PEAKUPs) with the A1 mirror were usually doubled up to center the target in the SSA. Acquiring a target in the SSA first requires a LSA acquisition (3 x 3 search) followed by a SSA acquisition (5 x 5 search).

The GHRS LSA was 74 arcseconds from the FOS Blue aperture. Starting with Cycle 5, it became possible to acquire a faint target with the FOS and slew the telescope to position the target into the GHRS LSA. It also became possible to acquire a bright target with the GHRS and slew the telescope to position the target into the FOS Blue aperture. Therefore, a GHRS proposal executed during Cycles 5 and 6 may contain FOS observations (which you would have to request from the archive separately). This can be seen by examining the Phase II proposal.

34.2.2 Detectors

Use of the various gratings or mirrors produces one of three kinds of GHRS data:

- An image of the entrance aperture, which may be mapped to find and center the object of interest.

- A single-order spectrum.

- A cross-dispersed, two-dimensional echelle spectrum.

The flux in these images was measured by photon-counting Digicon detectors; the portion of the image plane that was mapped onto the Digicon is determined by magnetic deflection coils. These detectors were the heart of the GHRS and they involve subtleties that must be understood if data are to be reduced properly and competently.

The Detectors and Their Diodes

There were two Digicons: D1 (also known as Side 1) and D2 (Side 2). D1 had a cesium iodide photocathode on a lithium fluoride window that makes D1 effectively *solar-blind*, i.e., the enormous flux of visible-light photons that dominates the spectrum of most stars will produce no signal with this detector, and only far-ultraviolet photons (1060 to 1800 Å) produce electrons that are accelerated by the 23 kV field onto the diodes. D2 had a cesium telluride photocathode on a magnesium fluoride window. Each Digicon had 512 diodes that accumulated counts from accelerated electrons. 500 of those are *science diodes*, plus there are *corner diodes* and *focus diodes*.

The 500 science diodes were 40 x 400 microns on 50 micron centers. The focus diodes were 25 x 25 microns and there were three located on each end of the array. Two 1,000 x 100 micron diodes were used to measure background and two 1,000 x 100 micron diodes were used to monitor high energy protons. Eight diodes mapped the LSA and the SSA was 1 diode wide and 1/8 diode high.

Figure 34.4: View from the Cross-Dispersers toward the Digicon Detectors (illustrates senses of *x* and *y* motions and of increasing wavelength)
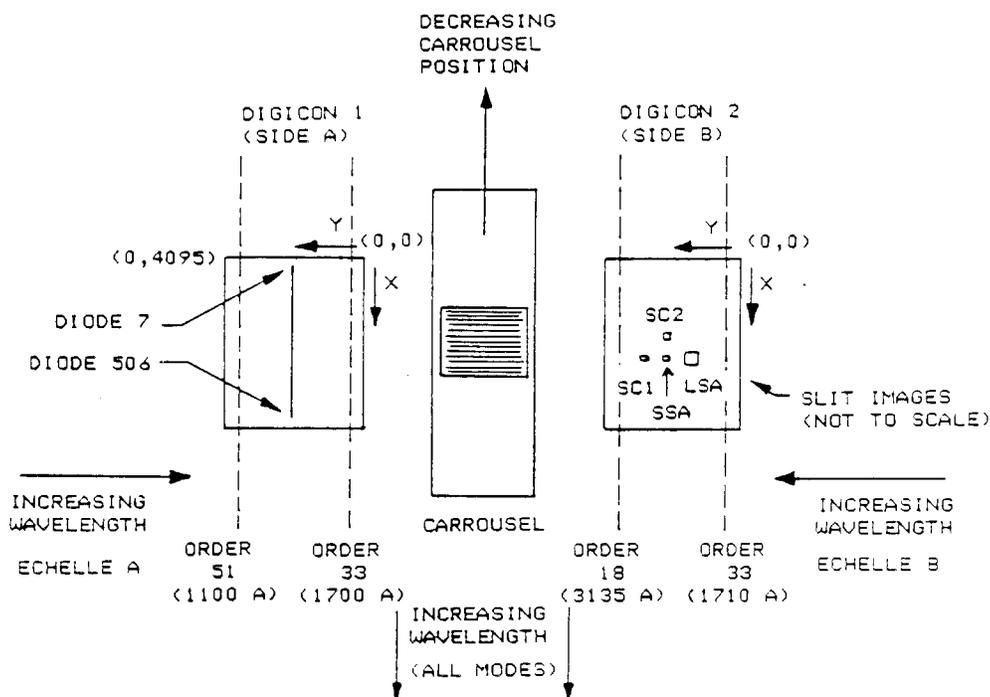
Photocathode Granularity and FP-SPLIT Observing

Both photocathodes had granularity—irregularities in response—of about 0.5% (rms) that could limit the S/N achieved, and there were localized blemishes that produced irregularities of several percent. The Side 1 photocathode also exhibited features called "sleeking," which are slanted, scratch-like features that have an amplitude of 1 to 2% over regions as large as half the faceplate. The effects of these irregularities could, in principle, be removed by obtaining a flatfield measurement at every position on the photocathode, but that was generally impractical. Instead, the observing strategy was to rotate the carrousel slightly between separate exposures and so use different portions of the photocathode. This procedure is called an FP-SPLIT, and with it each exposure was divided into two or four separate-but-equal parts, with the carrousel moving the spectrum about 5.2 diode widths each time in the direction of dispersion. These individual spectra could be combined together during the reduction phase.

Diode Irregularities and the Use of Comb-Addition

The diodes in the Digicons also had response irregularities, but these were very slight. The biggest effect was a systematic offset of about 1% in response of the odd-numbered diodes relative to the even-numbered ones. This effect could be almost entirely defeated by use of the default COMB addition procedure. COMB addition deflected the spectrum by an integral number of diodes between subexposures and had the additional benefit of working around dead diodes in the instrument that would otherwise leave image defects.

Sampling and Substepping with STEP-PATT

The Digicons' diodes were about the same width as the FWHM of the point spread function (PSF) for HST. Thus the true resolution of the spectrum could not be realized unless it was adequately sampled. That was done by making the magnetic field move the spectrum by fractions of the width of a diode, by either half- or quarter-diode widths, and then storing those as separate spectra in the onboard memory. These were merged into a single spectrum in the data reduction phase. The manner in which this was done was specified by the STEP-PATT parameter, described in more detail in Chapter 35 (see Table 35.3). The choice of STEP-PATT also determined how the background around the spectrum was measured. Figure 34.5 shows the diode arrangement; note the six large corner diodes and six focus diodes (numbers 4, 5, and 6, for example).

Figure 34.5: Diode Layout in the Digicon Detectors

DIMENSIONS IN INCHES UNLESS OTHERWISE NOTED
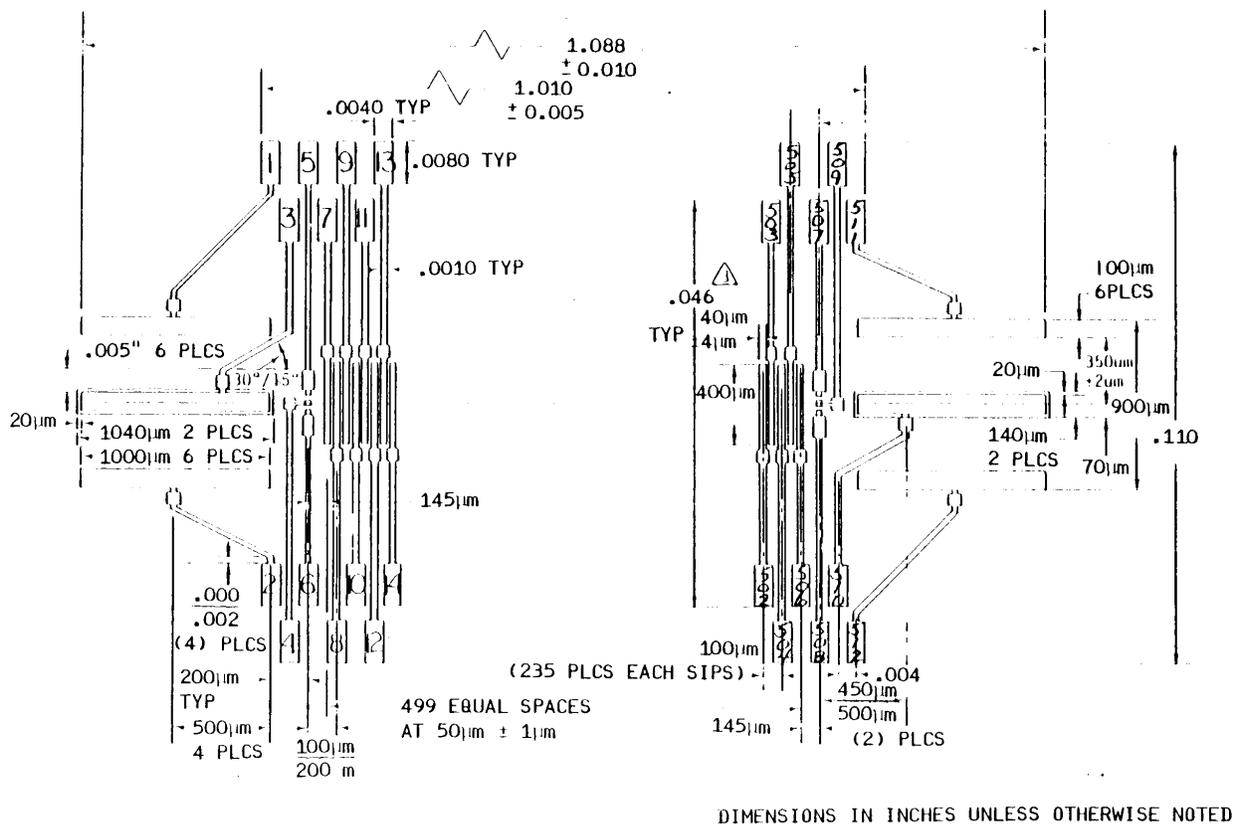
34.2.3 Internal Calibration

The GHRS was built with two Pt-Ne hollow-cathode lamps to provide a rich spectrum of emission lines for accurate calibration of wavelengths. The locations of these lamps and the way in which they illuminated the spectrograph optics are illustrated in the *GHRS Instrument Handbook*. The apertures through which calibration exposures were made were the same size as the Small Size Aperture (SSA). Moreover, calibration aperture SC2, the one most frequently used, was offset from the SSA in the x direction (the direction of dispersion), but was aligned in the y direction (see Figure 34.1). This offset in x introduced a systematic shift in wavelength between the SSA and SC2 because light from them hit the gratings at different angles. By convention, the wavelength scale of the GHRS was calculated so as to be correct for the SSA.

These wavelength calibration lamps were also used for other internal instrumental calibrations, such as DEFCALs (deflection calibration) and SPYBALs (Spectrum-Y-Balance). Only one of these lamps was available for use after the failure of Side 1 in 1991. A wavelength calibration exposure (WAVECAL) was obtained by specifying an ACCUM in the Phase II Proposal with a target of WAVE and an aperture of SC2. (Prior to 1991, SC1 was a valid aperture designation and so older observations may show it.)

A WAVECAL is not the only way to assess the quality of the wavelength scale for observations. As will be noted in the example for R136a, a SPYBAL was obtained just before an ACCUM that used a grating for the first time. A SPYBAL was just a WAVECAL that was obtained at a predetermined carrousel position for each grating, and SPYBALs were done to align the spectrum on the diodes in the y direction (perpendicular to dispersion). A SPYBAL contains wavelength information that can be used to check for zero-point offset.

34.2.4 Side 1

The installation of the GHRS Redundancy Kit during the first servicing mission (December 1993) eliminated the risk of a Side 1 power supply failure affecting Side 2. With this risk removed, Side 1 operations were resumed during Cycle 4. These operations were nominal.

When the Side 1 carrousel was commanded through the Side 2 electronics during a Side 1 observation, the telemetry word containing the carrousel position would read the Side 2 commanded position during carrousel configuration, and the Side 1 encoder position after integration. The Side 1 GHRS data headers do contain the correct Side 1 position of the carrousel.

GHRS Side 1 observations cover the time spans April 1990 to June 1991 and February 1994 to the Second Servicing Mission.

34.2.5 COSTAR

The spherical aberration of the HST primary mirror was corrected by the first servicing mission (December 1993) with the installation of the Corrective Optics

Space Telescope Axial Replacement (COSTAR) assembly. COSTAR deployed corrective reflecting optics in the optical path of the GHRS. The post-COSTAR GHRS has a different response with wavelength than the pre-COSTAR instrument. Interim sensitivity files were installed in CDBS on April 16, 1994, and updated during Cycle 4 and 5 when calibration observations became available. GHRS observations obtained early in Cycle 4 will require recalibration.[1]

34.3 Operating Modes and Data Types

The GHRS had two principal science data acquisition modes: accumulation (ACCUM) and rapid readout (RAPID or DIRECT READOUT), as well as onboard target acquisition modes and a rudimentary image mode which was sometimes used to image the sky through the science aperture. We provide a high-level overview of these modes here, with more detail provided in Chapter 35.

34.3.1 Acquisitions and Images

Almost all GHRS visits began with an acquisition of an object. Most GHRS targets were point sources (i.e., stars), but there were also many observations of planets, nebulae, and galaxies. Almost all acquisitions were of the ONBOARD type, i.e., they were done autonomously by the GHRS. In a few cases, especially soon after launch, acquisitions were interactive. There are also some cases of "early acquisitions," in which an image was first obtained with WF/PC, FOC, or WFPC2, well in advance of the GHRS observation.

IMAGE mode was used to create an image of the GHRS aperture being used. Obviously this would be a very small region of the sky, but it would be taken in the ultraviolet, and it would show how the light of the object was distributed in the aperture, which was sometimes helpful for after-the-fact analysis of what was observed. A similar mode was invoked if a MAP were requested. GHRS acquisitions are explained in "Understanding GHRS Acquisitions" on page 35-19.

34.3.2 ACCUMs

ACCUM mode was by far the most commonly used mode of the GHRS as it allowed the use of all the automatic procedures for optimizing the data acquisition (FP-SPLIT, substepping, and comb addition—see "Detectors" on page 34-7). The calibrated data (.c1h and .c0h files) for a typical ACCUM mode observation will have multiple groups. Each of these groups is an independent (sub)integration and they must be added together (realigning the data in wavelength space before adding) to produce the total calibrated spectrum for your observation. See

___

1. We recommend, as a rule, that archival researchers recalibrate *all* GHRS observations in order to take advantage of the best calibrations and knowledge that is available.

"Assessing GHRS Science Data" on page 35-29 for examples of ACCUM data and a description of how to reduce and analyze such data.

WSCAN was a variant of ACCUM in which one could specify a range of wavelengths to be observed and the software would determine how to space grating movements to accomplish that. OSCAN was another variant of ACCUM that applied only to the echelle gratings (scanning through orders); it was used almost exclusively for calibrations.

34.3.3 RAPID Mode

For observations of targets whose spectra varied on shorter timescales, there was *rapid* (or *direct*) readout mode. In RAPID mode, individual integrations could be obtained as often as once every 50 milliseconds. However, RAPID mode did not allow use of the FP-SPLIT or substepping producedures and observations of the detector background were not interspersed with the on-target observations. In RAPID mode data, each subintegration was stored sequentially in separate groups in both the raw and the calibrated data.

RAPID mode resulted in huge data quantities, and was used to search for forms of time variability. See "RAPID Mode (and a Little About Spatial Scans)" on page 35-34 for examples of RAPID mode data and a discussion of how to work with it.

34.4 Documentation and References

34.4.1 STScI GHRS Documentation

Many of the documents described in this section are available only as paper. Archival users should not generally need them, but if needed, copies are cataloged[2] and stored in the STScI Library.

Instrument Handbooks

The *GHRS Instrument Handbook* is the single most useful reference about the GHRS except for this data handbook; it describes instrument operating modes as well as observing strategies. The instrument handbook is critical for understanding why a series of observations may have been obtained in a particular manner at a particular time. The flight software and operating procedures for the GHRS changed continually over its life as errors were corrected and new features installed. The different versions of the instrument handbook document the history of these efforts (as do the ISRs, described below).

---

2. If you search the library's on-line catalog for GHRS documents, try the string "HRS" because many older documents pre-date the addition of "Goddard" to the name.

Eight versions of the *GHRS Instrument Handbook* were issued by STScI between October, 1985, and June, 1995. The first four versions (1.0, 2.0, 2.1, and 3.0) exist as paper-only documents, and they pertain to the pre-COSTAR instrument. The last four versions (4.0, 4.1, 5.0, and 6.0) are available on-line as Adobe Acrobat and world wide web documents, and were written for the post-COSTAR instrument.

The instrument handbook contains information pertinent to specific time periods and cycles of HST operation. Archival researchers should not need to refer to these documents but we list them in Table 34.2 for completeness.

Table 34.2: GHRS Instrument Handbook Versions

IH version	Date of Issue	HST Cycle
2.0	May, 1989	1, 2
3.0	January, 1992	3
4.0	January, 1993	4
5.0	May, 1994	5
6.0	June, 1995	6

Instrument Science Reports

Instrument Science Reports (ISRs) are technical papers issued by STScI that summarize, for example, calibrations, or new operating features. Ninety-one GHRS ISRs were written. Sometimes ISRs provide details not available elsewhere, but in general we have tried to encapsulate the contents of ISRs into this data handbook so that archival researchers will not need to refer to them. There are some cases where the ISR treats a specialized subject that is beyond the scope of this handbook, and we note those where appropriate.

34.4.2 GHRS Web Resources

STScI maintains extensive resources on the World Wide Web. GHRS resources can be found by using the search mechanism. You should always check there for changes or updates. STScI's home page is at:

```
http://www.stsci.edu/
```

34.4.3 GHRS Bibliography

The following papers include discussions of GHRS construction and performance or provide detailed explanations of particularly useful data analysis techniques. A more complete list of references is available on the web and as *GHRS ISR* 91.

GHRS / 34

Primary Reference for GHRS Performance

The following paper should, in most cases, be cited when referring to GHRS observations:

- Heap, S.R., et al., "The Goddard High Resolution Spectrograph: In-Orbit Performance," 1995, *PASP*, 107, 871.

Ultraviolet Reddening and Extinction

- Bless, R.C., and B.D. Savage, "Ultraviolet Photometry from the Orbiting Astronomical Observatory. II. Interstellar Extinction." 1972, *ApJ*, 171, 293–308.

- Nandy, K., G.I. Thompson, C. Jamar, A. Monfils, and R. Wilson, "Studies of Ultraviolet Interstellar Extinction with the Sky-survey Telescope of the TD-1 Satellite." 1976, *A&A*, 51, 63–69.

- Code, A.D., J. Davis, R.C. Bless, and R. Hanbury Brown, "Empirical Effective Temperatures and Bolometric Corrections for Early-Type Stars." 1976, *ApJ*, 203, 417–434.

- Seaton, M.J., "Interstellar Extinction in the UV" 1979, *MNRAS*, 187, 73P–76P.

- Savage, B.D., and J.S. Mathis, "Observed Properties of Interstellar Dust" 1979, *ARA&A*, 17, 73–112.

GHRS-Related Technical Papers

- Ebbets, D.C., J.C. Brandt, and the HRS Investigation Definition Team, "Ultraviolet High-Resolution Spectroscopy from the Space Telescope," 1983, *PASP*, 95, 543–549.

- Reader, J., N. Acquista, C.J. Sansonetti, and J.E. Sansonetti, "Wavelengths and Intensities of a Platinum/Neon Hollow Cathode Lamp in the Region 1100–4000 Å," 1990, *ApJS*, 72, 831–866.

- Ebbets, D.C., J. Brandt, and S. Heap, S.,"Status of the Goddard High Resolution Spectrograph in May 1991," in *The First Year of HST Observations*, edited by A.L. Kinney and J.C. Blades, 1991, p. 110-122.

- Cardelli, J.A., D.C. Ebbets, and B.D. Savage, "Scattered Light in the Echelle Modes of the Goddard High Resolution Spectrograph Aboard the Hubble Space Telescope. I. Analysis of Prelaunch Calibration Data." 1990, *ApJ*, 365, 789–802.

- Cardelli, J.A., D.C. Ebbets, and B.D. Savage, "Scattered Light in the Echelle Modes of the Goddard High Resolution Spectrograph Aboard the Hubble Space Telescope. II. Analysis of Inflight Spectroscopic Observations." 1993, *ApJ*, 413, 401–415.

- Gilliland, R.L., S.L. Morris, R.J. Weymann, D.C. Ebbets, D.C., and D.J. Lindler, "Resolution and Noise Properties of the Goddard High Resolution Spectrograph," 1992, *PASP*, 104, 367–382. (Discusses deconvolution of the effects of the GHRS PSF and LSF.)

- Brandt, J.C., et al., "The Goddard High Resolution Spectrograph: Instrument, Goals, and Science Results," 1994, *PASP*, 106, 890–908. (Publication of record for the pre-COSTAR GHRS.)

- Blades, J.C., and S.J. Osmer, editors., *Calibrating Hubble Space Telescope: Proceedings of a Workshop Held at STScI* published by STScI. (Contains several papers of relevance for data analysis.)

- Lyu, C.-H., F.C. Bruhweiler, and A.M. Smith, "Tomography/Power Spectrum Techniques for Removal of Fixed Pattern Noise from Hubble Space Telescope Spectra," 1995, *ApJ*, 447, 880–888.

- Lallement, R., J.-L. Bertaux, J.T. and Clarke, "Deceleration of Interstellar Hydrogen at the Heliospheric Interface" 1993, *Science*, 260, 1095–1098. (Provides a good illustration of geocoronal Ly-α with the LSA and Echelle-A.)

- Lambert, D.L., Y. Sheffer, R.L. Gilliland, and S.R. Federman, "Interstellar Carbon Monoxide toward ζ Ophiuchi," 1994, *ApJ*, 420, 756–771. (Discsses how to achieve very high signal-to-noise with the GHRS.)

GHRS / 34

GHRS / 34

GHRS Data Structures and Data Assessment

This chapter presumes that you have selected and retrieved some GHRS observations from the Hubble Data Archive. We will describe the contents of the delivered data and how to assess those data. To more fully understand archival observations it sometimes helps to look at the Phase II proposal for the program that first requested them. We use some examples of actual GHRS programs to illustrate how Phase II proposals were turned into observations and data products. Complete explanations are provided later for reference.

35.1 Contents of Delivered Data

Most HST data are retrieved over the Internet, but it is still possible to get a tape. In either case, you will receive various FITS files containing science data and other information. StarView gives you the option of obtaining sets of uncalibrated, calibrated[1], data quality, observation log, and used and best reference files.

---

1. As we noted in the previous chapter, we urge you to recalibrate all GHRS observations in order to take advantage of the latest and best calibrations and knowledge of the instrument. However, it can be helpful to look at the calibrated observations to judge the quality of the data and their suitability for your needs.

In this section we provide a description of the information stored in each file. The STSDAS routine for unpacking your data is **strfits**. The resulting files will have default suffixes, as described in Table 35.1 below.

The suffixes for the headers of the raw science data images you will have after running **strfits** are listed in the first column in Table 35.1; they are the output of the Routine Science Data Processing (RSDP) pipeline generic conversion process and are discussed in more detail below. You generally need all of these files in order to calibrate GHRS data.

The third column in Table 35.1 lists the header suffixes for the calibrated data created by running **calhrs**, as well as some additional engineering files available from the Archive. The RSDP pipeline usually runs **calhrs** on all GHRS data when it is taken, but due to updates to reference images and tables, we strongly recommend that you recalibrate the data.

Table 35.1: File Name Suffixes

Suffix	File Contents	Suffix	File Contents
.d0h	Raw science data	.c0h	Calibrated wavelength solution
.q0h	Data quality for raw science image	.c1h	Calibrated science data (fluxes)
.d1h	Return-to-Brightest & SSA ACQ/PEAKUP	.c2h	Propagated statistical error
.q1h	Data quality for RTB & SSA ACQ/PEAKUP	.c3h	Calibrated special diodes
.x0h	Extracted engineering data	.c4h	Special diodes data quality
.xqh	Data quality for extracted engineering data	.c5h	Background
.shh	Standard Header Packet	.cqh	Calibrated science data quality
.ulh	Unique Data Log	.jit, .jih	Jitter files (post- and pre-COSTAR)
.trl	Trailer file	.pdq or .ocx	PODPS data quality files

35.1.1 Uncalibrated Raw Data

Science Data (.d0h and .q0h)

The science data (.d0h image) contains the single-precision floating point values representing the number of detected counts accumulated for each diode, just as it comes from the spacecraft. Depending on the stepping pattern (STEPPATT) used for the observation, there may be only one, or up to six groups of science data per exposure. The default STEPPATTs are listed in Table 35.3 and the implications are discussed more in "File Sizes" on page 35-5. The science data are read out from the 500 science diodes (see the *GHRS Instrument Handbook*).

The data quality image (.q0h) associated with the science data records whether there is "fill" data due to technical problems with the observation or due to problems in transmitting the data from the telescope. The .q0h file contains

zeroes where the data are good, and ones for Reed-Solomon errors (related to data transmission) and 16 for fill data (see "Calibration Quality Files" on page 37-22 for a more complete explanation).

Return-To-Brightest and Small Science Aperture ACQ/PEAKUP (.d1h and .q1h)

Most acquisitions of point sources since mid-1993 used the return-to-brightest algorithm, in which the aperture (LSA or SSA) was rastered in a 3 x 3 or 5 x 5 pattern, and the pointing with the most counts was returned to for peakup and observation. The return-to-brightest (RTB) target acquisition record is in the .d1h image and also in the trailer file (.trl). This image contains the total counts at each dwell point in the spiral search performed by the RTB acquisition algorithm.

SSA ACQ/PEAKUPs use the same algorithm as RTB target acquisitions. Therefore they will also have a .d1h file whose header file contains information on which dwell point (MAPFND) contained the largest flux (FLUXFND).

The data quality image (.q1h) associated with the RTB data records whether there is fill data due to technical problems with the observation or due to problems in transmitting the data from the telescope.

Extracted Engineering Data (.x0h)

For ACCUM and RAPID mode observations, the extracted engineering data image (.x0h) consists of 24 pixels which contain the values of the twelve special diodes (i.e., focus, background monitor, and radiation monitor diodes; see the *GHRS Instrument Handbook*) in the detector and twelve pixels of engineering trailer and flight software data relevant to each pattern execution (see Table 35.2). The data quality file (.xqh) records whether any of the data represent fill due to technical problems with the observation or telescope during the observation. These data are sometimes used for determining the background count rate.

Standard Header Packet (.shh)

The standard header packet (SHP, image suffix .shh) contains the telemetry values from the engineering data and some GHRS-unique data. The engineering data includes temperatures, currents, and voltages at various points in the instrument. The header packet also contains information used in the operation of the spacecraft, such as target name, position, and velocity of the telescope, the right ascension and declination of the target, Sun, and Moon, and other proposal information used in the observation which was provided in the Phase II part of the proposal. There is one group of .shh data per pattern used in the observation. Various items from the SHP are used in various steps of the reduction process.

Unique Data Log (.ulh)

The unique data log (UDL, image suffix .ulh) contains the command values (i.e., the Observation Control Table) used to control the aperture, detector, carrousel, Digicon deflections, observing modes, and flux measurements as well as some observation data produced by the flight software. There are two groups of .ulh data per pattern per observation. For images and standard ACCUM mode, a leading and following UDL are readout that bracket the observation.

GHRS / 35

Trailer File (.trl)

The trailer file (suffix `.trl`) contains many messages generated by the conversion of the data from what is on-board the spacecraft into STSDAS images. These messages include information on missing or filled packets, RTB information for some acquisitions, and the informational messages produced by **calhrs** as it is used to calibrate the data.

35.1.2 Calibrated Data

Calibrated Wavelength Solution (.c0h)

The calibrated wavelength solution (`.c0h`) image contains the wavelengths in Angstroms for each corresponding pixel in the `.c1h` file. The dimensions and number of groups is the same as the `.c1h` file. This file is produced when ADC_CORR is set to PERFORM.

Calibrated Science Data (.c1h)

The calibrated science data (`.c1h`) image contains the calibrated science data, and is always produced by **calhrs**. The number of groups and dimensions of the spectra depends on the stepping pattern used (STEPPATT, see Table 35.3 and "File Sizes" on page 35-5) in the observation and also which calibration steps are performed. The contents can range from being an exact copy of the raw science data (found in the `.d0h` image) to a fully flux-calibrated spectrum.

Propagated Statistical Error (.c2h)

The propagated statistical error (`.c2h`) image contains the propagated statistical error associated with the `.c1h` science data. The number of groups and dimensions of this file will be the same as the `.c1h` image. The units of the error will also be the same as the final units of the science data.

Calibrated Special Diodes (.c3h)

This twelve-pixel image contains the calibration of the special diodes whose raw values correspond to the first twelve pixels in the `.x0h` file (see Table 35.2).

Special Diode Data Quality (.c4h)

The special diode data quality (`.c4h`) image contains the data quality flags for the special diodes. See Table 37.5 for data quality flags.

Background (.c5h)

The background (`.c5h`) image contains the actual subtracted background. The units of the background will be either in counts or count rate, depending on the setting of the EXP_CORR switch. This file is produced when a background correction is performed. You have several options for calculating the background rate; these are described in "Calibration Steps Explained" on page 36-2.

Calibrated Science Data Quality (.cqh)

The calibrated science data quality (`.cqh`) image contains the data quality flags associated with each pixel in the calibrated science data image. The flags are num-

bers; the higher the value, the worse the data in the corresponding pixel. See Table 37.5 for calibrated data quality flags.

Table 35.2: Special Diodes

Diode Array Index	.c3h or .x0h Pixel #	Description
1	1	Upper left background (corner) diode
2	2	Lower left background (corner) diode
3	3	Left high-energy diode
4	4	Middle focus (disabled) diode
5	5	Upper left focus diode
6	6	Lower left focus diode
507	7	Upper right focus diode
508	8	Lower right focus diode
509	9	Middle focus diode
510	10	Right high-energy diode
511	11	Upper right background (corner) diode
512	12	Lower right background (corner) diode

GHRS / 35

35.1.3 File Sizes

As mentioned above, the size (number of pixels and number of groups) of your raw science file (.d0h) will depend on the substepping strategy used in the original observations, and that is determined by the setting of the STEPPATT keyword. The default STEPPATTs are listed in Table 35.3. Quarter-stepping, i.e., four output pixels per diode, was ordinarily done with science observations in order to achieve full resolution, but the default background measurement strategy may differ depending on the grating and order being observed. The different STEPPATTs you may encounter with GHRS data are listed in Table 35.3.

A typical raw science file (.d0h) will have a STEPPATT=5 and, like other data from STEPPATTs with quarter-stepping and two interorder background bins, will contain six 500-pixel groups per exposure. The first four groups (or bins) are the science data (each bin shifted by 1/4 diode) and the next two are interorder background measurements, one above the spectrum, one below. Mathematically, the number of raw science groups can be represented by the following formula;

number(.d0h groups) = (spectrum + background bins)*(RPTOBS + 1) * *fpsplits*

- The number of spectrum and background bins are determined by the STEPPATT, see Table 35.3.

- RPTOBS and STEPPATT are available in the header.

- *fpsplits* = 1 (FP_SPLIT=DEF) or 2 (FP_SPLIT=TWO or DSTWO) or 4 (FP_SPLIT=FOUR or DSFOUR).

The .q0h, .x0h, .xqh, and consequently, .c3h and .c4h files will have the same number of groups as the .d0h file. Patterns which use the corner diodes for background measurements may still create measured background bins in the raw data, although they are not used by **calhrs**.

Table 35.3: Stepping Pattern Properties for the GHRS

| STEP-PATT number | Bins Measured | | Spectrum/ Background Ratio | Diodes used for Background | On-target Efficiency | Appropriate Gratings | Minimum Exposure Time (sec)[a] |
	Spectrum	Background					
1	1	0	1		1.00	all	0.8
2	2	0	1		1.00	all	1.6
3	4	0	1		1.00	all	3.2
4	2	2	8	science	0.89	first-order	14.4
5[b]	4	2	8	science	0.94	first-order	27.2[b]
6	2	2	8	science	0.89	echelle	14.4
7[c]	4	2	8	science	0.94	echelle	27.2
8	2	2	8	corner	0.89	echelle	14.4
9[d]	4	2	8	corner	0.94	echelle	27.2
10	2	2	1	science	0.50	first-order	3.2
11	4	2	1	science	0.67	first-order	4.8
12	2	2	1	science	0.50	echelle	3.2
13	4	2	1	science	0.67	echelle	4.8
14	2	2	1	corner	0.50	echelle	3.2
15	4	2	1	corner	0.67	echelle	4.8

a. Calculated using COMB=4, STEP-TIME=0.2, and FP-SPLIT=NO. Scale these values by 4, for example, if using FP-SPLIT=STD.
b. Default STEPPATT for first-order gratings.
c. Default STEPPATT for Ech-A orders < 51 and Ech-B orders < 31.
d. Default STEPPATT for Ech-A orders ≥ 51 and Ech-B orders ≥ 31.

The size (number of pixels and number of groups) of your calibrated output flux file (.c0h, .c1h, .c2h, .c5h, .cqh) will depend on the switch settings and the substepping strategy used in the original observations. In a typical observation, the four groups of science data are merged (see the MER_CORR description in "Calibration Steps Explained" on page 36-2) and the combined background groups subtracted from that merged spectrum (see the BCK_CORR description in "Calibration Steps Explained" on page 36-2) to create one 2000-pixel group of calibrated science data per exposure. (Half-stepped data would create a 1000-pixel

calibrated exposure.) Unmerged data, such as RAPID-mode, remain in groups of 500 pixels. Mathematically, the number of calibrated flux file groups is:

number (`.clh` groups) = (RPTOBS + 1) * *fpsplits*

RAPID-mode data are slightly different and will have a number of raw groups equal to three plus the exposure time divided by the sample (or step) time:

number (raw RAPIDs) = 3 + (EXPTIME / STEPTIME).

The number of calibrated data will be three less than that because the first two and last groups of raw RAPID data are hysteresis and are thrown away.

The pipeline calibration does not combine RAPID, FP-SPLITs, or repeat exposures.

35.1.4 Observation Log Files

As of February 1995, the observation log files (`.jih`) and jitter files (`.jit`), which are provided by the Observatory Monitoring System (OMS), were routinely available. These can give valuable information, such as telescope performance during the observation and the position of the target within the aperture. A so-called *jitter ball* is a routine portion of all GHRS paper products for which jitter files exist. This plot shows the motions of the FGSs needed to keep the target centered, recorded every six seconds throughout the exposure. See Appendix C in Volume I of this handbook for a description of these files and additional quantities available in the jitter files.

35.1.5 PODPS Data Quality

OPUS (formerly OSS and PODPS) staff performed a quick data quality assessment of the target acquisitions and the science observations. This assessment was performed to identify any target acquisition failures, guide star acquisition failures, other spacecraft anomalies, or instrumental problems. This assessment was recorded in the data quality keywords contained in the PDQ (Procedural Data Quality) file. The PDQ files are archived to data class PDQ and can be retrieved from the HST Archive using StarView. OCX files (Observation Support System (OSS) Observer Comment files) contain information about the success or failure of target acquisitions and science observations. Before April 17, 1992, OCX files were not always archived separately, and, in some cases, were prepended to the RSDP pipeline history file, the `.trl` trailer file. After February 1995, OCX files were produced only to document real-time activity (interactive target acquisition) in support of an observation. After October 1996, OCX files may contain information about observation execution problems.

Please note that the PDQ files and their comments should not be overinterpreted. These remarks were based on a quick visual examination of the data and the experience of the OPUS staff. The technical remarks are usually sound, but some comments about the "quality" of the observations can arise from an incomplete knowledge of the science goals of the original proposer. Unless the object was significantly miscentered, for example, the achieved signal-to-noise is proba-

GHRS / 35

bly close to what was expected, even if it may appear low in a single exposure. To assess whether or not a low flux is meaningful, you should examine the jitter file or other records of spacecraft performance, or simply look at the total number of counts achieved.

35.1.6 Reference Files

The Archive will also give you the opportunity to retrieve the "used" or "best" reference files that go along with the data you are retrieving from the Archive. The "used" reference files are those listed in the calibration reference file keywords, and are those actually applied to the observations to produce the calibrated files in the Archive. The "best" reference files are meant to reflect accumulated experience on GHRS calibration and performance and so are recommended. For more information, please see "Recalibrating GHRS Data" on page 36-13.

35.2 Header Keywords

The header files provide all the information needed to calibrate GHRS data. The headers are divided into groups of keywords that deal with specific types of information (i.e., observing information, engineering information, and processing and calibration information). Table 35.4 lists a few of the important GHRS header keywords.

An HST observation is composed of packets of information sent down to the ground, and each observation packet has an embedded packet format code to identify the packet as SHP, UDL, or science. Each science packet has a packet format code (PKTFMT) that identifies the type of science. The default GHRS calibration switches are set by the PKTFMT keyword value, specified by the type of observation (Target ACQuisition, IMAGE, ACCUM, or RAPID mode). The default calibration switches have been selected to achieve the best possible calibration. The PKTFMT values are set when the observations are scheduled. They are used to determine the values of the science header keywords. This information is stated here for completeness.

The GHRS calibration steps are listed and described in "Recalibrating GHRS Data" on page 36-13.

GHRS / 35

Table 35.4: Important GHRS Header Keywords

Keyword	Description and Values
GCOUNT	Number of data groups
FILETYPE	shp, udl, ext, sci, img, wav, flx
NBINS	Number of substep bins in this pattern
RPTOBS	Expected number of observation repeats
STEPPATT	Step pattern sequence
FP_SPLIT	FP-SPLIT (NO, TWO, FOUR, DSTWO, DSFOUR)
COMB_ADD	Comb-addition (NO, TWO, FOUR, DSTWO, DSFOUR)
FINCODE	Observation termination code
OBSMODE	Observation mode (ACCUM, RAPID, SPYBAL, DEFCAL, ACQ,)
DETECTOR	Detector in use (1 or 2)
GRATING	Grating, echelle, or mirror in use
APERTURE	Aperture name
DATE	Date this file was written (dd/mm/yy)
KZDEPLOY	COSTAR deployed for the HRS (T or F)
APER_FOV	Aperture field of view (arcsec), N/A for cal
FGSLOCK	Commanded FGS lock (FINE, COARSE, GYROS, UNKNO
DATE-OBS	UT date of start of observation (dd/mm/yy)
TIME-OBS	UT time of start of observation (hh:mm:ss)
EXPTIME	Exposure duration (seconds)—calculated

GHRS / 35

35.3 Paper Products

The term "paper products" refers to the package of text and graphical information that can be generated, for example, for a visit's worth of GHRS data[2]. The GHRS paper products have been automatically generated as part of the RSDP pipeline process since September, 1996. Also, a task can now be run on any HST data by using **pp_dads** which is in the **hst_calib.paperprod** package. Refer to the help file for information on how to run this task. It is often useful to inspect the paper products to obtain a quick overview of data you have retrieved from the Archive.

---

2. A *visit* is the sequence of observations obtained on a single target during one continuous use of HST.

The GHRS paper products produce title pages for an observation and a one-page summary for each rootname (excluding DEFCALs, which are deflection calibrations) in an observation. The page is divided into quadrants: summaries of the observation, the calibration, the image statistics, and OMS (or jitter) data. Quadrants may contain different information depending on the type of file being displayed.

An example of GHRS paper products is shown below for reference to these remarks (see Figure 35.1 through Figure 35.4). We have not included the title page to save space, but we show an LSA acquisition and an SSA peakup so that you can see an example of both.

35.3.1 Title Pages

The first page produced by **pp_dads** is a page which lists the proposal number and the name of the Principal Investigator. The next page(s) contains a list of targets for the observations and a list of the observations, similar to the exposure logsheet.

35.3.2 The Observation Summary

A separate sheet is produced for each individual exposure. The Observation Summary in the upper left quadrant contains information from keywords which characterize an exposure, such as the proposal ID, instrument, target and its location, grating, observation mode, exposure time, wavelength information, etc. The information for target acquisitions or images will be slightly different from science observations. For instance, target acquisitions will list the settings of the return-to-brightest indicator (RTBRIGHT) or the bright and faint limits, the size of the spiral search (SRCHSIZE), the highest flux in an RTB acquisition (FLUXFND), and the total flux on the eight target acquisition diodes at the end of the acquisition (ZFLUXM). At the bottom of the quadrant, the number of groups for the image displayed in the quadrant below (Image Statistics Summary) is listed.

35.3.3 The Calibration Summary

The Calibration Summary (upper right quadrant) will be blank for target acquisitions and images. For data that are calibrated, it will contain a list of the calibration images and tables, on the right; and a list of all the calibration switch settings, on the left. Two new additions (SAAHFILE and CCRE) to the headers, if added during any eventual reprocessing, may not show up in this section, since they were added after the paper products task was created. This quadrant also contains the "instrument: rootname" label for the observation being summarized on this sheet.

Figure 35.1: Target and Observation List
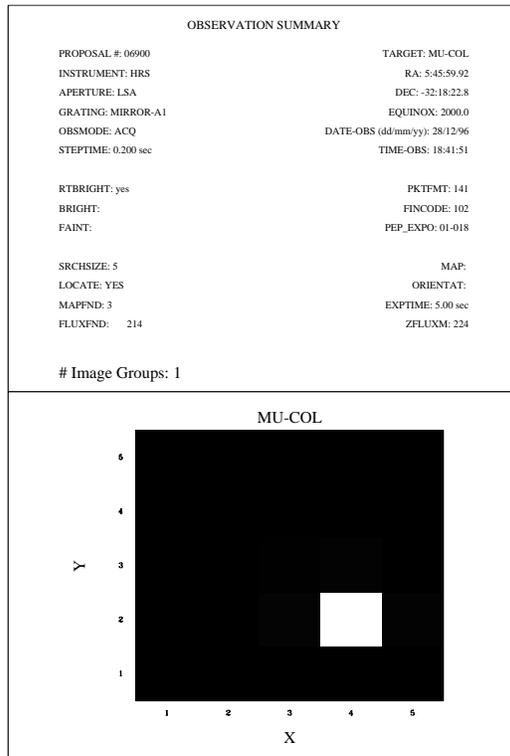
Visit: 01	Proposal: 06900	*GHRS*

Target List

Target Name	R.A. (J2000)	Dec. (J2000)	Description
MU-COL	5:45:59.92	-32:18:22.8	CALIBRATION,PHOTOMETRIC,

Observation List

Logsheet Line#	Rootname	Target Name	Config	Observation Mode	Aperture	Spectral Element	Wavelength (central)	Exposure (sec)	Quality Flags Obs	Proc
1.018	Z3JN0102T	MU-COL	HRS	ACQ	LSA	MIRROR-A1	(N/A)	5.0		
1.100	Z3JN0114T	MU-COL	HRS	ACQ/PEAKUP	SSA	MIRROR-A1	(N/A)	25.0		
2.060	Z3JN020MT	MU-COL	HRS	ACCUM	LSA	ECH-B	1703	230.4		

Quality flags: ○ = OK   ● = Not OK   Blank = Unknown or file missing

Figure 35.2: Observation Summary—LSA Acquisition

OBSERVATION SUMMARY

PROPOSAL #: 06900	TARGET: MU-COL
INSTRUMENT: HRS	RA: 5:45:59.92
APERTURE: LSA	DEC: -32:18:22.8
GRATING: MIRROR-A1	EQUINOX: 2000.0
OBSMODE: ACQ	DATE-OBS (dd/mm/yy): 28/12/96
STEPTIME: 0.200 sec	TIME-OBS: 18:41:51
RTBRIGHT: yes	PKTFMT: 141
BRIGHT:	FINCODE: 102
FAINT:	PEP_EXPO: 01-018
SRCHSIZE: 5	MAP:
LOCATE: YES	ORIENTAT:
MAPFND: 3	EXPTIME: 5.00 sec
FLUXFND: 214	ZFLUXM: 224

Image Groups: 1

MU-COL

GHRS: Z3JN0102T

Space Telescope Science Institute 3700 San Martin Drive Baltimore, MD 21218   PaperProd 2.41   Wed 13:55:47 27-Aug-97

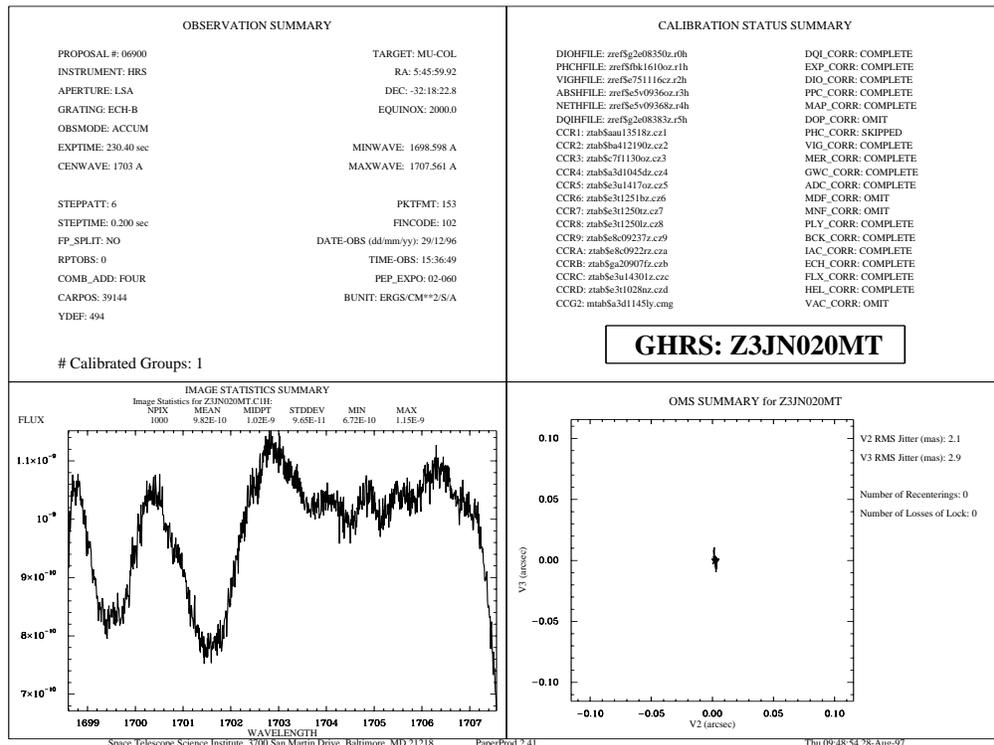**Figure 35.3:** Observation Summary—SSA Peakup

Figure 35.4: Observation, Calibration, Image, and OMS Summaries

35.3.4 The Image Statistics Summary

The first thing you will notice in the Image Statistics Summary (lower left quadrant) for calibrated data is the plot of flux versus wavelength. Most data are coadded for this plot; the number of groups corresponding to the output display is printed at the bottom of the Observation Summary quadrant. At the top of the plot, image statistics for this observation are found, including the number of pixels, mean and mid-point (similar to a median; see the **imstat** help file), standard deviation, minimum and maximum. For RTB target acquisitions and SSA ACQ/PEAKUPs, there is a greyscale representation of the spiral search. Images will also be displayed in this quadrant.

35.3.5 The OMS Summary

The lower right corner contains the OMS (Observatory Monitoring System) Summary. Here you will find, if the information is available, the jitter plot (jitter ball) which shows the movement of the HST in V2 and V3 coordinates measured in arcseconds off center. The plot is made to be about the size of the Small Science Aperture (SSA), i.e., 0.25 arcsec on each side, unless the observation is a target acquisition in which case the full resolution of the spiral search is shown (3 x 3 or 5 x 5). Also listed is a summary of the rms jitter in V2 and V3 in milliarcsec, in addition to the number of recenterings and losses of lock during the observation. More information about OMS engineering data is available in Appendix C of Volume I of this handbook.

GHRS / 35

35.4 Assessing GHRS Data

To help you assess GHRS data we will walk through actual proposals containing examples of many of the observing modes available. A short description of a program being used in the science assessment example is provided and a description and picture of the exposure logsheet, followed by assessment descriptions for the different observing modes represented in the example program.

Every observation in the Archive resulted from a detailed Phase II proposal created by the original observer. It is not usually necessary to examine the Phase II proposal to make sense of the data, but it is sometimes helpful to understand the structure of the observations.

35.4.1 An Example: R136a in the LMC

Program 5297 was executed in the spring of 1994 as an Early Release Observation (ERO), following the 1993 servicing mission. During that mission, COS-TAR mirrors were deployed so that the full optical quality of HST could be realized by the GHRS. Also, a repair kit was installed that allowed Side 1 of the GHRS to be used once again (Side 1 capabilities were lost in 1991 due to the failure of a low-voltage power supply).

Program 5297 was designed to take advantage of and demonstrate these capabilities by obtaining low-resolution spectra of closely-spaced hot stars in a young cluster (R136a) in the Large Magellanic Cloud (LMC). Two of the stars to be observed were only about 0.12 arcsec apart, less than the size of the GHRS Small Science Aperture (SSA), which is 0.22 arcsec square. Thus precise positioning was needed. To achieve this, the telescope was first to acquire and center on the brightest object in the R136a field. That object was itself the convolution of two stars, so that some allowance had to be made for the apparent centroid of what was acquired. This was done using information from a WF/PC-1 image of R136a obtained before the servicing mission. Once centered on R136a1, the SSA could then be moved with high relative precision, but to ensure understanding of what was observed, IMAGEs were taken at each position.

35.4.2 The Exposure Logsheet

An abridged version of the Phase II Proposal for 5297 is shown in Figure 35.5. The first portion of the figure is the Target List and the bottom half is the Exposure Logsheet. Here are some notes to go with individual lines of the Exposure Logsheet:

Line 1: R136a1 was acquired with the Large Science Aperture (LSA). The LSA is denoted as "2.0" but has a true size of 1.74 arcsec square with the COSTAR mirrors in place. SEARCH-SIZE=5 is specified to ensure a good acquisition by providing a wider search area. (The default SEARCH-SIZE=3 was adequate in nearly all cases, but the crowding of this field led to using a more liberal value.) The specified exposure time of 25 seconds implied a STEP-TIME of 1.0 second; STEP-TIME is the dwell per point in the spiral search pattern. MIRROR-N2 was used because these stars were faint. Using MIRROR-N1 would have been preferable if these stars were bright enough because then it would have been unnecessary to switch from using detector D2 on Side 2 (implied by MIRROR-N2) to detector D1 on Side 1 (implied by using Spectral Element G140L on line 20). Switching from one Side of the GHRS to the other took about 40 minutes because of the need to let the electronics stabilize. However, MIRROR-N1 reflected light only from about 1200 to 1700 Å, and the STEP-TIME needed to acquire these stars would have exceeded the maximum permitted value of 12.75 seconds. Note the comment explaining how the exposure time was estimated and the Special Requirements that tie this acquisition to the subsequent exposures. Acquisitions are explained in detail in the *GHRS Instrument Handbook*. The comment about BRIGHT=RETURN means that the onboard acquisition algorithm will determine which dwell point had the most counts and will center the LSA at that point.

Figure 35.5: Exposure Logsheet for Program 5297

```
PROPOSAL FOR HUBBLE SPACE TELESCOPE OBSERVATIONS ID 5297
1.Proposal Title: FIRST SPECTRA OF O STARS IN R136A
-------------------------------------------------------------------------------
TARGET LIST    a) Fixed Targets                                 ID = 5297        [  3]
-------------------------------------------------------------------------------
 1 |    2     |         3          |          4          |   5    |   6   |  7  |        8
-------------------------------------------------------------------------------
Tar|  Target  |      Target        |       Target        | Coord  |Radial |Acqui|FLX|   Flux data
No |  Name    |    Description      |      Position       | Eqnx   | Vel.  |Prblm|REF|
-------------------------------------------------------------------------------
 1  R136a1     B,103,D,203           RA = 05H 38M 42.438S +/-  2000             1  V=12.77
                                     0.1S,                                      2  B-V=+0.43
                                     DEC = -69D 06' 02.294" +/-
                                     0.5"
       Comments: V,B-V from Malumuth & Heap (1993)
-------------------------------------------------------------------------------
 2  R136a2     B,103,D,203           RA = 05H 38M 42.4576S +/- 2000             1  V=13.38
                                     0.1S,                                      2  B-V=+0.43
                                     DEC = -69D 06' 02.242" +/-
                                     0.5"
       Comments: WN star in R136a; coordinates and V,B-V
                 from Malumuth & Heap (1993)
-------------------------------------------------------------------------------
 5  R136a5     B,105,D,203           RA = 05H 38M 42.4785S +/- 2000             1  V=13.73
                                     0.1S,                                      2  B-V=+0.12
                                     DEC = -69D 06' 02.096" +/-
                                     0.5"
       Comments: O star in R136a; coordinates and V,B-V
                 from Malumuth & Heap (1993)
-------------------------------------------------------------------------------
EXPOSURE LOGSHEET                                               ID = 5297        [  4]
-------------------------------------------------------------------------------
 1  |   2   |    3     |  4   |  5  |   6   |   7    |  8   |      9      |10 |  11  |  12  |13|14|     15
-------------------------------------------------------------------------------
Line  |  Seq  |  Target  |Instr |Oper.|Aper  |Spectral|Central| Optional     |Num| Time |S/N   |Flx|Pr|  Special
Number|  Name |  Name    |Config| Mode|or FOV|Element |Waveln.| Parameters    |Exp|      |Rel. Time|Ref|  |  Requirements
-------------------------------------------------------------------------------
 1              R136a1     HRS    ACQ   2.0   MIRROR-N2         SEARCH-SIZE=5  1  25S         1  1 CYCLE 4/1-101
                                                                                              ONBOARD ACQ FOR 2-
                                                                                              3
                                                                                              SEQ 1-101 NO GAP
       Comments: Time=(128*Nmap +SS2)*StepT =(0
                 +5x5)*1.0S = 25S GHRS HDBK/Fig
                 7.3 gives N1 c/s=2500 for
                 V=13.0, (B-V)o=-.3, E(B-V)=.4
-------------------------------------------------------------------------------
 2              R136a1     HRS    ACQ/  2.0   MIRROR-N2                        1  102S        1  1 CYCLE 4
                                  PEAKUP
       Comments: Time=Fapt*StepT =102 * 1S
-------------------------------------------------------------------------------
 3              R136a1     HRS    ACQ/  0.25  MIRROR-N2         SEARCH-SIZE=5  1  25S         1  1 ONBOARD ACQ FOR 4-
                                  PEAKUP                                                       52
       Comments: Time=SSIZE^2 * StepT =25 * 1S
                 BRIGHT=RETURN assumed
-------------------------------------------------------------------------------
 4              R136a1     HRS    IMAGE 0.25  MIRROR-N2         NX=13          1  169S        1  1
                                                               NY=13
                                                               DELTA-X=1
                                                               DELTA-Y=1
       Comments: Time=13*13*1S=169S
-------------------------------------------------------------------------------
 5              R136a2     HRS    IMAGE 0.25  MIRROR-N2         NX=13          1  169S        1  1
                                                               NY=13
                                                               DELTA-X=1
                                                               DELTA-Y=1
       Comments: Time=13*13*1S=169S
-------------------------------------------------------------------------------
20              R136a2     HRS    ACCUM 0.25  G140L    1300     STEP-PATT=3    1  10M            1
                                                               FP-SPLIT=NO
-------------------------------------------------------------------------------
21              R136a2     HRS    ACCUM 0.25  G140L    1610     STEP-PATT=3    4  10M            1
                                                               FP-SPLIT=NO
-------------------------------------------------------------------------------
50              R136a5     HRS    ACCUM 0.25  G140L    1610     STEP-PATT=3    4  30M            1
                                                               FP-SPLIT=FOUR
       Comments: total texp=120M
-------------------------------------------------------------------------------
51              R136a5     HRS    ACCUM 0.25  G140L    1300     STEP-PATT=3    1  30M            1
                                                               FP-SPLIT=FOUR
       Comments: total texp=30M
-------------------------------------------------------------------------------
52              WAVE       HRS    ACCUM SC2   G140L    1300     STEP-PATT=3    1  25.6S          1
                                                               FP-SPLIT=NO
       Comments: WAVECAL FOR SPECTRA
-------------------------------------------------------------------------------
99              R136a5     HRS    IMAGE 0.25  MIRROR-N2         NX=13          1  169S        1  1
                                                               NY=13
                                                               DELTA-X=1
                                                               DELTA-Y=1
       Comments: Time=13*13*1S=169S
-------------------------------------------------------------------------------
100             R136a5     HRS    IMAGE 2.0   MIRROR-N2         NX=22          1  968S        1  1
                                                               NY=22
                                                               DELTA-X=2
                                                               DELTA-Y=2
       Comments: Time=22*22*2S=968S
-------------------------------------------------------------------------------
101             R136a5     HRS    ACQ   2.0   MIRROR-N2         SEARCH-SIZE=3  1  1161S       1  1
                                                               LOCATE=NO
                                                               MAP=ALL-POINTS
       Comments: Time=(128*Nmap +SS2)*StepT
                 =(128*9 +3X3)*1.0S=1161S
-------------------------------------------------------------------------------
```

GHRS / 35

- **Line 2:** Here the object R136a1 was centered in the LSA. The exposure time of 102 seconds implied a STEP-TIME of 1.0 seconds, as for the initial acquisition. As we noted, what is called "R136a1" is not a single object but is a convolution of R136a1 with R136a2 because of the finite resolution of HST and the size of the LSA. An estimate of the centroid of a1+a2 was made from a pre-COSTAR WF/PC-1 image.

- **Line 3:** Here R136a1 was centered in the SSA, with SEARCH-SIZE=5 and an implied STEP-TIME of 1.0 second. The true post-COSTAR size of the SSA is 0.22 arcsec square. As for line 1, the acquisition algorithm automat-

ically determined which dwell point had the most counts and moved the SSA to that point. (The SSA ACQ/PEAKUP algorithm is the same as the LSA BRIGHT=RETURN acquisition algorithm.)

- **Line 4:** An IMAGE of R136a1 in the SSA was obtained. The values of NX, NY, DELTA-X, and DELTA-Y were chosen to fully cover the SSA with the minimum spacing between points. The time spent at each point was 1.0 seconds, as implied by the 169 second total exposure time.

- **Line 5:** This is the same as line 4 except that the object was R136a2. This implies that the telescope has been moved 0.052 arcsec north and 0.105 arcsec east, for a net motion of 0.117 arcsec, about half the size of the SSA. An IMAGE was taken to confirm the positioning.

- **Line 20:** This line obtained a ten-minute exposure on R136a2 with grating G140L centered at 1300 Å. The STEP-PATT value chosen (3) was not the default value of 5, but was selected to maximize the time on target at the cost of some uncertainty in the background. Because the object was faint and low signal-to-noise was anticipated, FP-SPLIT=NO has been chosen. Using a Side 1 spectrum element (G140L) implied a wait of about 40 minutes between lines 5 and 20 to allow one detector to be turned off and the other to be turned on and brought to a stable configuration.

- **Line 21:** Here a second spectrum centered at 1610 Å was obtained. Lines 20 and 21 together provided as much spectrum as G140L was capable of delivering.

- **Line 50:** Now the target was R136a5, implying a small motion of the telescope. The central wavelength was the same as for line 21 to eliminate a grating movement. A longer exposure of 30 minutes was needed for this fainter target. In this case the FP-SPLIT feature has been used.

- **Line 51:** Same as line 20, but for R136a5. Again, FP-SPLIT was used.

- **Line 52:** A wavelength calibration exposure obtained at the previous position for G140L.

- **Line 99:** An IMAGE of R136a5, analogous to line 5. As before, the use of MIRROR-N2 implied waiting about 40 minutes to switch Sides.

- **Line 100:** An IMAGE of R136a5 in the LSA with MIRROR-N2.

- **Line 101:** This "acquisition" at the end of the sequence of operations may seem odd, but what it achieved was a coarse image over a broader area (SEARCH-SIZE=3) than an IMAGE itself was capable of.

Each of these lines was an operation specified by the observer, and they corresponded closely to the operations performed by the instrument and the data files that were generated, as shown in Table 35.5. For example, each of the ACQuisitions, ACQ/PEAKUPs, and IMAGEs resulted in a data file, but each is also preceded by a DEFCAL. This is a DEFlection CALibration, in which an internal lamp illuminated an aperture (SC2) which the acquisition mirror then imaged onto the photocathode. Software on the spacecraft then determined where the actual image of the aperture was falling on the diodes so that the image could be properly centered. The image moved slightly due to thermal effects and the earth's

magnetic field. These DEFCALs were essential for proper operation of the GHRS, but the information they contain is rarely of use to the observer.

You will note that many, but not all, of the ACCUMs were preceded by a SPYBAL exposure. SPYBAL stands for SPectrum Y BALance, and it, like a DEFCAL, was performed to ensure proper alignment of the spectrum on the science diodes. However, a SPYBAL was an actual spectrum recorded at a selected wavelength for each grating (chosen to provide a uniform distribution of comparison lines) and it was performed each time a different grating was used for the first time. In longer programs, SPYBALs will appear about every 90 minutes of alignment time as well, in order to compensate for thermal drifts and the like. An exposure was not interrupted to insert a SPYBAL, however. Also, in some

Table 35.5: Relationship Between Proposal Lines and Files for Program 5297

Exposure Logsheet Line #	OBSMODE	Aperture	Mirror or Grating	Targname	FP_SPLIT	Central Wavelength (Å)	ROOTNAME for output file
1	DEFCAL						z2bd0101t
	ACQ	LSA		R136a1			z2bd0102t
2	DEFCAL						z2bd0103t
	ACQ/PEAKUP	LSA		R136a1			z2bd0104t
3	DEFCAL						z2bd0105t
	ACQ/PEAKUP	SSA		R136a1			z2bd0106t
4	DEFCAL						z2bd0107t
	IMAGE	SSA	N2	R136a1			z2bd0108t
5	DEFCAL						z2bd0109t
	IMAGE	SSA	N2	R136a2			z2bd010at
20	SPYBAL	SC2	G140L	WAVE	NO	1414.899	z2bd010bt
	ACCUM	SSA	G140L	R136a2	NO	1304.579	z2bd010ct
21	ACCUM	SSA	G140L	R136a2	NO	1608.027	z2bd010dt
50	SPYBAL	SC2	G140L	WAVE	NO	1414.903	z2bd010et
	ACCUM	SSA	G140L	R136a5	FOUR	1598.548	z2bd010ft
51	SPYBAL	SC2	G140L	WAVE	NO	1414.728	z2bd010gt
	ACCUM	SSA	G140L	R136a5	FOUR	1294.922	z2bd010ht
52	ACCUM	SC2	G140L	WAVE	NO	1313.492	z2bd010it
99	DEFCAL						z2bd010jt
	IMAGE	SSA	N2	R136a5			z2bd010kt
100	DEFCAL						z2bd010lt
	IMAGE	SSA	N2	R136a5			z2bd010mt
101	DEFCAL						z2bd010nt
	ACQ	LSA	N2	R136a5			z2bd010ot

cases the PI suppressed SPYBALs in order to keep the carrousel from moving during a sequence of observations.

Table 35.6 shows some of the different kinds of files generated in this program for the different operations that resulted from the Exposure Logsheet. The entries are Exposure Logsheet line numbers. The lines at the bottom of the table show what kinds of files are generated for the different kinds of operations. For example, all observations generate log files with suffixes `.shh`, `.ulh`, and `.trl`. The "*" next to the acquisition files for lines 1 and 3 indicate that these observations also generate `.d1h` files and the corresponding `.q1h` data quality files. `.d1h` files are generated for Return-to-Brightest (RTB) acquisitions and SSA peakups (which use the RTB algorithm). Notice that LSA peakups do not generate `.d1h` files; nor would an LSA acquisition that does not use the RTB algorithm.

Table 35.6: Breakdown of Files by Proposal Line Number for Program 5297

Target	DEFCAL	ACQ	ACQ/PEAKUP	IMAGE	(MAP)	SPYBAL	WAVECAL	ACCUM	FP-SPLIT
R136a1	1	1*							
	2		2						
	3		3*						
	4			4					
R136a2	5			5					
						20		20	
								21	
R136a5						50			50
						51			51
							52		
	99			99					
	100			100					
	101				101				
Header File Suffixes	Log files: .shh, .ulh, .trl.			All log files, plus *raw data files*: .d0h, .q0h, .x0h, .xqh		All log files, all raw data files, plus *calibrated files*: .c0h,.c1h,.c2h, .c3h, .c4h, .c5h, .cqh			

35.5 Assessing GHRS Acquisitions

There are no jitter files available for the example we just discussed, program 5297, and so in this section we show another case drawn from *GHRS ISR* 079. We will return to program 5297 when we discuss the science assessments.

35.5.1 Understanding GHRS Acquisitions

Most GHRS targets were point sources (stars) and were acquired with the normal on-board target acquisition mode. Other types of targets were acquired either by blind offsetting from a nearby star, with an FOS acquisition, or offsetting from coordinates determined from a WFPC2 image. FOS acquisitions and WFPC2 offsets were discussed in the *GHRS Instrument Handbook*. The LSA is larger than the GHRS PSF, and using a blind offset to position a target into the LSA could introduce a wavelength shift in the data. Each OnBoard Acquisition is composed of up to eight steps, some of which are optional. The first and last steps always occur:

1. Initialization.

2. Deflection calibration (DEFCAL).

3. Target Search: 3 x 3 (or 5 x 5) spiral search.

   Search stopped when within BRIGHT/FAINT limits or pointing returned to dwell scan position with most counts.

4. Locate: center the target in the LSA.

   - Y balance.
   - Coarse X balance.
   - Fine X balance.

5. Peakup in SSA.

6. Blind offset.

7. Post-offset peakup.

8. Final Flux measurement (ZFLUXM).

A DEFCAL is an internal calibration that used the calibration lamps to locate the spectrum on the photocathode. The location of the spectrum on the photocathode depended on thermal and geomagnetic factors. This spectrum was not saved, but the location of the spectrum on the photocathode was compared to coordinates stored in the onboard data base. An offset was determined and used by the onboard computer during the subsequent Search and Locate phases of the LSA ACQ. A DEFCAL observation only generated log files (`.shp`, `.udl`), not science data.

The target search phase slewed the telescope in a spiral search pattern. At each dwell point, the flux in the aperture was measured. All targets were first acquired using the LSA because the SSA is so small. (Note, however, that the SSA

GHRS / 35

ACQ/PEAKUP algorithm is the same as that used for the LSA Return-to-Brightest (RTB) target search.) The target is assumed to be somewhere within the LSA 3 x 3 (or 5 x 5) spiral search pattern. The separation between dwell points during the LSA search was 1.52 arcsec on the sky (for an SSA ACQ/PEAKUP 5 x 5 spiral search, the separation was 0.052 arcsec). Figure 35.6 displays normal LSA 3 x 3 and SSA 5 x 5 spiral search patterns (from OMS jitter files). The spiral searches are plotted in V2,V3 space.

Most LSA acquisitions from mid-1993 on specified the BRIGHT=RETURN (RTB) option. This feature automatically returned the spacecraft pointing to the dwell position with the highest total counts. Since a 32-bit onboard register was used to store and compare the measured counts, overflow was not a problem. Alternatively, BRIGHT and FAINT limits may have been specified for the spiral search. For this case, a 16-bit register was used to store the measured counts and wrapping of the counter could result if a diode exceeded about 65,000 counts. The spacecraft pointing stopped at the first dwell position that had a flux between the selected limits. If no dwell position was found to meet the requirements, the spacecraft pointing remained at the last position.

The locate phase consisted of y balance, coarse-x balance, and fine-x balance. This process determined the location of the target in the aperture, and commanded the telescope to slew to position the target in the center of the aperture. The y balance routine compared the counts in the upper and lower half of the aperture and used single step offsets to find the optimum centering of the target. The x balance algorithm computed a coarse offset to place the peak of the target on one of the two center acquisition diodes. The peak was then single stepped toward the other center diode until the peak count was sensed on the second diode. Offsets in y and x were computed and used to slew the telescope. Sometimes this phase helped pull targets into the aperture that were not well-centered by the search.

A small angle maneuver was performed to move the target to the SSA. The LSA shutter is closed when the SSA is used. An SSA ACQ/PEAKUP was used to perform the centering in the SSA. In practice, the SSA ACQ/PEAKUP is identical to the LSA RTB except the SSA was used and the Locate and balance phases are not performed. The pointing was returned to the dwell position with the most counts. For the SSA example in Figure 35.6, the target was found at the first dwell position. The offset in the return path to the first dwell position was due to a velocity aberration correction.

The flux was summed over the eight target acquisition diodes after the completion of the locate phase (and any additional peakups); this value was written into the keyword ZFLUXM, available in the Unique Data Log (.udl or .ulh) and the target acquisition science header, if one was generated. Executing the following IRAF command returns the flux value:

```
cl> hsel z2il0102t.ulh $I,zfluxm yes
z2il0102t.ulh   16092
```

Figure 35.6: Normal LSA 3 x 3 and SSA 5 x 5 Spiral Search Patterns (OMS Obs Logs)
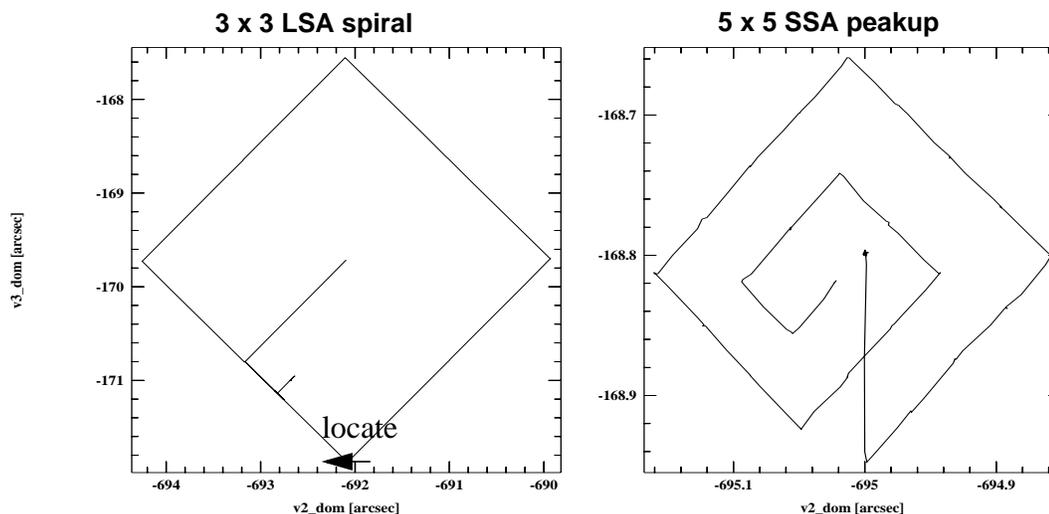
35.5.2 Return-to-Brightest

Not every GHRS target acquisition method produces data to examine. After the acquisition, if specified in the proposal, IMAGEs or MAPs will create science (.d0h) files. The Return-to-Brightest (RTB) acquisitions, implemented in 1993, record the flux at each dwell position. At first (April 27, 1993, SOGS Build 31.1) this information was dumped only to the trailer files (where the first dwell position is numbered 00) but eventually .d1h files were created to contain this data. See *GHRS ISR* 079 for more details.

Figure 35.7 shows examples of contour plots for two LSA ACQ .d1h/.d1d pseudo-images. The target was found at the first dwell position for the first example, while for the second example, the target was found at dwell position 6. For both examples, the spacecraft pointing was returned to the dwell position with the maximum flux.

During the spiral search, the telescope slews were parallel to the GHRS *x* and *y* detector coordinates. The first slew in the sequence is in the positive *x* direction. The next slew is in the negative *y* direction, followed by a slew in the negative *x* direction. All subsequent slews are performed to complete the spiral pattern. Figure 35.6 displays the spiral search geometry and the corresponding detected counts at each dwell position for the two LSA ACQs presented in Figure 35.7. Figure 35.8 displays two examples of the SSA 5 x 5 spiral search. The upper search pattern found the target (a Cepheid binary star) at dwell position 1. The lower search pattern found the target (a B0-B2III-I star) on the edge of the spiral pattern at position 19. The spectra for this program were fine, indicating the target was found and subsequently moved to the center of the aperture.

Figure 35.7: LSA 3 x 3 Spiral Search Contour Plots
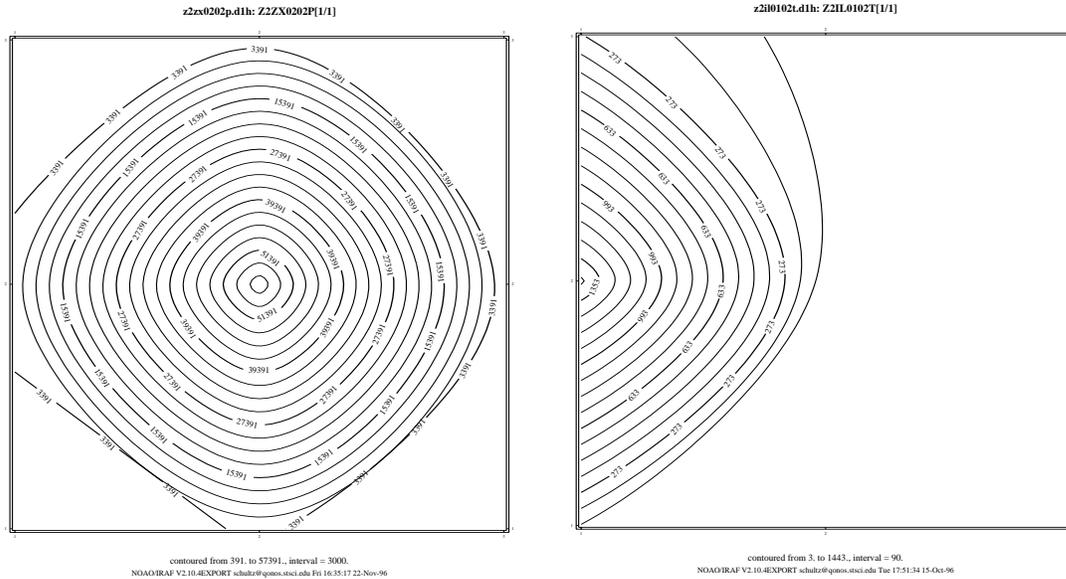
Figure 35.8: Examples of SSA 5 x 5 Spiral Search Patterns in Aperture Space (X and Y)

Dwell Positions						Detected Counts				
21	22	23	24	25		481	956	1211	1095	643
20	7	8	9	10		1384	3312	3242	2746	803
19	6	1	2	11		2701	5246	5366	4974	1036
18	5	4	3	12		2707	4993	5104	4827	950
17	16	15	14	13		2311	4300	4391	4108	673
21	22	23	24	25		49	12	3	4	2
20	7	8	9	10		516	45	20	23	3
19	6	1	2	11		1202	146	22	7	4
18	5	4	3	12		1187	162	64	13	7
17	16	15	14	13		673	158	37	14	7

35.5.3 OMS Products and Guiding

The guide stars used for pointing control during an observation can be found in the Observatory Management System (OMS) observation log header and in the SHP (.shd/.shh) header file. The OMS data header file (.cmh or .jih) contains information about the observation. The header is divided into groups of keywords that deal with a particular topic (e.g., spacecraft data, background light, pointing

control data, line of sight jitter summary). A more complete description of OMS products can be found in Appendix C of Volume I.

There were three commanded guiding modes: FINE LOCK, FINE LOCK/GYRO, GYRO. If the acquisition of the second guide star failed, the spacecraft guidance could drop from FINE LOCK to FINE LOCK/GYRO or even to GYRO which could result in a target rolling out of an aperture. It must be noted that single guide star guiding is acceptable. A GHRS target could remain in the SSA even over multi-orbit exposures. The guiding at the time of the observation can be found in the OMS header keyword GUIDEACT.

```
cl> hsel z2il0102j.cmh $I guideact yes
z2il0102j.cmh    "FINE LOCK"
```

You can check the OMS header keywords to verify that the guiding mode was the one requested. Archive users should check the guiding mode to verify that no changes occurred during the observation. If you suspect that a target rolled out of the aperture during an exposure, you can check the counts in each group of the raw science data.

A "type 51" slew was used to track moving targets (planets, satellites, asteroids, comets). Observations were scheduled with FINE LOCK acquisition, i.e., with two or one guide star. Usually, a guide star pair stayed within the pickle during the entire set of observations (obset), but if two guide stars were not available, a single guide star may have been used. This assumes the drift was small or perhaps that the observer stated the roll was not important for the program. An option during scheduling was to drop from FGS control to GYRO control when the guide stars moved out of the pickle. Guide star handoffs (which are not a simple dropping of the guide stars to GYRO control) could affect the guiding and may be noticeable when the jitter ball (V3 vs. V2) is plotted.

On January 19, 1996, there was a failure in tape recorder #2. This recorder had been used for recording engineering data for subsequent playback to the ground. The failure was permanent, causing engineering data to be obtained only during real-time TDRSS availability (typically 80% or so during each orbit). Consequently, there are gaps in the engineering data and gaps in the OMS products.

Displaying Spacecraft Motion

IRAF/STSDAS tools are available to read the OMS tables and graphically display the spacecraft motion during an observation. The package of tools to work with tables is called **ttools**. For most observers, the .cmi or .jit STSDAS table will contain all the information needed to determine if there was motion or jitter during an observation.

For example, plotting "v2_dom" versus "v3_dom" will generate a plot that looks like a ball of string, which is why it is sometimes called the *jitter ball*. The same plot for a target acquisition will display the spiral search and locate phase that occurred. See fifth page of paper product example.

```
st> sgraph "z2o40402j.cmi v2_dom v3_dom"
```

After entering the plotting command, the command will plot the data in the graphics window and auto scale using the minimum and maximum data values. The plot may be misleading due to the auto scaling of the axis units, so be careful.

35.5.4 Acquisition Anomalies

Status Codes

If a target was not in the aperture, the acquisition may have failed and generated an error message also known as a Status Buffer Message, or the acquisition software may have centered on noise or a background object. All of the flight software status messages have their corresponding numbers placed into the keyword FINCODE. The FINCODE value for each data group are stored in the UDL (.uld/.ulh) file. The STSDAS task **obsum** can be used to display the individual group FINCODE values. The FINCODE value of the last data group is extracted and written to the science header (.d0d/.d0h). FINCODE=102 is a normal end of an observation. Any other value of the keyword indicates a possible problem, see Table 37.7.

The GHRS Carrousel

All acquisition mirrors and gratings were mounted on a rotating carrousel. There were times when the carrousel failed to lock into position if a target acquisition took longer than expected to complete, due to carrousel movement. The subsequent observations may have been affected and exposure times shortened (FINCODE=106).

Figure 35.9 shows an example of a SSA ACQ/PEAKUP that started late and completed later than the expected time as specified by the SMS (Science Mission Specification). A guide star re-acquisition took longer to complete than normal and there were two loss of locks before the start of the SSA ACQ/PEAKUP 5 x 5 spiral search. The acquisition did not complete normally. The time window used by OMS to extract the telemetry was for the originally scheduled time. The OMS .jit table contains part of an unrelated slew as well as the start of the spiral search pattern. For this unique case, a request was sent to the STScI help desk (help@stsci.edu) for a new OMS observation log. The software engineers determined that the OMS software could not handle this special case, moving the start time of the observation to extract the spiral search pattern information. OMS software was to be modified to handle these special cases. Currently, the anomalous observation log is in the archive.

Figure 35.9: SSA ACQ/PEAKUP Started Late Due to Long Guide Star Re-acquisition
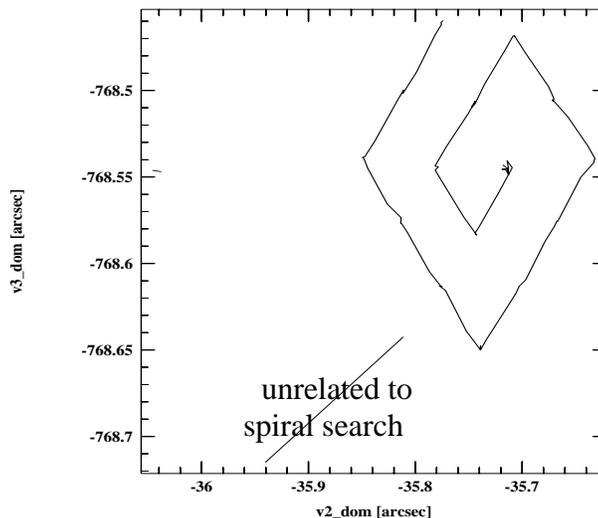
False Fine Lock

A false lock, an anomaly that is not specific to GHRS, was simply a failure of an FGS (Fine Guidance Sensor) to lock onto the null point of the S-curve for the acquired guide star. Instead, it locked onto noise, onto a fake fine error signal at the edge of the FGS interference field of view, or onto a very weak S-curve. These sources of noise may be influenced by:

- Large noise in the FGS of faint stars.
- Star fainter than FGS magnitude limit due to magnitude error.
- Large star magnitude error of relatively bright star.
- Double star.
- Mask misalignment.

Figure 35.6 shows an example of a GHRS spiral search target acquisition while in a normal fine lock condition. The path indicates a very smooth travel during the slewing maneuver. Figure 35.10, on the other hand, exhibits a very ragged and irregular travel, a false fine lock.

The potential impacts of a false lock may include:

- Prolonged acquisitions.
- Loss of lock.
- Positioning errors.
- Loss of science in subsequent orbits.

It is also possible that a roll in the spacecraft could be introduced, causing the target to drift toward the edge of an aperture. Positioning errors, occurring as a result of an undetectable false lock, could result in a misinterpretation of the spacecraft attitude error. When corrected, the end result would be a real HST

pointing error, virtually impossible to identify without examining the data. However, such errors will not exceed 2.5 arcsec due to the maximum allowed drift. Loss of science in subsequent orbits could occur in cases where a re-acquisition results in a good, true lock following a false lock orbit. In a case such as this, it is entirely possible that the target would not be found in the aperture upon successful re-acquisition.

Prolonged acquisitions could delay subsequent science activities or result in the loss of science altogether. False locks, while possible, were not frequent. During 1995, false locks represented only 0.7% of the total number of acquisitions with HST. Unfortunately, however, most of the factors contributing to false locks were not preventable or fixable.

Figure 35.10: Example of False Fine Lock
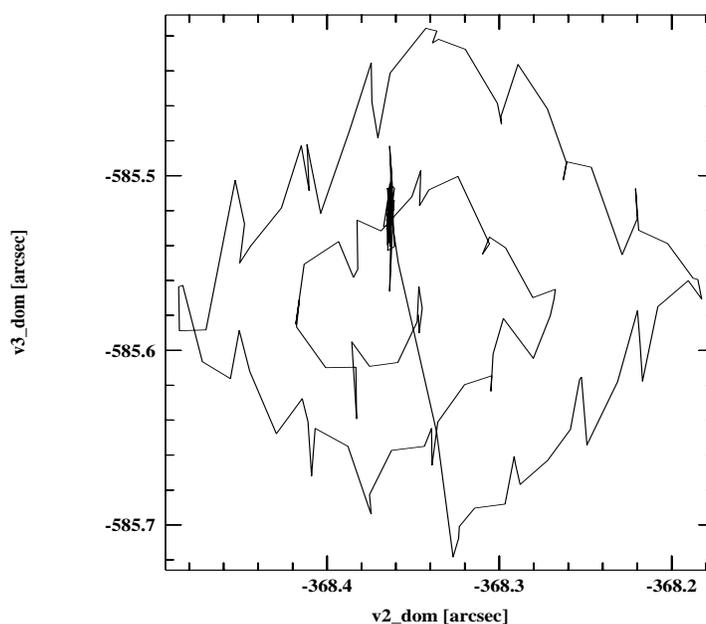
Loss of Lock

During a loss of lock, spacecraft motion can be large (>0.2 arcsec). FGS control of the spacecraft is given up, and the FGSs execute a sequence of maneuvers to re-acquire the guide stars (sort of an on-the-spot guide star re-acquisition). During a loss of lock recovery, the spacecraft Take Data Flag (TDF) was set to "no." The function of the TDF is to provide a simple reference for the science instruments to query about the stability of the spacecraft pointing. During a loss of lock, the GHRS stops acquiring data, but the LSA shutter does not close. (If an observation is taken in the SSA, the LSA shutter is already closed.) Once fine lock pointing control has been re-established, the TDF was set to "yes."

A loss of lock did not necessarily result in the loss of science if the guide stars could be re-acquired and the observation completed before the next scheduled activity. However, this was unlikely for most GHRS observations and a delay usually forced an observation to time-out.

Suspect Spoiler Guide Stars

The Guide Star Catalog (GSC) was created with entries down to 15th magnitude from digitized photographic Schmidt plates. Suitable guide stars were selected for each observation by the Guide Star Selection System (GSSS) to be used for fine pointing and guiding of HST. Most (>98%) guide star acquisitions and guiding were successful. The main source of problems was very close binary stars that were unresolved on the Schmidt plate, causing FGS fine lock failures. There were infrequent failures (1 to 3 a year) due to misclassification of an object in the GSC (blend of two stars or a faint circular galaxy).

A spoiler star could result in acquiring the wrong star with the FGS and the target would not be in the aperture due to this mispointing of HST. This could also result in a shift in the pointing following a guide star re-acquisition when the scheduled star was acquired. The target could roll in and out of the aperture resulting in changes in the counts between observations obtained during different orbits.

The differences between the predicted (PREDGSEP) and the actual (ACTGSSEP) measured separation between Guide Stars can be used to test for a spoiler star. For the following example, the science observation z2zx0207 started with the target in the aperture, was halted for earth occultation, and the observation completed on the following orbit. However, the guide star re-acquisition (REACQ) locked up on a spoiler star. The target was not centered in the aperture during the remaining exposure time. Observation z2zx0208 was noise. Observation z2zx0209 was halted for earth occultation and upon the REACQ, the target was moved into the aperture. For this observation, the first part of the exposure resulted in noise, while for the second orbit, the target was in the aperture.

```
cl> hedit z2zx020*.jih PREDGSEP,ACTGSSEP .
z2zx0204j.jih,PREDGSEP = 1328.046 <-- SSA ACQ/PEAKUP
z2zx0204j.jih,ACTGSSEP = 1326.466
z2zx0205j.jih,PREDGSEP = /         <-- SPYBAL
z2zx0205j.jih,ACTGSSEP = /
z2zx0206j.jih,PREDGSEP = /         <-- WAVECAL
z2zx0206j.jih,ACTGSSEP = /

z2zx0207j.jih,PREDGSEP = 1328.046 <-- first science obs.
z2zx0207j.jih,ACTGSSEP = 1328.019     guide star REACQ
z2zx0208j.jih,PREDGSEP = 1328.046     wrong pointing
z2zx0208j.jih,ACTGSSEP = 1328.019
                                  <-- guide star REACQ
z2zx0209j.jih,PREDGSEP = 1328.046 <-- correct pointing
z2zx0209j.jih,ACTGSSEP = 1326.475

z2zx020aj.jih,PREDGSEP = 1328.046 <-- no further problems
```

Figure 35.11 presents the overplotting of the pointing for each observation (v2_dom versus seconds). This shows the change in HST pointing for this program. An HST Observation Problem Report (HOPR) was filed by the PI and the observations were repeated using different guide stars.

GHRS / 35

Figure 35.11: Jump in HST Pointing due to a Spoiler Guide Star
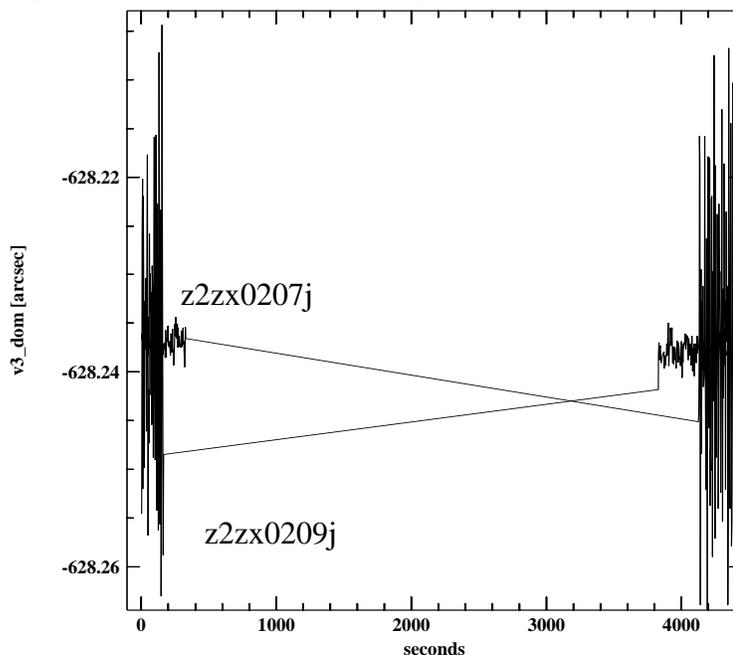
Single FGS Mode

On February 12, 1993, FGS 2 was temporarily turned off. Some observations shortly thereafter were executed with guiding from a single FGS. Later, a guide star acquisition could fail, resulting in use of a single guide star. For GHRS this could become a problem if the observation was being done in the SSA because the star could roll out of the aperture, as seen by a decrease in counts in the data. At some point, it was decided that single FGS mode was perfectly all right for LSA observations because the amount of expected roll wouldn't take the star out of the LSA, but it was not to be done for SSA observations. If you see a large drop-off in counts with SSA data, one explanation could be use of a single FGS.

Recentering Events

During a recentering event, pointing control of the telescope by the Fine Guidance Sensors was paused until the spacecraft motion excursions became small enough that FGS guiding could be resumed. Recenterings typically lasted a few seconds, the total spacecraft motion was less than 0.1 to 0.2 arcsec, and after the recentering was finished the pointing position should be the same as before the recentering (to within ~7 milliarcsec).

During a recentering event, the GHRS continued to acquire data. The PI (or archival researcher) is the only one who can determine whether or not a recentering event affected the target acquisition or data. Careful comparison of the time of recentering and the time during which the individual exposures were made can be obtained from the OMS Obs Log. Plotting the OMS "recenter" column versus "seconds" will indicate whether or not a recentering event occurred. The recentering event may have occurred during a time when data were being read out, in which case there is no problem. If the recentering was short compared to the exposure time of a given group of data, it probably had no effect on the data.

35.5.5 Images and Maps

Location of Targets Within the SSA

The location of a single star within the Small Science Aperture cannot be determined with an SSA image.[3]

Orientation

To determine the orientation of the GHRS apertures on the sky, you need the value of the PA_APER keyword in the SHP header (.shh). This number is the position angle of the $+y$ axis of GHRS measured from north through east. The $+y$ axis is the direction from the LSA to the SSA. The $+x$ axis is the direction of increasing wavelength.

The trick is to figure out how to display your image so that it has the same directional sense as Figure 34.1. The problem is that tasks typically display $+y$ up and $+x$ to the right but what is needed is $+y$ down and $+x$ to the right. In IRAF this would be something like:

```
cl> display test.hhh[*,-*].
```

Once you have this orientation then you apply the offset angle (PA_APER) to get northeast lined up.

You should also know that RA_APER1 and DECAPER1 are the predicted RA and Dec of the center of the aperture used, for the beginning of the observation. GHRS PEAKUPs effectively re-zero the coordinate system so one would need to use the OBS logs (jitter files) to get the actual pointing.

35.6 Assessing GHRS Science Data

35.6.1 Examining the ACCUMs

Here we return to our examination of program 5297. There are many, many data files for this program, but to start you would probably like to look at the reduced spectra, and then go back to understand how they got the way they are and how the calibrations might be improved.

The reduced wavelength and flux files have suffixes of .c0h and .c1h (for a complete explanation of file suffixes, see Table 35.1). GHRS observations have separate files for wavelengths because they are on a non-linear scale; i.e., there is a distinct wavelength associated with each output data point, and those wavelengths are not necessarily evenly spaced. For a quick look, we need to use **fwplot**, a task in **stsdas**. The **fwplot** task will display flux versus wavelength and it can find the right wavelength file automatically (unless you changed its name), so we use the following to examine the first group of a repeat observation containing R136a2:

---

3. Malumuth, E., in *Calibrating HST: Post Servicing Mission*, 1995, pp. 227.- 241.

```
cl>fwplot z2bd010ct.c1h
```

This produces the plot shown in Figure 35.12. Plots of the other spectra can be obtained by changing the rootname. **fwplot** can also plot error bars and the like, which we will explain in a moment.

Figure 35.12: Flux vs. Wavelength for R136a2
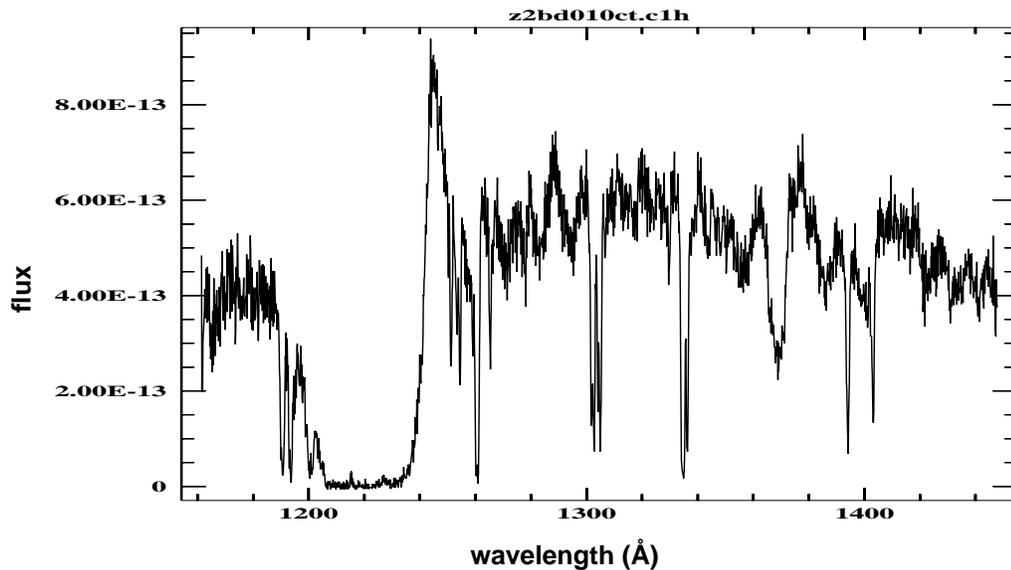
Now that we have seen the spectrum, let's understand better why it looks the way it does. First let's look at counts versus pixel to get a sense of the quality of the observations. Since there are three repeats in this observation, we will look at all four of the corresponding groups of data. We must create a listing of the file names with the group numbers attached, so we use **grlist** and redirect the output to a file. Then we stack the spectra using **sgraph**.

```
cl> grlist z2bd010ct.d0h - > lis
cl> sgraph @lis st+
```

Note how few counts we have at the short-wavelength (left) end (Figure 35.14). We can see the effect of this in the reduced spectrum. If we use **fwplot** to plot the a small part of the reduced spectrum with its errors (Figure 35.13) we get essentially the same information in a more compact form, and we can see that the errors are the statistical ones calculated from raw counts.

Figure 35.13: Reduced Spectrum of R136a2 with Error Bars
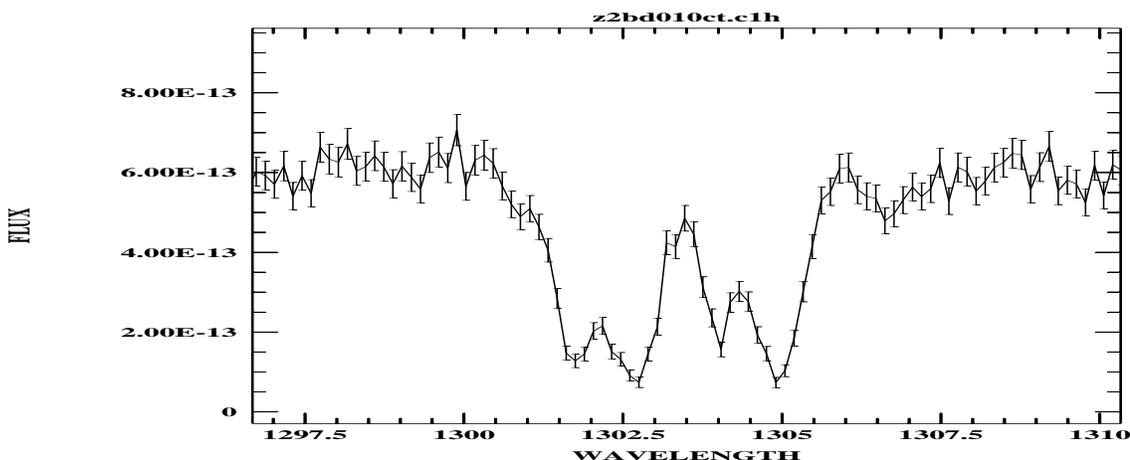
Figure 35.14: Raw Counts vs. Diode Number for Four Spectra in z2bd010c
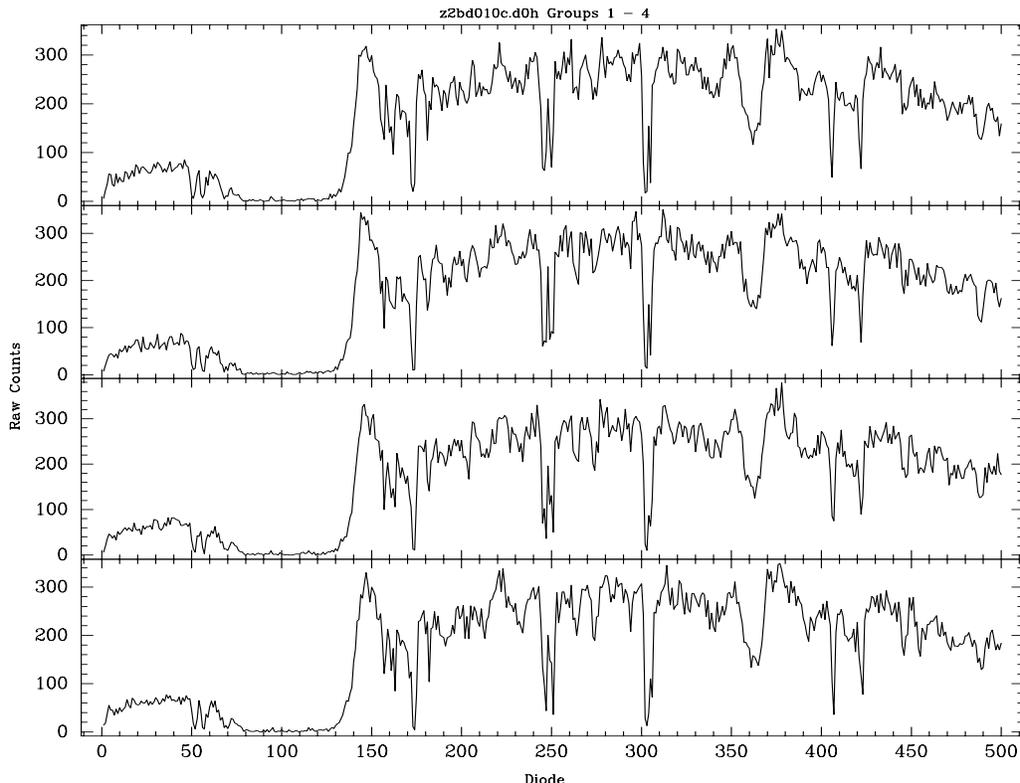
The reduced spectrum in Figure 35.13 has a wavelength scale that is the default from the pipeline reduction system. There are two ways to improve on this, either by using a wavelength calibration exposure or by using a SPYBAL. For example, we can take the SPYBAL z2bd010bt and process it with **waveoff**. The SPYBAL exposure is shown in Figure 35.15, and the net result is that we compute a wavelength offset of 0.708 Å. See the help file for **waveoff** for examples of how to use it.

Figure 35.15: SPYBAL Exposure z2bd010bt
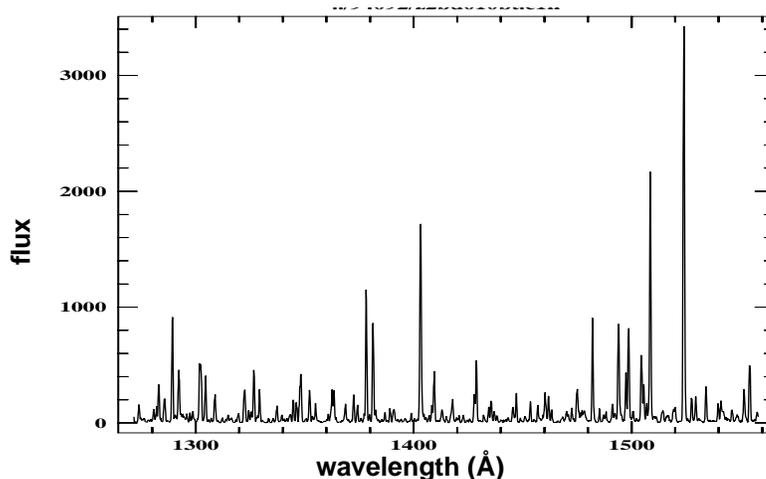
35.6.2 Putting FP-SPLITs Back Together

Specifying FP-SPLIT=FOUR (or any value except "NO") on the exposure logsheet resulted in small motions of the grating carrousel between individual subexposures. This moved the source spectrum slightly on the diode array, making it possible to distinguish fixed-pattern noise from true spectrum features and to correct for that pattern.

The most sophisticated use of FP-SPLITs involved iteration to determine a function representing the fixed-pattern noise. This could be augmented by obtaining spectra with larger discrete motions of the grating as well.[4] Here we describe the simplest use of FP-SPLITs for achieving more modest gains in signal-to-noise. This involves simply realigning the individual subexposures so that spectrum features line up, and then adding up the spectra.

The best way to align the subexposures is by cross-correlating them against the first exposure obtained. When there is not enough signal-to-noise for that, it is possible to determine the shift to apply from knowledge of instrument parameters, but the factors that limit the quality of the wavelength scale (see "Wavelength Data Quality" on page 37-26) make that method inferior to cross-correlation.

The cross-correlations to restore FP-SPLITs are done in **stsdas** with the **specalign** task. An example of raw data produced by an FP-SPLIT is shown in Figure 35.16.

---

4. See the discussion by Cardelli et al,. 1993, *ApJ*., 402, L17; Cardelli and Ebbets 1994, in *Calibrating Hubble Space Telescope*, J.C. Blades and A.J. Osmer eds., (Baltimore: STScI), 322.

Figure 35.16: Raw FP-SPLIT Observations for R136a5
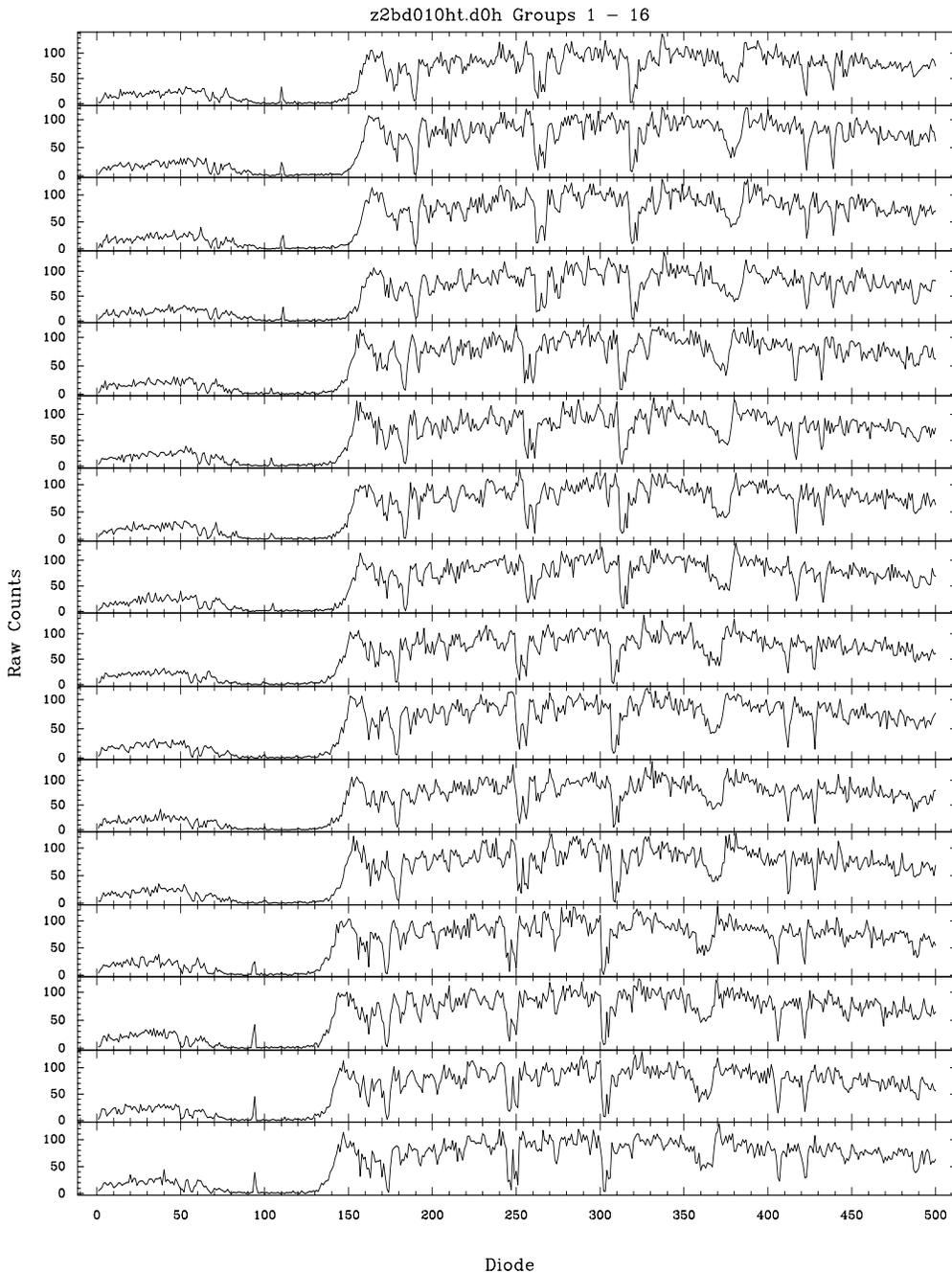
Note that there are four groups of four (due to STEPPATT=3), with a shift in wavelength after every fourth spectrum (due to the FP-SPLIT setting). The result of shifting and adding all the subexposures for R136a5 is shown in Figure 35.17 using **sgraph** to show that there are more pixels in the combined spectrum than in the output of the pipeline software.

Figure 35.17: Summed Spectrum for R136a5
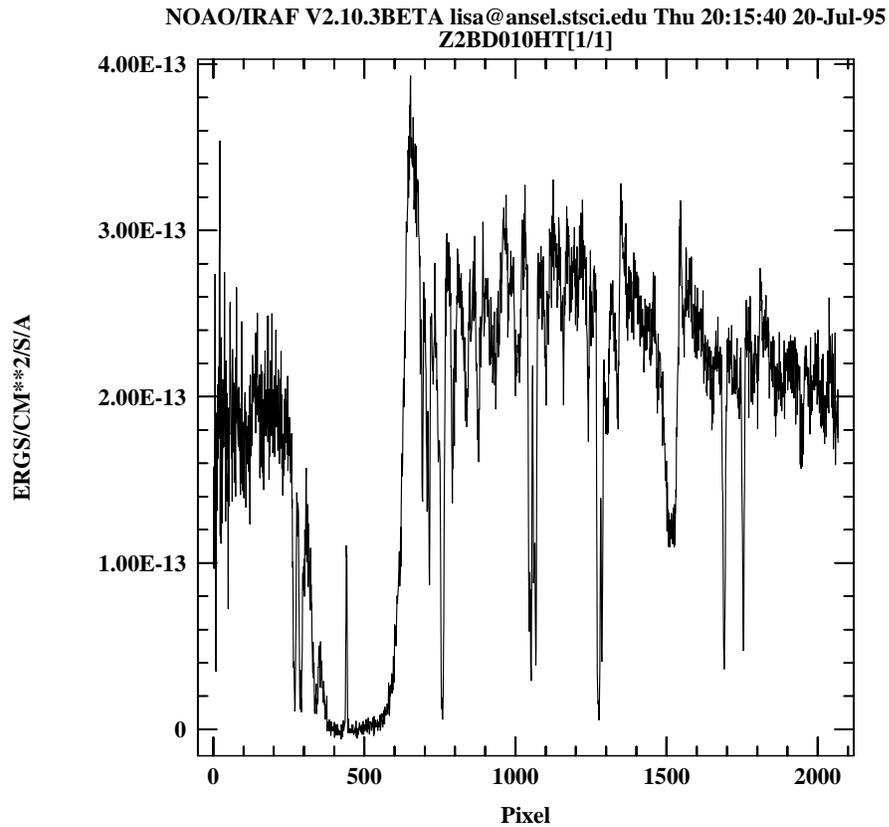
35.7 RAPID Mode (and a Little About Spatial Scans)

RAPID mode was used relatively rarely, but it had some unique capabilities. There are also some unique problems that arise in treating the resultant data.

Proposal 5745 was a calibration test designed to map out the central portion of the PSF as presented to the GHRS apertures by COSTAR. This particular test made use of a spatial scan to map out the PSF while collecting data in RAPID mode.

35.7.1 The Exposure Logsheet

An abridged version of the Phase II Proposal for 5745 is shown in Figure 35.18. Here are some notes to go with individual lines of the Exposure Logsheet:

- **Line 10:** Sk–65°21 was acquired with an ONBOARD ACQ using MIRROR-N1.

- **Line 15:** A confirmation IMAGE was taken as a sanity check for this program. In general, an IMAGE was unnecessary.

GHRS / 35

Figure 35.18: Exposure Logsheet for Program 5745

EXPOSURE LOGSHEET   ID = 5745   [4]

1	2	3	4	5	6	7	8	9	10	11	12	13	14	15
Line Number / Seq Name	Target Name	Instr Config	Oper. Mode	Aper or FOV	Spectral Element	Central Waveln.	Optional Parameters		Num Exp	Time Rel. Time	S/N Time	Flx Ref	Pr Pr	Special Requirements
10	SK-65D21	HRS	ACQ		MIRROR-N1		SEARCH-SIZE=5 BRIGHT=RETURN		1	25S		1		ONBOARD ACQ FOR 15 -20 CYCLE 4 / 10-40
Comments: STEPTIME=1.0S EXPECT APPROX. 2800 COUNTS/S TARGET IS IN CVZ														
15	SK-65D21	HRS	IMAGE		MIRROR-N1	2.0	NX=16 NY=16 DELTA-X=4 DELTA-Y=4		1	256S		1		
Comments: STEPTIME=1.0S														
20	SK-65D21	HRS	ACQ/ PEAKUP		MIRROR-N1	0.25	SEARCH-SIZE=5		1	25S		1		ONBOARD ACQ FOR 25
Comments: STEPTIME=1.0S														
25	SK-65D21	HRS	ACQ/ PEAKUP		MIRROR-N1	0.25	SEARCH-SIZE=5		1	25S		1		ONBOARD ACQ FOR 40
Comments: STEPTIME=1.0S														
40	SK-65D21	HRS	RAPID		G140L	1400	SAMPLE-TIME=1.0	1	1	112.5M		1		SPATIAL SCAN SINGLE-EXP
Comments: 15X15 GRID WITH 0.053 ARC SEC SPACING EXPTIME AT EACH DWELL POINT=30S														

Scan Paramters Form   Proposal ID: 5745   [5]

```
Data ID: 1
Exposure Logsheet lines: 40

FGS Scan:                         DWELL     Dwell Only: dwell points/line:  15    Seconds per dwell:                15
Scan width (arc-secs):           0.7420     Scan length (arc-secs):       0.7420  Angle between sides (degrees):    30.00
Number of lines:                    15      Scan rate (arc-sec/sec):      0.0000  PA of first scan line (degrees): 270.00
Scan frame (CEL or S/C):           S/C      Length Offset (arc-sec):      0.3710  Width Offset (arc-sec):           90.000
                                                                                                                    0.3710
```

- • The geometry of the spatial scan is shown in Figure 35.19. The **splot** display shows the relative orientations of the GHRS *x*, *y* and HST V2-V3 coordinate systems. Data points are delta distances in units of arcseconds.

Figure 35.19: Geometry of a Spatial Scan

z2i3010aj.cmi
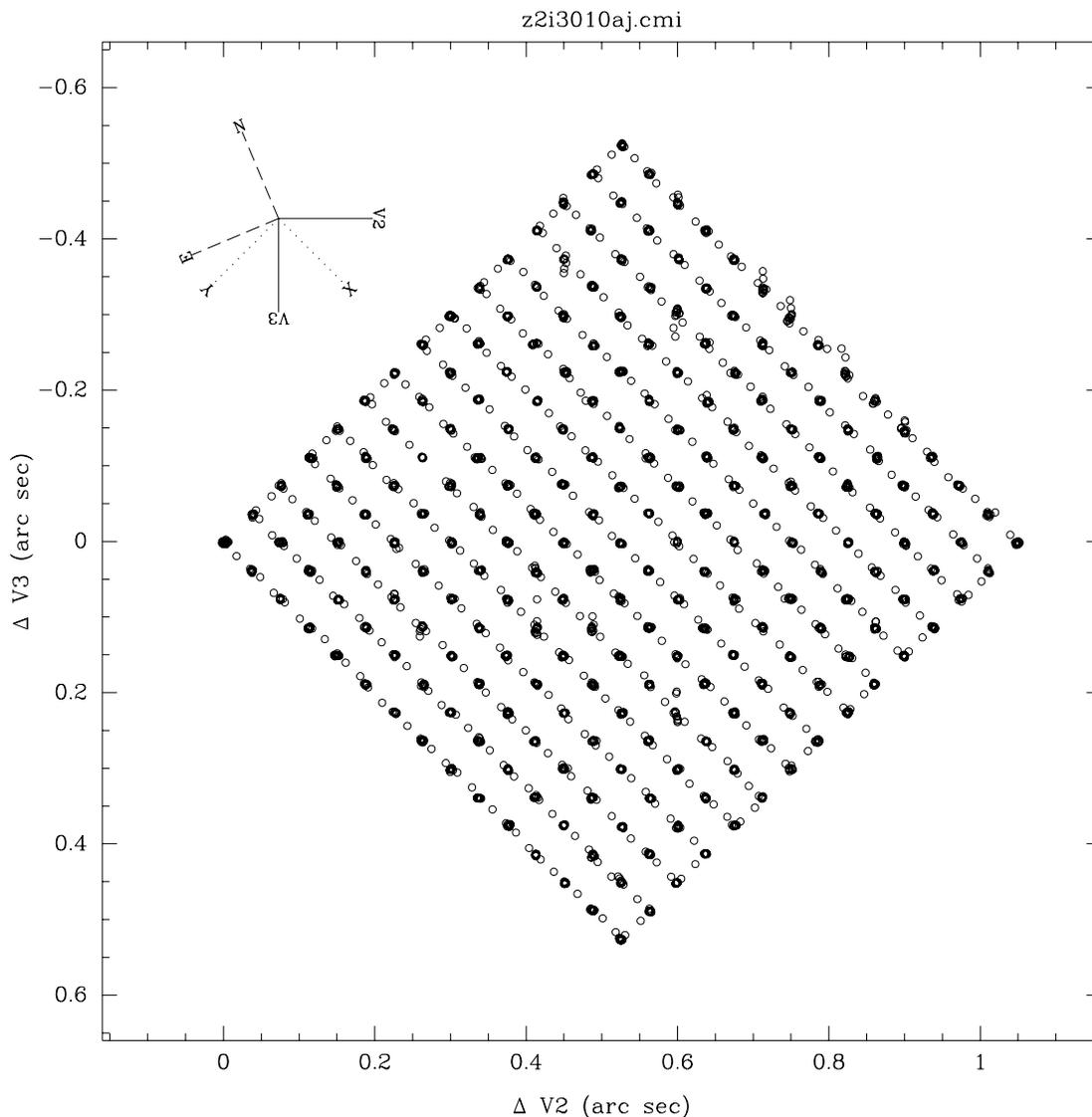
- • **Line 20:** Sk–65°21 was moved to the SSA using an ACQ/PEAKUP. The STEP-TIME was increased to compensate for the reduced throughput of the SSA relative to the LSA and to increase the signal-to-noise for the PEAKUP algorithm.

- • **Line 25:** Another ACQ/PEAKUP. Again this is an exception rather than the rule for SSA ACQ/PEAKUPs (except when using MIRROR-A1).

- • **Line 40:** This is the line where the spectra were obtained. A RAPID of 112.5 minute duration with a SAMPLE-TIME of 1.0 seconds was specified. We expected to get about 6750 individual spectra from this observation.

- **Spatial Scan:** The spatial scan specified a dwell scan that was 15 dwell points by 15 dwell points in extent. The spacing between dwell points was 0.053 arc seconds (about two deflection steps). The time spent at each dwell point was 30 seconds. Note that the total number of spectra was 30 one-second exposures, times 15 dwell points, times another 15 dwell points in the other direction, for a total of 6750.

35.7.2 Examining the RAPID Data

First let's look to see how many individual spectra we have:

```
cl> imhead ../data/z2i3010at.d0h,../data/z2i3010at.c1h l-
../data/z2i3010at.d0h[1/9024][500][real]: Z2I3010AT[1/9024]
../data/z2i3010at.c1h[1/9021][500][real]: Z2I3010AT[1/9021]
```

The **imheader** task shows that we have many more spectra than expected. Further investigation turned up the fact that ten seconds was allocated for the slew from dwell point to dwell point. So we ended up having an extra ten seconds for each slew. Not all of these extra spectra are useful since the telescope was actually moving, but we ended up getting about 35 seconds per dwell point instead of the anticipated 30 seconds. The **imheader** output also shows that there are three less spectra in the calibrated output than in the raw data. Keep in mind that since there is no substepping or FP-SPLITs possible when using RAPID mode, that a single raw spectrum maps to a single calibrated spectrum. (Contrast this with a standard ACCUM with the default STEP-PATT: the raw data would contain six individual spectra—four substeps and two background spectra—which would be merged into a single calibrated spectrum.) In the case of RAPID mode, the first two readouts were generated during a hysteresis sequence that preceded every observation, and the last readout was produced by a final pass deflection made at the end of every observation. These readouts contain no useful science data and are not included in the calibrated data.

Manipulating a very large image can be difficult. For demonstration purposes, let's examine an arbitrary subsection of the original raw image in Figure 35.20. The **gcopy** task was used to extract a subset of groups from the original multi-group image. **gstat** computed the statistics for the new image.

Examining RAPID data as a two-dimensional image can be instructive. A simple way to convert the multi-group subset.hhh into a two-dimensional image is to use the **gftoxdim** task.

```
cl> gftoxdim subset.hhh subset_d2.hhh
```

The new image is now two-dimensional: the first dimension runs from diode 1 to 500 while the second dimension marks time.

```
cl> imhead subset_d2.hhh l-
subset_2d.hhh[500,41][real]: SUBSET_2D[1/1]
cl> display subset_d2.hhh 1 z1=0 z2=40 zr- zs-
```

Figure 35.20: Manipulating a Large Image

```
cl> gcopy ../data/z2i3010at.d0h subset.hhh groups=4604-4644
../data/z2i3010at.d0h -> subset.hhh
cl> gstat subset.hhh groups=*
# Image Statistics for subset.hhh
# GROUP      NPIX      MEAN     MIDPT     STDDEV       MIN       MAX
    1        500     10.048   9.00849   5.7949        0.        28.
    2        500      9.68    9.87606   5.31584       0.        24.
    3        500      10.     9.12097   5.48161       0.        27.
    4        500     10.334   9.88548   5.68217       0.        27.
    5        500     10.174   9.94917   5.75412       0.        28.
    6        500     10.166   9.00516   5.83254       0.        28.
    7        500     10.014   9.06106   5.56919       0.        25.
    8        500      10.04   9.8603    5.64465       0.        29.
    9        500      9.792   9.00807   5.29384       0.        28.
   10        500      9.886   9.92473   5.40587       0.        26.
   11        500      9.818   8.99274   5.39881       0.        28.
   12        500     10.072   9.82091   5.79603       0.        27.
   13        500     10.092   9.89125   5.59913       0.        25.
   14        500      9.856   9.10092   5.50562       0.        29.
   15        500     10.004   9.05718   5.64195       0.        29.
   16        500      9.822   9.01055   5.71381       0.        35.
   17        500      9.952   9.88586   5.57313       0.        24.
   18        500     10.054   9.94277   5.68822       0.        30.
   19        500      9.856   9.01978   5.35805       0.        25.
   20        500      9.958   8.97168   5.75312       0.        28.
   21        500      9.916   8.98258   5.69824       0.        26.
   22        500      10.07   9.86902   5.49741       0.        23.
   23        500      9.834   9.90083   5.55231       0.        25.
   24        500     10.206   9.83871   5.75446       0.        32.
   25        500     10.122   9.00645   5.72859       0.        28.
   26        500     10.148    10.128   5.65137       0.        31.
   27        500     10.286   10.0233    5.7052       0.        28.
 28 500          9.76   9.03122    5.41859            0.        25.
   29        500     10.068   9.04799   5.69493       0.        25.
   30        500      10.12   10.0108   5.52473       0.        28.
   31        500      9.908   8.98854   5.53071       0.        26.
   32        500      9.856   9.09568   5.40905       0.        29.
   33        500     10.076   9.90533   5.61045       0.        25.
   34        500      9.942   9.84996   5.42379       0.        27.
   35        500      9.822   9.88937   5.39598       0.        25.
   36        500      9.832   9.87903   5.58553       0.        25.
   37        500     10.206    9.8606   5.54952       0.        27.
   38        500      10.05    9.8626   5.61128       0.        26.
   39        500     10.102   9.97581   5.49509       0.        25.
   40        500     10.304   9.91161   5.80646       0.        27.
   41        500      9.926   8.99917   5.49809       0.        32.
```

GHRS / 35

We can sum the two-dimensional image in each dimension for further inspection:

```
cl> blkavg subset_2d.hhh subset_sum_y.hhh b1=1 b2=41 option=sum
cl> blkavg subset_2d.hhh subset_sum_x.hhh b1=500 b2=1 option=sum
cl> imhead subset_sum_?.hhh l-
subset_sum_x.hhh[500,1][real]: SUBSET_SUM_X[1/1]
subset_sum_y.hhh[1,41][real]: SUBSET_SUM_Y[1/1]
```

Figure 35.21 shows plots of three images. At the top is a greyscale plot of the extracted two-dimensional image, in the middle is a plot of the sum of the 500 diodes as a function of time, and at the bottom is a summed plot of the spectra over time.

Figure 35.21: RAPID Data Displays

GHRS / 35
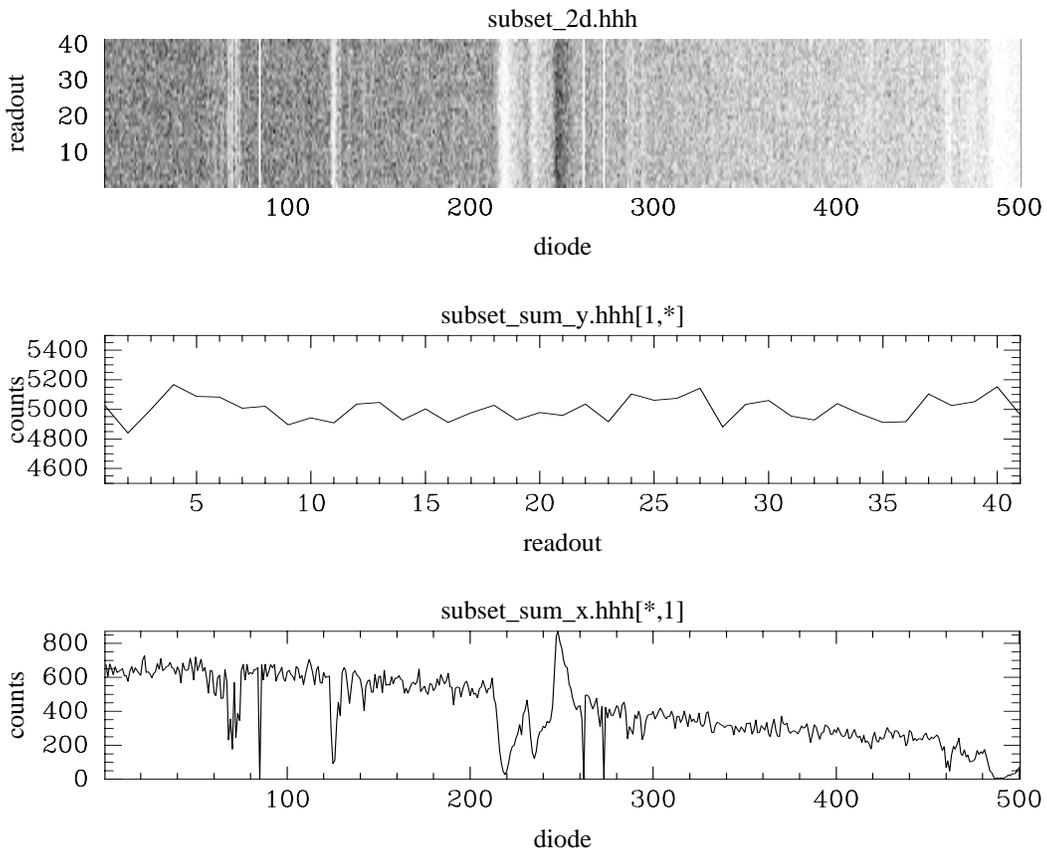
Calibrating and Recalibrating GHRS Data

This chapter explains what happens to GHRS observations when they are processed through the calibration pipeline—the Routine Science Data Processing (RSDP) system at STScI. You should *always recalibrate* GHRS observations to exploit the latest and best information available. The recalibration task, **calhrs**, is the same as the software used in RSDP, so you will need to know how it works. The distinction between "calibration" and "recalibration" is partly artificial, but by "recalibration" we mean applying **calhrs** data to observations of your choice in a way that you control. Recalibration can also include some tasks that RSDP could not do, such as applying an improved wavelength calibration or accounting for background counts in a different way.

The GHRS calibration task **calhrs**, part of STSDAS, was developed and is maintained at STScI. For the GHRS, the calibration process assigns flux and wavelength values to each raw data point. In addition, **calhrs** corrects for non-uniformity in diode response and for diodes that have been turned off (dead diodes). **calhrs** produces, as output, the calibrated spectrum, wavelength solution, error estimates, and data quality images. The calibration software used in the RSDP pipeline to calibrate GHRS observations is the same software used within the **calhrs** task. The **calhrs** task can be found within the STSDAS **hst_calib** package. We will emphasize here the calibration steps themselves, deferring a discussion of error and uncertainty to the next chapter.

36.1 Pipeline Calibration Process

The way in which the routine calibration pipeline handled data depended on how the observations were originally obtained. Please review the previous two chapters to learn more about operating modes and the details of observation specifications. As we emphasized in the previous chapter, an examination of the Phase II proposal for a particular set of observations is helpful in understanding the structure of the data. The Phase II proposal can often be retrieved over the web.

Calibrated data in the archive result from the calibration steps specified by *switches* in the raw science header (.d0h). If there were problems with the observation, it was set aside for repair. If there were missing packets (due to data transmission problems), and no further packets were forthcoming from the spacecraft, the pipeline replaced missing data with fill data. Information about missing packets and fill data can be found in the trailer file (.trl).

36.2 Calibration Steps Explained

Each calibration step is described in this section along with the corresponding calibration switch and various reference files required by that step. A flowchart of the process is illustrated in Figure 36.1.

Data Quality Initialization (DQI_CORR)

This step applies data quality initialization using the reference file dqihfile, which contains a data quality flag for each diode. Each data quality flag in the .q0h file (Table 37.10) is compared with the corresponding flag in the data quality initialization file (.r5h), and the most severe flag is kept. Quality flags are not additive and are never decreased. The most severe data quality flags are written to the output file (.cqh). Table 37.5 defines these flags (by order of decreasing severity).

Conversion to Count Rates (EXP_CORR)

This step converts the input data to count rates by dividing by the exposure times. The exposure time is computed for each bin as:

$$EXPOSURE = n_{coadd} \times (0.05 \times \text{intper} - 0.002)$$

<div align="right">Eq. 36.1</div>

where:

- *EXPOSURE* is the exposure time per bin as found in the keyword in the calibrated data headers.

- *intper* is the integration period in 0.05 second intervals.

- 0.002 is the overhead required to read out the data.

- n_{coadd} is the number of coadds to the bin.

If any value contains fill, no exposure time can be computed and the entire bin is flagged as unusable. The values for n_{coadd} and *intper* are read from the extracted engineering file. If this step is omitted, then the paired pulse correction (PPC_CORR) will also be omitted, regardless of its setting.

Diode Response Correction (DIO_CORR)

The diodes within the Digicons of the GHRS do not have identical sensitivities. This calibration step divides the observed count value (or count rate) by the diode's response (near unity) to correct for diode nonuniformity using the diode response file `diohfile`. When COMB addition is used, a smooth diode response array is computed using a weighted average of diode responses. Data with a diode response value less than the minimum diode response value set in the `ccr3` table are set to 0.0.

Paired Pulse Correction (PPC_CORR)

This step corrects count rate data for the finite response time of the detector electronics. The measured deadtime is 10.2 μsec, determined for detector D1 and assumed to apply to D2 as well. What this means is that the correction is only 1% at an input rate of 2,000 counts per second, which occurs only for very bright stars. The values used are stored in table `ccg2`.

Photocathode Mapping (MAP_CORR)

This step computes where the spectrum was located on the detector's photocathode. This mapping of the location is performed in LINE and SAMPLE space. LINE position is perpendicular to dispersion, and SAMPLE is parallel to the dispersion. This calculation is used by the following calibration steps: ADC_CORR, VIG_CORR, PHC_CORR, and MER_CORR. If MAP_CORR is omitted, then those steps will also be omitted, in spite of their settings.

The position of the individual substep bins are mapped into photocathode space using the following:

$$\text{SAMPLE(bin)} = x_0 + b \times XD + c \times XD^2 \qquad \text{Eq. 36.2}$$

$$\text{DELTAS(bin)} = e \qquad \text{Eq. 36.3}$$

$$\text{LINE(bin)} = L0 + A \times YD \qquad \text{Eq. 36.4}$$

where:

- *SAMPLE* is the sample position of the first diode.

- *DELTAS* is the spacing between sample positions.

- *LINE* is the line position of the diodes.

- *XD* is the X-deflection minus 2048.

- *YD* is the Y-deflection minus 2048.

- *s0*, *b*, *c*, and *e* are coefficients in table `ccr2`, interpolated for the given Y-deflection.

- *L0*, and *A* are coefficients in table `ccr1`.

GHRS / 36

Doppler Compensation (DOP_CORR)

This step corrects for Doppler compensation when removing photocathode nonuniformities (i.e., when PHC_CORR is set to PERFORM) or vignetting effects (VIG_CORR set to PERFORM). Do not confuse this with the on-board Doppler compensation indicated in the science header by the value of the DOPPLER (DPOZER and DOPMAG) keywords. The on-board Doppler compensation is needed to avoid blurring of the spectrum because of apparent shifts introduced by the spacecraft motion. The on-board compensation involves moving the spectrum on the photocathode in the opposite sense to the effect caused by the spacecraft. That means that the spectrum is not at a fixed location over the course of the exposure, and this step attempts to correct for that fact.

This DOP_CORR step computes the percentage of time spent at each Doppler offset in the original observation. These are computed by dividing the observation into time segments and computing the deflection offset for each segment. The SHP packet time is used as the start of the readout and the packet time of the first science packet is used as the ending time of the readout. This step is not applied in the pipeline because GHRS observations are interruptible. We may know the start time of the observation and that it was interrupted, but we have no way of knowing when the interruption began, so we don't know where we are in Doppler space.

Photocathode Nonuniformity Removal (PHC_CORR)

This step removes the photocathode granularity using a reference file that has a granularity map, `phchfile`, when MAP_CORR is also performed. The GHRS pipeline does not use this feature because obtaining the flatfield exposures for all possible grating positions was impractical. Therefore the `phchfile` used by the pipeline is a dummy file that is populated with ones and zeroes. FP-SPLITs were generally used for high signal-to-noise work. However, post-COSTAR G140L flatfields are available; they are especially useful for data having S/N > 30, see *GHRS ISR* 076 for more information.
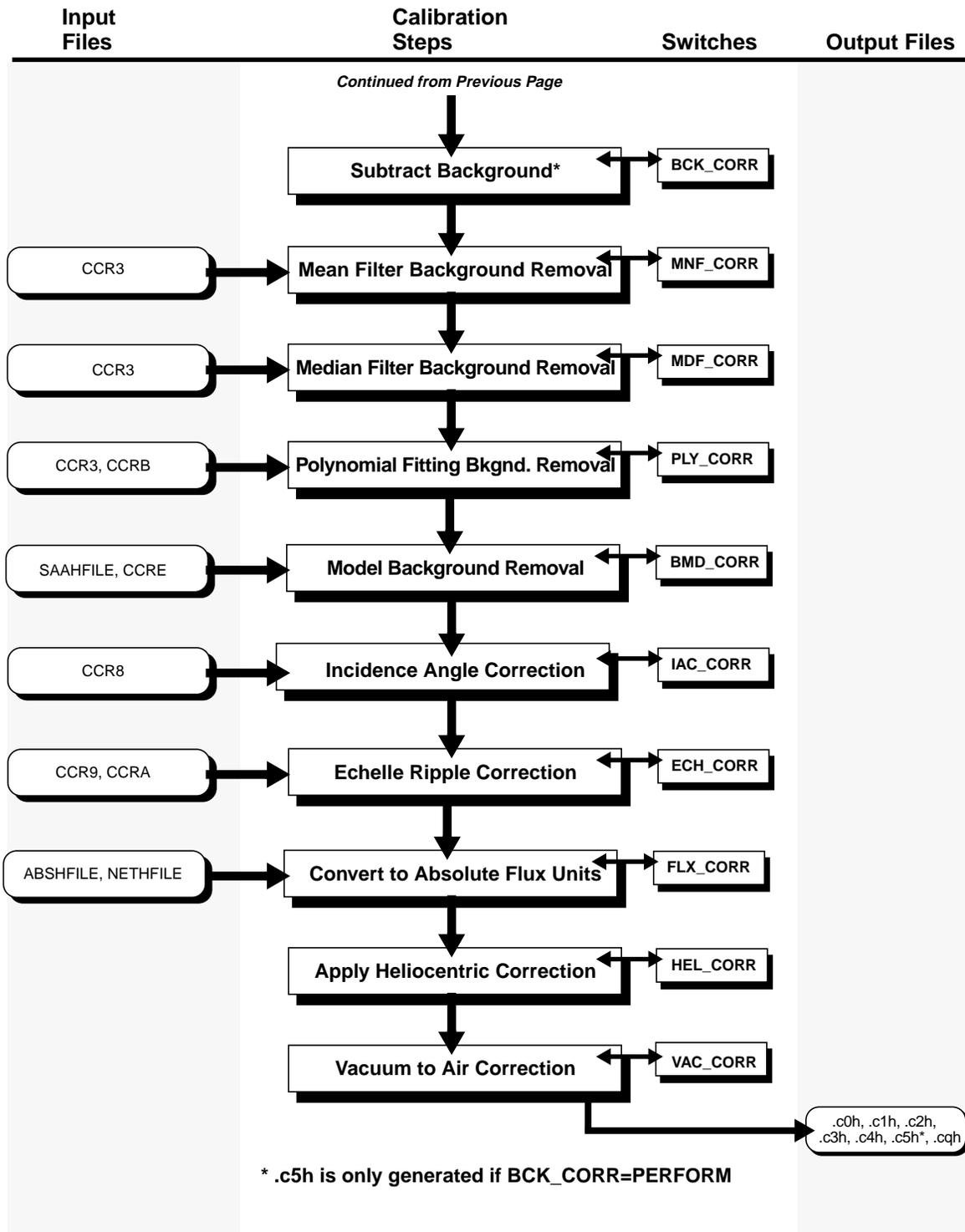
This map is intended to have a granularity vector for multiple line positions. At each line position, the granularity is tabulated with a constant starting sample for all lines and a constant delta sample. To compute the response for a given line and sample, bilinear interpolation is used within the reference file. If Doppler compensation is specified (DOP_CORR = 'PERFORM'), the response is smoothed by a weighting function describing the motion of the data samples along the photocathode.

Vignetting Removal (VIG_CORR)

The response of the detector to light of a given wavelength depends on the grating used, but there is also a dependence on position on the photocathode. The first effect is the overall sensitivity, and the second is called *vignetting*. This vignetting resembles optical vignetting in that it is not present at the center of the detector but causes lower counts (by a few percent) near the edges; however, the cause is in the detector, not in the optics. The vignetting was determined by observing standard stars at enough grating settings so that there was redundancy at any one wavelength, allowing sensitivity and vignetting to be disentangled.

Figure 36.1: GHRS Calibration Process

Input Files	Calibration Steps	Switches	Output Files

Raw Science Images (.d0h, .x0h, .shh, .ulh, .q0h, .xqh) → **Compute Exposure Times**

DQIHFILE, CCRD → **Data Quality Initialization** ← DQI_CORR

Convert to Count Rate ← EXP_CORR

DIOHFILE, CCR3 → **Diode Response Correction** ← DIO_CORR

CCG2 → **Paired Pulse Correction** ← PPC_CORR

CCR1, CCR2 → **Mapping Function** ← MAP_CORR

Compute Doppler Correction ← DOP_CORR

PHCHFILE → **Remove Photocathode Granularity** ← PHC_CORR

VIGHFILE → **Remove Vignetting** ← VIG_CORR

Merge Data ← MER_CORR

CCR5, CCR6, CCR7, CCRC → **Apply Dispersion Coefficients** ← ADC_CORR GWC_CORR

Continued on Next Page

GHRS / 36

GHRS / 36

Input Files	Calibration Steps	Switches	Output Files

Continued from Previous Page

Subtract Background* — BCK_CORR

CCR3 → **Mean Filter Background Removal** — MNF_CORR

CCR3 → **Median Filter Background Removal** — MDF_CORR

CCR3, CCRB → **Polynomial Fitting Bkgnd. Removal** — PLY_CORR

SAAHFILE, CCRE → **Model Background Removal** — BMD_CORR

CCR8 → **Incidence Angle Correction** — IAC_CORR

CCR9, CCRA → **Echelle Ripple Correction** — ECH_CORR

ABSHFILE, NETHFILE → **Convert to Absolute Flux Units** — FLX_CORR

Apply Heliocentric Correction — HEL_CORR

Vacuum to Air Correction — VAC_CORR

.c0h, .c1h, .c2h, .c3h, .c4h, .c5h*, .cqh

* .c5h is only generated if BCK_CORR=PERFORM

The VIG_CORR routine removes the vignetting and low frequency photocathode response using a reference file that has a vignetting map, `vighfile`, when MAP_CORR is also performed. The vignetting map has a vector for multiple line positions and carrousel positions. At each line position the vignetting response is tabulated with a constant starting sample for all lines and a constant delta sample. To compute the response for a given line and sample, tri-linear interpolation is used within the reference file over carrousel position, line position and sample position. If doppler compensation is specified (DOP_CORR = 'PERFORM'), the response is smoothed by a weighting function describing the motion of the data samples along the photocathode.

Merging Substep Bins (MER_CORR)

This routine merges the spectral data when MAP_CORR is also performed. If MER_CORR is omitted, then the background correction (BCK_CORR) will also be omitted. Unmerged output data are then just a copy of the input data. BINID# keyword value are used by **calhrs** to determine how many groups of data are to be merged. Any STEPPATT that accumulates two or more bins of spectra as listed in Table 35.3 will generally require merging. To illustrate the merging, consider input data having values D*bin.diode* for bin number *bin* and diode number *diode*. The data would look like the following:

```
bin 1   D1.1  D1.2  D1.3  D1.4 ...
bin 2   D2.1  D2.2  D2.3  D2.4 ...
...
...
bin 7   D7.1  D7.2  D7.3  D7.4 ...
```

The position of the data points in the two-dimensional data array mapped into a one-dimensional data array are $500 \times bin + diode - 1$. This routine maps the data into the output array for half-stepped data as:

```
D1.1  D2.1  D1.2  D2.2  D1.3  D2.3 ...
```

And for quarter-stepped data as:

```
D1.1  D2.1  D3.1  D4.1  D1.2  D2.2  D3.2  D4.2  D1.3 ...
```

Determine Wavelengths (ADC_CORR, GWC_CORR)

This step converts the sample positions on the photocathode to wavelengths by applying the dispersion constants using tables `ccr5`, `ccr6`, `ccr7`, and `ccrc`; these contain spectral order, dispersion, and thermal constants. ADC_CORR computes spectral orders and wavelengths, when MAP_CORR is also performed. For the first order gratings, the spectral order is set to 1. For the echelle gratings, the spectral order is computed from the following formula:

$$order = NINT\left(\frac{b \times A \times \sin((C - carpos)/B)}{ydef - a - d \times A \times \sin((C - carpos)/B)}\right)$$
Eq. 36.5

where:

- *NINT* is the nearest integer.

- *A, B, C* are in table `ccr5`.

- *a*, *b*, and *d* are in table `ccr5`.

- *carpos* is the carrousel position.

- *ydef* is the Y-deflection adjusted for the proper aperture (LSA: 128 added to it, SC1: 128 subtracted from it).

The wavelengths are computed by solving the dispersion relation for wavelength using Newton's iterative method. The dispersion relation is described by the following equation:

$$s = a0 + a1m\lambda + a2(m\lambda)^2 + a3m + a4\lambda + a5m^2\lambda + a6m\lambda^2 + a7(m\lambda)^3 \qquad \text{Eq. 36.6}$$

where:

- *m* is the spectral order.

- *l* is the wavelength.

- *a0,a1,...* are the dispersion coefficients.

- *s* is the sample position.

The dispersion constants are calculated in one of two ways. If the switch GWC_CORR is set to PERFORM, then the dispersion coefficients are calculated from the `ccrc` table's set of global coefficients which define a function based on carrousel position. If ADC_CORR is PERFORM but GWC_CORR is set to OMIT, then the dispersion coefficients are read from the `ccr6` table, which contains the dispersion coefficients for a few carrousel positions. Therefore, when GWC_CORR is OMIT, interpolation is performed between two sets of coefficients bracketing the required position, if that particular position is not in the `ccr6` table. If ADC_CORR is omitted, then many other switches relying on it are also omitted, namely: IAC_CORR, VAC_CORR, HEL_CORR, FLX_CORR, ECH_CORR, BCK_CORR, and GWC_CORR. The subject of wavelength calibrations and their improvement is treated in the next chapter.

Background Removal (MDF_CORR, MNF_CORR, PLY_CORR, BCK_CORR, BMD_CORR)

This step removes the background, or dark counts, from the observed flux. The switch BCK_CORR determines whether or not background removal is done. The other switches, MDF_CORR, MNF_CORR, PLY_CORR, and BMD_CORR determine how the background is smoothed before subtraction. If BCK_CORR is omitted, then MDF_CORR, MNF_CORR, PLY_CORR, and BMD_CORR are all omitted, too. If the dispersion constants are not applied (ADC_CORR is omitted), then no background subtraction is done.

If MDF_CORR is set to PERFORM, then a median filter is applied to the background. This size of the filter box is found in table `ccr3` in columns SKY_MDFWIDTH and INT_MDFWIDTH. This switch is not normally applied in RSDP: it is provided as a recalibration option.

If MNF_CORR is set to PERFORM, then a mean filter is applied to the background. The size of the filter box is found in table `ccr3` in the columns SKY_MNFWIDTH and INT_MNFWIDTH. This switch is not normally applied in RSDP: it is provided as a recalibration option.

GHRS / 36

If PLY_CORR is set to PERFORM, then a polynomial is fit to the background and the function is subtracted. The order of the polynomial is found in table `ccr3` in columns SKY_ORDER and INT_ORDER. Currently the order is set to 0 but can be modified in your own copy of the `ccr3` table as a recalibration option.

It is possible to have all three filter options set, in which case, they are all performed in the order given above. However, if any of the above are set to PERFORM and BMD_CORR is set to PERFORM, then the background model correction is omitted.

There are three ways to calculate the background counts: the first involving resampling by linear interpolation and the other two internally measuring the background.

Resampling Method

If the science data are composed of multiple substep bins, the sky background will be resampled by linearly interpolating adjacent smoothed background data values. The background will then be scaled by:

$$B_{scale} = B_{res} \times N_{aper}$$

<div align="right">Eq. 36.7</div>

where

- B_{scale} is the background to subtract from the science.

- B_{res} is the resampled sky background.

- N_{aper} is the normalization factor to compensate for the different sizes of the apertures.

Internal Measurement Methods

The two other methods involve internal measures of the background. Both methods use the same formula for determining the background vector:

$$B_i = 0.5(a \times U_i + b \times L_i) - c \times N_i + d \times N_{ave}$$

<div align="right">Eq. 36.8</div>

where:

- B_i is the background at diode i.

- a, b, c, d, are scattered light coefficients from table `ccrb`.

- U_i is the upper inter-order background at diode i.

- L_i is the lower inter-order background at diode i.

- N_i is the net on-order count rate.

- N_{ave} is the average of N over all science diodes.

  N_i is determined by:

$$N_i = D_i - 0.5(U_i + L_i)$$

<div align="right">,Eq. 36.9</div>

and D_i is the on-order count rate at diode i.

GHRS / 36

The two internal methods differ in how the U_i and L_i data are determined.

1. The background can be measured from inter-order spectra. The background is measured by the science diodes by observing the photocathode above and below the science data. U_i is set to the upper background spectrum and L_i is set to the lower background spectrum.

2. The background can be measured from the corner diodes. There can be up to six substep bins sampling both the upper and lower background diodes. The background for each corner diode is the average of all measurements for that particular corner diode:

$$B_{corner} = B_{ncorner}/n \qquad \text{Eq. 36.10}$$

where

- *corner* is the corner diode identifier: *UL* - upper left, *UR* -upper right, *LL* - lower left, *LR* - lower right.

- B_{corner} is the effective background measured by the corner diode.

- $B_{ncorner}$ is the individual background measurement by the corner diode.

- *n* is the number of measurements from the corner diode.

The U_i and L_i vectors are then calculated by interpolating between the corner diodes as follows:

$$U_i = \frac{(C - C_1) \times (B_{UR} - B_{UL})}{(C_2 - C)} + B_{UL} \qquad \text{Eq. 36.11}$$

and

$$L_i = \frac{(C - C_1) \times (B_{LR} - B_{LL})}{(C_2 - C)} + B_{LL} \qquad \text{Eq. 36.12}$$

where

- U_i is the upper background at diode *i*.

- L_i is the lower background at diode *i*.

- *B* is explained above.

- *C* is the channel for diode *i*.

- C_1 is the effective channel or diode for the left corner diodes.

- C_2 is the effective channel or diode for the right corner diodes.

The observation can specify any combination of corner diodes using the substep bin identifications (BINID) found in Table 36.1. If no specific corner diodes are specified, then all four corner diodes are used for each science substep bin.

GHRS / 36

Table 36.1: Background Diodes Used by Substepping

BINID	Corner Diodes Determining Background	BINID	Corner Diodes Determining Background
8	Right and Left Upper	12	Right Upper
9	Right and Left Lower	13	Right Lower
10	Left Upper	14	Upper and Lower Left
11	Left Lower	15	Upper and Lower Right

3. The background can be calculated using a model. There are good reasons for doing this. Sometimes the number of counts accumulated in the background diodes is very small because the exposures are fairly short. When this occurs, the counting statistics limit the accuracy of the background correction. The model, on the other hand, is based on the cumulative experience of the GHRS in orbit. There are also reasons to avoid the model. In particular, if the observations span a range of orbital conditions, then the model's estimate of background may be significantly wrong. This is especially a problem in the region around the South Atlantic Anomaly. Also, for longer observations, the measured background may be well-measured anyway.

BMD_CORR is provided as a recalibration option; it controls the application of the background count rate model available in **calhrs** v.1.3.11 (March 1997). When performed, the background model correction will calculate and subtract a model background based on location of the telescope in its orbit instead of using the background bins obtained with an observation. Because results from the background count rate model are not reliable in or near the SAA, the SAA Model 7 contour (defined in SAAHFILE) is used to issue warning messages per readout of an observation. The `ccre` table contains mean derived background count rates as a function of geomagnetic latitude and longitude. The model is actually the blue FOS model derived by Rosenblatt, et al. (1992) multiplied by a GHRS-detector-specific scaling factor. Header keywords in the table contain the multiplicative scaling factors required to scale the results from the model to the appropriate GHRS detector. See *GHRS ISR* 084.

Apply the Incident Angle Correction (IAC_CORR)

All GHRS wavelengths are referenced to the SSA. After the dispersion constants are applied (ADC_CORR is performed), this routine adjusts the zero-point of the wavelength array for the effects on wavelength of the difference in incidence angle of apertures LSA, SC1, and SC2 from the SSA. New post-COSTAR LSA offsets were determined in 1997 and are now available (*GHRS ISR* 080).

The `ccr8` table is searched for the correct grating, spectral order, aperture, and carrousel position to obtain two coefficients, *A* and *B*. Interpolation of the coefficients (in carrousel position) is used if an exact match is not found. These coefficients are then used to compute an offset using the following formula:

$$\lambda = \lambda + (A + Bs)/m \qquad \text{Eq. 36.13}$$

where:

- l is the wavelength.

- A and B are coefficients from ccr8.

- s is the photocathode sample position.

- m is the spectral order.

Echelle Blaze Correction (ECH_CORR)

This step is appropriate only for observations made with an echelle grating. The large-scale change of response with wavelength is characterized as *sensitivity*, while *vignetting* accounts for minor detector effects. An echelle grating, however, produces a spectrum that drops as one goes away from the blaze peak; this is the *blaze function*, sometimes called the *ripple function*.

Tables ccr9 and ccra contain echelle blaze constants. This step performs the echelle ripple removal (if the data were taken with one of the echelle gratings) after the dispersion constants are applied (ADC_CORR is performed) by dividing the flux by the following echelle ripple function:

$$ripple = gnorm \times \mathrm{sinc}(ax + b)^2 \qquad \text{Eq. 36.14}$$

where

$$gnorm = \frac{\cos(\theta + \beta + \delta)}{\cos(\theta + \beta - \delta + e)} \qquad \text{Eq. 36.15}$$

$$x = \pi m \left(\frac{\cos(\theta + \beta + \delta) \times \sin(\theta + e/2)}{\sin(\theta + \beta + e/2)} \right) \qquad \text{Eq. 36.16}$$

$$e = \mathrm{atan}((samp - 280.0)/f) \qquad \text{Eq. 36.17}$$

$$\theta = \frac{2\pi \times (r0 - carpos)}{65536.0} \qquad \text{Eq. 36.18}$$

and

- m is the spectral order.

- *samp* is the photocathode sample position.

- *r0, b, d*, and *f* are grating parameters in the ccra table.

- a and b are coefficients from the ccr9 table.

The blaze function is normalized to 1.0 as the center of the order. The center of the order is defined to be the center of the photocathode at the carrousel position 27492 for Echelle-A and 39144 for Echelle-B.

Absolute Flux Conversion (FLX_CORR)

This step converts the input flux to absolute flux units, after the dispersion constants are applied (ADC_CORR is performed), by dividing the input count rate by a sensitivity stored in the abshfile (sensitivities) and the nethfile (wavelengths for the sensitivities) files. Quadratic interpolation is used within the sensitivity file to compute sensitivities for the input wavelengths.

The nature and quality of the flux calibrations is treated in the next chapter.

Heliocentric Correction (HEL_CORR)

This step converts wavelengths to a heliocentric system after the dispersion constants are applied (ADC_CORR is performed). This step corrects for the Earth's motion around the Sun and its rotation, and modifies the wavelengths appropriately. The wavelength correction is computed as follows:

$$\lambda = \frac{\lambda_{obs}}{1 - \left(\frac{V}{c}\right)}$$

Eq. 36.19

where

- λ_{obs} - is calculated by the dispersion correction (ADC_CORR).

- V is the velocity of *HST* in the direction of the target.

- $V = V_x \cos\alpha\cos\delta + V_y \sin\alpha\cos\delta + V_z \sin\delta$

- V_x, V_y, and V_z are computed from parameters in the SHP file.

- α and δ are right ascension and declination of the target.

- c is the velocity of light.

Vacuum Correction (VAC_CORR)

This step converts vacuum wavelengths to air wavelengths above 2000 Å, after the dispersion constants are applied (ADC_CORR is performed). This correction is *not* applied in the calibration pipeline. GHRS data are routinely calibrated to vacuum wavelengths. This step is provided as a recalibration option. The following formula is used:

$$\frac{\lambda_{vac}}{\lambda_{air}} = 1.0 + 2.735182\times10^{-4} + \frac{131.4182}{\lambda_{vac}^2} + \frac{2.76249\times10^8}{\lambda_{vac}^4}$$

Eq. 36.20

36.3 Recalibrating GHRS Data

The pipeline used the calibration reference files available at the time the observation was received. However, a number of factors about the instrument came to light as more experience was gained. For example, monitoring of the GHRS showed that it was stable over the lifetime of the instrument. However, some instrumental properties have changed slightly over time. Archive users should be aware that some GHRS observations were obtained before on-orbit calibration reference files were released to OPUS (formerly PODPS). Some calibration reference files are time-tagged, indicating that they should be used on data taken within specific range of dates.

Updated or more timely reference files sometimes become available after the data were processed. If there are unusual features in the data, or if your analysis requires a high level of accuracy, or if wavecal observations were obtained with the science observation, then you may want to determine whether or not a better calibration is possible and then recalibrate the data.

GHRS / 36

All users should perform a StarView search and check the list of reference files used during pipeline processing against the recommended calibration reference files. The decision to recalibrate depends upon which calibration image or table changed, and whether that kind of correction is likely to affect the analysis. Before deciding to recalibrate, retrieve the recommended and used calibration files and compare them to see if the differences are important.

All information needed to calibrate your GHRS observations is contained in the science data header keywords. **calhrs** opens the header file and determines which set of calibration steps to PERFORM or OMIT, and which calibration reference files and tables to use during the calibration process.

You can use the current set of calibration switches and specified reference files in the header file, or you can change certain keyword values. The STSDAS task **chcalpar** can be used to edit calibration parameters simply and reliably.

The IRAF task **imheader** can be used to examine the data header file.

```
to> imheader rootname.d0h l+ | page
```

Here is an excerpt from a GHRS science data header file showing the calibration reference files and switches:

Figure 36.2: GHRS Science Data Header

```
CALIBRATION REFERENCE FILES
DIOHFILE= 'zref$cce1504az.r0h' / diode response header file
PHCHFILE= 'zref$bcc11275z.r1h' / photocathode response header file
VIGHFILE= 'zref$e751116dz.r2h' / vignetting response header file
ABSHFILE= 'zref$e5v0936rz.r3h' / absolute flux header file
NETHFILE= 'zref$e5v0936az.r4h' / absolute flux wavelength net header file
DQIHFILE= 'zref$cce1505kz.r5h' / data quality initialization header file
CCR1    = 'ztab$aau13518z.cz1' / photocathode line mapping parameters table
CCR2    = 'ztab$ba412190z.cz2' / photocathode sample parameters table
CCR3    = 'ztab$c7f1130oz.cz3' / detector parameters table

CCR4    = 'ztab$a3d1045dz.cz4' / wavelength ranges table
CCR5    = 'ztab$e3u1417oz.cz5' / spectral order constants table
CCR6    = 'ztab$e3t1251bz.cz6' / dispersion constants table
CCR7    = 'ztab$e3t1250tz.cz7' / thermal constants table
CCR8    = 'ztab$e3t1250lz.cz8' / incidence angle coefficients table
CCR9    = 'ztab$e751042hz.cz9' / echelle interpolation constants table
CCRA    = 'ztab$e751041qz.cza' / echelle non-interpolation constants table
CCRB    = 'ztab$d8b1457az.czb' / scattered light correction factors
CCRC    = 'ztab$e3u14301z.czc' / global wavelength coefficients table
CCRD    = 'ztab$e3t1028nz.czd' / photocathode blemish table
CCG2    = 'mtab$a3d1145ly.cmg' / paired-pulse correction table

/ CALIBRATION SWITCHES
DQI_CORR= 'PERFORM ' / data quality initialization
EXP_CORR= 'PERFORM ' / division by exposure time
DIO_CORR= 'PERFORM ' / diode response correction
PPC_CORR= 'PERFORM ' / paired-pulse correction
MAP_CORR= 'PERFORM ' / mapping function
DOP_CORR= 'OMIT ' / doppler compensation
PHC_CORR= 'PERFORM ' / removal of photocathode nonuniformity
VIG_CORR= 'PERFORM ' / removal of vignetting nonuniformity
MER_CORR= 'PERFORM ' / merging of substep bins
GWC_CORR= 'PERFORM ' / use global wavelength coefficients
ADC_CORR= 'PERFORM ' / application of dispersion constants
MDF_CORR= 'OMIT ' / median filter of background spectra
MNF_CORR= 'OMIT ' / mean filter of background spectra
PLY_CORR= 'PERFORM ' / polynomial smoothing of background spectra
BCK_CORR= 'PERFORM ' / background removal
IAC_CORR= 'PERFORM ' / incidence angle correction
ECH_CORR= 'PERFORM ' / correction for echelle ripple
FLX_CORR= 'PERFORM ' / absolute flux calibration
HEL_CORR= 'PERFORM ' / conversion to heliocentric wavelengths
VAC_CORR= 'OMIT                ' / vacuum to air correction
```

GHRS / 36

The HST data headers are intended to be self-documenting. The data processing steps performed are listed within the headers as is the state of the telescope and instrumentation at the time of the observation. The trailer file (`.trl`) contains the history of the RSDP pipeline processing, including the history of the calibration steps executed.

36.3.1 Selecting the "Best" Reference Images and Tables

Over the past four years, several changes were made to both the reference images and tables and the calibration software that uses them. In general, software changes are backwards-compatible with earlier versions of reference tables. However, this has not always been the case. Consequently, the current version of the software will not always run properly with old data or old reference files. This is most likely to be a problem for data from before November 11, 1991, in its original form. The simplest work-around to any problem of this sort is to obtain officially-processed data and the latest (appropriate) reference images and tables from the HST Data Archive. StarView can retrieve calibration images and tables from the HST Archive: the GHRS calibration form provides a simple interface for identifying the best files.

Finding Appropriate Reference Files

The calibration reference files used and recommended for a particular observation can be determined by performing a StarView search of the HST Archive. The user should select the StarView |**Searches**| menu and follow the "GHRS" sub-menu to the "Reference Files" option. Type the proposal ID or observation rootname in the "Dataset Name" field and then choose **[Begin Search]** to list the calibration reference files and tables used during pipeline processing and the recommended reference files for calibration.

These files can be obtained from the HST Archive through a StarView retrieval request. Chapter 1 describes how to use the Archive.

StarView's Reference file screen contains four columns of useful information: Used and Recommended reference file names, Level of Change, and an indication if the correction associated with the files was performed. You will also find, for early science data, that not all the calibration switches currently used by the latest version of **calhrs** are in your raw science header. The StarView reference file screen will, however, retrieve all the latest recommended files that you need. By using **chcalpar** on the raw science file, the new switches and reference file keywords will automatically be placed in your header, including CCRE, SAAHFILE, and BMD_CORR keywords, which can be used to apply the model background subtraction instead of the pipeline default (see "Background Removal" on page 36-8) as well as the GWC_CORR and CCRD keywords used in the dispersion solution (see "Determine Wavelengths" on page 36-7). You will need to fill in the values of the switches and reference files within **chcalpar** (see "Running the STScI Recalibration Software" on page 36-16) before recalibrating, populating the names of the recommended reference files in place of those originally used by

the pipeline. We are now providing information on the Level of Change (SEVERE, MODERATE, TRIVIAL) for calibration images and table rows.

▽ Currently, **calhrs** looks for the incidence angle correction table for all science data taken through the SSA and the LSA. However, a correction does not need to be applied in the case of SSA data and the StarView Reference File screen will not, therefore, return a recommended reference file for data taken through the SAA. You will therefore need to set the IAC_CORR to "OMIT" before recalibrating data taken in the small science aperture.

Reference files consist of images and tables stored in FITS format in the HST Archive. You should probably run **strfits** on the files retrieved from the Archive before running **calhrs**. A calibration reference image is an STSDAS image (IRAF imtype = "hhh"). Once **strfits** is run, an image consists of two files: an ASCII header and a binary data file. A reference table is an STSDAS format table. This table is a single binary file which may contain data of several types. By convention, the suffix of a reference image begins with the letter "r" and that of a reference table begins with the letter "c." More information about FITS and STSDAS formats is provided in Chapter 2.

Running the STScI Recalibration Software

calhrs is a task in STSDAS. The STSDAS software runs under IRAF and is free to the astronomical community; it can be retrieved through the STSDAS web page. See Chapter 3 for information about setting up and using IRAF and STSDAS.

In order to recalibrate your data, you need to have all the reference images and tables that are specified by the calibration switches in the science data header (.d0h). If you want to change any of the files used by the RSDP pipeline calibration software to calibrate the dataset originally, the files can be retrieved from the HST Archive.

If you want to add or change the calibration switches or update the reference files, we recommend that you use the **chcalpar** task (in the **ctools** package under **hst_calib**). This task provides a simple and consistent method to change calibration parameters in any of the HST instrument headers.

The calibration software takes as input the raw data images (.d0h, .q0h, .shh, .ulh, .x0h, .xqh) and the calibration reference images and tables. The calibration software determines which calibration steps to perform and which reference files to use from the calibration keyword values (switches and reference files) in the header of the raw data (.d0h) file. The values of the calibration switches and reference file keywords depend on the instrumental configuration used, the date when the observations were taken, and any special pre-specified constraints. The header keyword values were populated in the raw data file in the RSDP pipeline.

All users should determine the values of the calibration switches and reference file keywords in the raw data and calibrated headers. Each observation mode will have calibration switches set to default values. Prior to calibration (.d0h), the cal-

ibration switches will have the value OMIT or PERFORM. Because some steps require that other calibration steps be completed first, there can be cases where a switch is set to PERFORM yet the step is not executed in the pipeline (these are noted in the descriptions of each step, "Calibration Steps Explained" on page 36-2). In this case, the calibration switch value will remain set to PERFORM in the output product (.c*h). After calibration (.clh), the switches for completed steps will have been assigned the value COMPLETE in the header keywords of the calibrated dataset, unless the software knows the reference file is a DUMMY file, in which case the value of the switch keyword will be SKIPPED.

The calibration task **calhrs** has only two user-selectable parameters: the input and output file names. If only the input name is specified, the output filenames will have the same rootname.

calhrs will write informational messages to the screen as it runs. These messages are saved in the trailer file (.trl) when RSDP calibrates the data. You can save them by redirecting the output into a file.

```
hr> calhrs oldrootname newrootname > output
```

The calibration process can logically be thought of in terms of two distinct steps: flux calibration and wavelength calibration. The file that contains the wavelength coefficients has the suffix .c0h, while the flux-calibrated image has .clh.

Each calibration step is described in the section "Calibration Steps Explained" on page 36-2, along with the corresponding calibration switch and various reference files required by that step.

36.3.2 SPYBALs and Wavecals

GHRS wavelength calibrations come in two varieties: SPYBAL and wavecal.

- *SPYBAL*: Automatic centering of a calibration lamp spectrum on the diode array in the direction perpendicular to the array (the *y*-direction) is called spectrum Y-balancing, or *SPYBAL*. This action ensures that the main spectrum features will be *y*-centered on the diode array during the acquisition of science data. The spectrum obtained during this action is dumped as science data with an observation mode called SPYBAL. In general, SPYBALs will be obtained at some wavelength that is different from the one at which you obtained your observations, at a specified setting for a particular grating.

- *wavecal*: Some programs requested wavelength calibrations (often called *wavecals*) at the same wavelength as the science observation. These data can then be used to obtain a better wavelength calibration for the science, with either a wavelength offset or complete redefinition of the dispersion coefficients (see "Using Wavelength Calibration Exposures" on page 36-18). However, the primary changes in wavelength occur in the zero point, not to the dispersion. As a result, if a programs lacks wavecals, SPYBALs may still be used to derive a zero-point correction to the default wavelengths that ends up being nearly as good as if a full wavelength cali-

bration had been obtained. By "nearly as good" we mean that the rms difference in wavelength between SPYBALs and wavecals when both were available was 19 mÅ, or about 3 km s^{-1}; see *GHRS ISR* 053 for details.

You may notice that a wavecal does not have exactly the same wavelength range as the science observations. This difference is primarily due to the incidence angle correction (the two spectra are through different apertures), with a slight contribution from the heliocentric wavelength correction (which is performed for science targets but not internal calibrations). *This difference in wavelength scales is not an error.*

The LSA had a shutter to block light from entering the spectrograph, while the SSA was always open. Therefore, scattered light from a target in the SSA sometimes contaminated a wavelength calibration exposure if the target was very bright. Usually the lines from the spectral cal lamp are strong enough to still be detected (by the **hrs.wavecal** task, for example) over the contaminating light; if, however, it interferes, the user can attempt to subtract the star's spectrum to decontaminate the wavelength calibration exposure.

36.3.3 Using Wavelength Calibration Exposures

The standard wavelength calibration can be improved by using a wavecal or SPYBAL observation taken close to the time of the science data to correct for zero-point offset: **calhrs** *does not do this automatically.* In addition, if a wavecal observation was deliberately obtained with the same carrousel position as the science data as part of the observations, and if the science observations were not obtained as an FP-SPLIT, you may choose to re-derive the wavelength dispersion constants and use them to create a new calibrated wavelength file (.c0h file) for the science observation. When re-deriving the dispersion, you should double check that the science data and the wavecal observation were obtained at the same carrousel setting by examining the value of the keyword parameter CARPOS in both files.

Correcting the Zero Point Offset

You can use the STSDAS **waveoff** task to derive a new zero point offset for the wavelength scale from either a wavecal or a SPYBAL.

hrs.waveoff prints the pixel, wavelength, and sample space offsets to the screen. You can then apply the wavelength offset to the science observations by using the **imcalc** task to add the calculated offset to each pixel (for all the groups) in the wavelength file. See the help file for **waveoff** for examples on how to do this.

Rederiving the Dispersion Coefficients

You can use the task **zwavecal** to re-derive the wavelength dispersion coefficients from a wavecal observation and create a new calibration table with these values. You can then recalibrate your data with **calhrs**, using the newly derived dispersion coefficients to create the calibrated wavelength file (.c0h file) for your science observations. Note that you can only use this method if you have a wavecal observation at the same carrousel position as your science data, taken close in

time to your science data, and your science data were *not* obtained as an FP-SPLIT. You can assure that the science data and the wavecal observation were obtained at the same carrousel setting by examining the value of the keyword parameter CARPOS in both files. Likewise, the value of the keyword FP_SPLIT should be set to "NO".

```
cl> hselect z29h0107t.c1h,z29h0108t.c1h $I,carpos,fp_split\
>>> yes
z29h0107t.c1h   50680   NO
z29h0108t.c1h   50680   NO
```

After running **zwavecal**, you can use **chcalpar** to change the value of the header keyword CCR6 (the dispersion constants reference table) in the science raw data header (.d0h) file to point to the newly created dispersion table. At the same time, change GWC_CORR to 'OMIT" and make sure that ADC_CORR is set to "PERFORM". Then re-run **calhrs** on the science observation. The **calhrs** task will produce a new set of calibrated files, including the new wavelength (.c0h) file reflecting the new dispersion solution. For example, if you had two observations, the first of which was a calibration lamp observation called z29h0107t that was requested at the same carrousel position as science observation z29h0108t, you could use the commands shown in Figure 36.3 to improve the wavelength solution.

Figure 36.3: Improving the Wavelength Solution

```
cl> zwavecal z29h0107t.c1h newdisp_0107
zwavecal: aperture SC2 carrousel position = 50680
wavefit: Iteration 1: 56 lines fit, chisq = 1.146993853700548

Removing 1 lines and fitting again...
wavefit: Iteration 2: 55 lines fit, chisq = 0.8818314073898266
Removing 1 lines and fitting again...
wavefit: Iteration 3: 54 lines fit, chisq = 0.7580552119929887
wavefit: maximum iterations reached.
cl> chcalpar z29h0108t.d0h
...
(ccr6   =      newdisp_0107.tab) dispersion coefficients table
...
(gwc_cor=               omit) Use global wavelength coefficients
...
cl> calhrs z29h0108t new_z29h0108t
```

36.3.4 Putting FP-SPLITs Together

If your data were taken in FP-SPLIT mode, then your calibrated data will have multiple groups that contain independent subintegrations taken at slightly offset carrousel positions. To obtain your final spectrum, with the full integration time, you need to combine the group spectra into a single spectrum. Recall that when taking data in FP-SPLIT mode, the grating carrousel is shifted slightly between subintegrations to assure that different portions of the photocathode are illuminated each time. Thus, each FP-SPLIT group in your calibrated spectrum is shifted in wavelength space with respect to the others. When the individual FP-SPLIT spectra are combined into a single spectrum, the effects of the granular-

ity of the photocathode response are reduced, since the flux measured in a single pixel in the final spectrum will have been collected over several (FP-SPLIT) different photocathode locations.

To combine the groups of an FP-SPLIT observation, you can use two **stsdas** tasks: **hrs.poffsets** and **hrs.specalign**. The **poffsets** task determines the shifts needed to align the spectra either by cross-correlating features in the individual spectra, or by using the information in the .c0h file which gives the wavelength at each pixel. The **specalign** task combines the spectra after first shifting them to align in wavelength space. These tasks are not specific to GHRS data, but can be used on any spectra which you wish to co-align and co-add. They are, however, of particular use in combining the FP-SPLIT groups in an ACCUM mode GHRS observation since for high-signal-to-noise FP-SPLIT data, the tasks can also be used to derive the photocathode response function (i.e., the photocathode flatfield) for your observations. You can then use the photocathode response function to assess the reliability of the features in your final spectrum.

A detailed description of how to use **poffsets** and **specalign** to combine the groups of an FP-SPLIT observation can be found in the help files for the tasks. This topic was also discussed in "Putting FP-SPLITs Back Together" on page 35-32.

GHRS / 36

Chapter 37

GHRS Error Sources

A GHRS spectrum has several dimensions, each with associated error and uncertainty. The two most obvious dimensions are flux and wavelength, which we plot to show the spectrum. But time is also a dimension of the spectrum, in the sense of when the spectrum was obtained, how long the exposure lasted, and the extent of interruptions of that exposure. Spatial dimensions—the positioning of the object within the aperture—are also relevant. Finally, there are instrumental and spacecraft errors that influence the data.

In Table 37.1, we provide a summary of the accuracies you can expect from your data when you have recalibrated it with the latest **calhrs** software and the best reference files (as recommended by StarView's Best Reference File screen—see Chapter 1 in Volume 1), assuming your target acquisition was successful and appropriate for your science slit, and, for photometry, assuming a wide aperture was used. In some cases improvements can be made further by using the calibration information and post observation refinement tasks described in this Data Handbook—these cases are noted in the table.

In this chapter we will discuss each of the dimensions affecting the accuracy of your data in turn and examine what is known about them from the experience gained since the GHRS started operation.

Table 37.1: Summary of GHRS Errors and Uncertainties[a]

Attribute	Accuracy	Limiting Factors
Flux, absolute	5%	Confidence in absolute flux scale
Flux, relative: same star, same wavelength	2–4%[b]	Grating at same position for all observations
Flux, relative: within an exposure	2 to 4%	2% typical, 4% worst case (G140L, 100 Å away)
Flux, relative: different setups	4%	2% typical; vignetting, sensitivity determinations
Flux, relative: pre-COSTAR	4%	Centering in LSA, poor PSF
Wavelengths, relative: within an exposure	<0.1 diode	Dispersion highly reliable
Wavelengths, absolute: default wavelength calibration	1.1 diodes	Assumes worst case from Table 37.8
Wavelengths, absolute: use of SPYBAL	0.4 diode	GIM effects and carrousel uncertainty
Wavelengths, absolute: use of wavecal	0.3 diode	GIM effects

a. See page 37-17 for applicability to G270M.
b. Can vary to 4% at shortest wavelength. For side 2, can be improved by correction for time-dependent variations, as in Figure 37.3.

37.1 About Flux Calibrations

The concept we discuss here as "flux" has several components. First, is the overall level of the spectrum, or "Has the correct flux scale been applied to the observations?" Second, is the shape of the spectrum, or "Is the curve I see in the continuum real or an artifact?" Finally, there is structure in the spectrum on the scale of a diode's width, or "Is that noise or a bad diode?" The first component has a length scale of tens to hundreds of Ångstroms and is embodied in the sensitivity function for a grating. The second component is incorporated primarily into the vignetting function, which depends on the particular setting for a grating, although other effects can contribute on this scale as well. The small-scale structure, as noted, is seen on diode-sized scales.

37.2 Spectrum Level and the Sensitivity Function

The sensitivity functions quantify the relationship between the observed flux from a point source and the count rate detected by the GHRS. For calibration purposes the fluxes of the reference stars are expressed in the cgs units traditional to astronomy: ergs cm^{-2} sec^{-1} $Å^{-1}$. Raw GHRS data have units of counts per diode per second. The sensitivity functions simply show the ratio of these quantities, with no other constants, scale factors or transformations included. The post-COSTAR sensitivity functions for all GHRS gratings are listed in Chapter 8 of the *GHRS Instrument Handbook*[1]. (See *GHRS ISR* 060 for the pre-COSTAR sensitiv-

ity functions.) For planning purposes, a known or estimated flux can be multiplied by the sensitivity to estimate what the GHRS count rate will be for a particular grating. During data reduction, an observed count rate can be divided by the sensitivity function to calibrate the data in flux units by setting the value of the `FLX_CORR` switch to `PERFORM` in the `.d0h` header.

The sensitivity functions depend on several factors. The telescope contributes its unobscured geometrical collecting area, the reflectivity of both mirrors, and the fraction of the light which manages to pass through the instrument's entrance aperture. The GHRS optics introduce a finite reflectivity at each surface and transmission at each filter and window, the blaze efficiency and linear dispersion of the gratings. The detectors have an overall quantum efficiency (QE) at each wavelength, spatial gradients related to vignetting or real QE variations, isolated scratches and blemishes, pixel-scale irregularities, finite sampling by the diodes, and diode-to-diode gain variations. As we noted, to simplify this problem, the calibration is broken into several components. The basic function relates flux and count rate measured at the center of the diode array, for a star centered in the LSA, at a range of wavelengths for each grating. The echelle blaze function is quantified separately for each order. Gradients of sensitivity across the diode array are described by vignetting functions which vary with wavelength for each grating or echelle order. The SSA throughput is measured relative to the LSA at several wavelengths, and is assumed to be independent of grating mode. Blemishes are tabulated as departures from the local sensitivity for each grating. Diode response functions are tabulated as detector properties, which depend on threshold settings, but not optical modes. Finally, the pixel to pixel granularity can be identified and suppressed as photometric noise.

Each of these factors that affects the flux measurement has some uncertainty, which we will discuss below.

37.2.1 Standard Stars

The stars used for flux references are members of the set of standards established and maintained by STScI. Targets for specific observations are selected primarily on the basis of UV brightness and nonvariability, since we want to obtain count rates high enough to achieve adequate S/N (>50) in short exposure times.

We used the ultraviolet standard stars BD+28D4211 and μ Columbae as our primary flux references. We have also used BD+75D325 and AGK+81D266 on occasion. None of these are known to exhibit significant variability in the ultraviolet. BD+28D4211 is a hot white dwarf that was used for the sensitivity monitors for the low- and medium-dispersion gratings. The corresponding observations for the echelle, and other long-term monitoring programs, were done with the bright late-O super giant μ Col. An example of a Cycle 4 BD+28D4211 observation is in Figure 37.1.

---

1. The values in the *GHRS Instrument Handbook* were for purposes of observation planning and are not the final nor best information available. The CDBS files are up-to-date and based on our cumulative experience since launch.

Sensitivity determination is done by comparing an observed spectrum to the reference spectrum for that star. The reference spectrum is the current best estimate of the true flux versus wavelength for a particular star, and therefore represents "truth." The flux scale for the GHRS and other HST instruments has been modified such that observations of the star G191B2B match theoretical models.

37.2.2 Procedures for Determining Sensitivity and Vignetting Functions

A series of observations for the characterization of the post-COSTAR GHRS was made shortly after SMOV, in 1994. A similar series was done early after launch for the pre-COSTAR instrument. To illustrate how these observations were used to determine sensitivity and vignetting, we borrow from *GHRS ISR* 085, which discusses G140L sensitivity.

If it were possible to record the full useful wavelength range of a grating in a single exposure, then it would also be possible to determine a single "sensitivity function" for that grating. That function, which we will denote by S_λ, would have units of flux per count rate[2], or, more physically, S_λ is in units of (erg cm^{-2} s^{-1} Å^{-1}) per (counts s^{-1} diode^{-1}), where knowledge of the instrument's properties indicates the appropriate wavelength at a given diode. We will denote the flux by F_λ and the count rate by C_λ, so that $S_\lambda = F_\lambda/C_\lambda$.

The work would be much easier if we could observe a "perfect" star, by which we mean one with a flat or nearly-flat spectrum which is not variable in time and which is largely free of any structure (such as absorption lines). We also wish we had a "perfect" detector to work with, which would be one with a flat response across its face, that response being independent of wavelength, spatial position, or time.

Real stars, in particular those used as standards for UV flux calibration, have many spectrum features, and those lie at astrophysically-critical wavelengths. The biggest of these, like Lyman-α, are "potholes" in that they must be worked around carefully. There are also weaker features—the "barbs"—that make it difficult to divide one spectrum by another. Real detectors, like those in the GHRS, have response functions that vary with wavelength, and, to some degree, with time. What is particularly difficult to treat is the very steep decline in sensitivity below Lyman-α.

The gratings of the GHRS can be positioned to almost any wavelength within their nominal ranges. When this is done, other effects must be taken into account. In particular, GHRS spectra have a *vignetting* correction applied after the initial sensitivity calibration. This vignetting is only partially so in the classic optical sense, and, in fact, includes several effects that lead to variations in the spectrum of a few percent over scales of tens of pixels. "Sensitivity," on the other hand, is meant to refer to the gross dependence of observed count rate on stellar flux. Thus "sensitivity" should not depend on how a spectrum is placed on the detector; those

---

2. More properly this is the inverse sensitivity. We will ignore the distinction here.

GHRS / 37

spatially-dependent effects come under "vignetting." Variations on even finer scales also occur and have to do with diode-to-diode gain variations, granularity, etc. Those small-scale (one to a few diodes in scale) variations will not be treated here.

The underlying concepts used to determine S and separate it from V, the vignetting function are simple:

1. Observe a standard star over the full useful range of the grating, ensuring that any given wavelength is observed twice by stepping the grating by half its bandwidth. This produces the observed standard star spectrum, in count rate units, $C_\lambda(O)$, as a function of wavelength.

2. Plot these overlapping spectra in the units they are observed (count rate) versus wavelength. The central region of each spectrum should form an upper envelope to what is seen.

3. Compare this upper envelope to a reference flux spectrum for the standard star, $F_\lambda(R)$. The reference spectrum is the official version of what the flux at each wavelength of the standard star is supposed to be.

4. The initial estimate of sensitivity is then $S_1 = F_\lambda(R)/C_\lambda(O)$.

5. Use this initial estimate S_1 to derive deviations for each individual spectrum. These are V_1, determined as a function of position on the detector photocathode, the detector being the presumed source of the variations ascribed to vignetting.

6. Iterate S and V until satisfactory closure occurs, to get S_{final} and V_{final}. The goal is to determine vignetting to within about 1%.

In practice, of course, determining S_λ and V_λ is not so simple, and involves some estimates and compromises. For example, we accepted the existing CDBS G140L vignetting files as final versions and did not rederive the vignetting: the residuals in overlapping areas of the spectra were within acceptable limits.

Figure 37.1 shows the first step in this process. The upper frame shows the observed spectrum, $C_\lambda(O)$, of standard star BD+28 in units of count rate, while the bottom frame shows the reference spectrum, $F_\lambda(R)$. Please note that this reference spectrum already takes into account the proper white dwarf flux scale, and that no secondary correction is needed.

Problems and Limitations

The procedure outlined above quickly produces satisfactory results. There remain, however, some difficult nagging problems.

Far-UV Reference Fluxes

The existing reference spectrum of our standard star, BD+28˚4211 is based on FOS observations, and are on the fundamental UV scale of G191-B2B. However, the GHRS can observe further into the UV than can the FOS, which means that we lack a reference spectrum below about 1140 Å.

GHRS / 37

Lyman-α and Other Major Features

It is difficult to determine the calibration in the region of Lyman-α because it is such a large feature. Also, Lyman-α lies on a portion of the observed spectrum with a steep slope (Figure 37.1). Lyman-α is very broad, and, moreover, there is little spectrum left shortward of Lyman-α, and the sensitivity there is declining rapidly. As a result the intrinsic uncertainty in fluxes in the region of Lyman-α is higher than at other wavelengths.

Figure 37.1: Observed Spectrum $C_\lambda(O)$ of Standard Star BD+28 (above) Compared to Reference Spectrum $F_\lambda(R)$ for the Star (below).
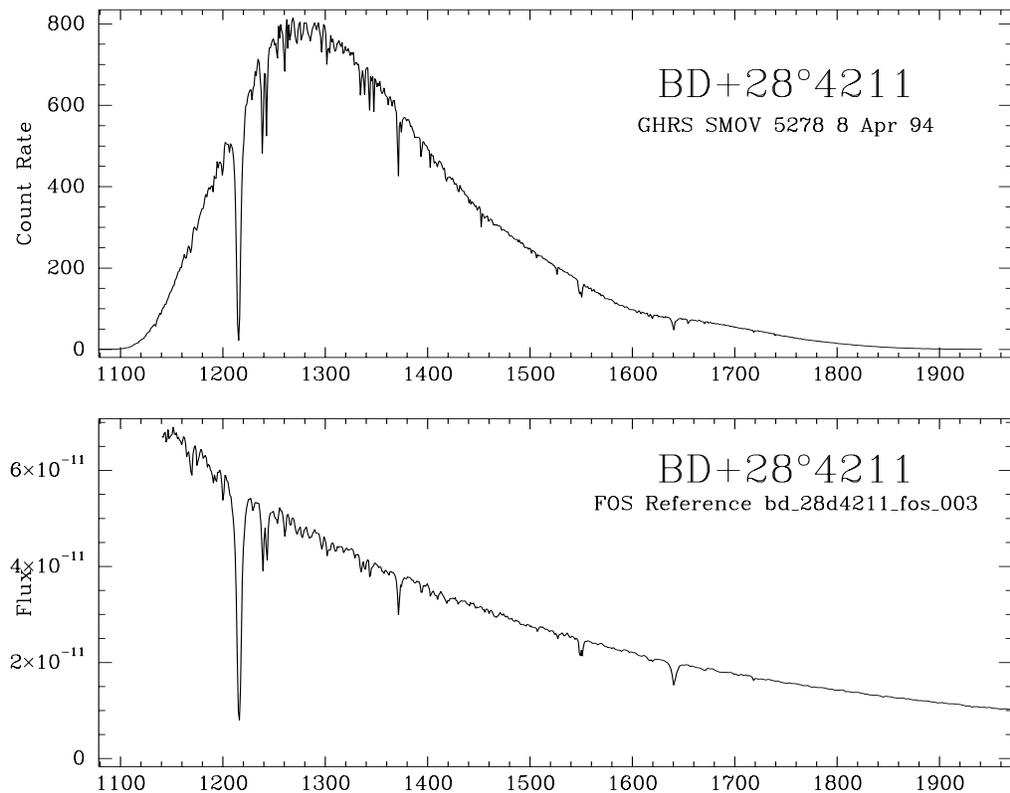
Various features show up in all parts of the spectrum of the standard star, but they are moderate in effect, making it possible to form a reliable estimate of the spectrum. Recall that the reference spectrum is defined in terms of the total stellar flux within some bandpass, meaning that it is *not* the flux in the continuum. The reference spectrum has its origins in FOS observations, at resolution lower than those of the GHRS. Therefore we interpolate both spectra to get the resolution of the GHRS spectra to a level similar to that of the reference spectrum.

Small Science Aperture (SSA)

The amount of light seen through the Small Science Aperture (SSA) is sensitive to the centering of the object in the SSA. The baseline SSA sensitivity curve was created by multiplying the baseline LSA sensitivity curve by the SSA to LSA ratio. The process used is discussed in greater detail later in this document.

Effects of Time

Ratios of our regular sensitivity monitoring data to the baseline SMOV data show changes in GHRS Side 1 sensitivity over time since the installation of COS-TAR. Each time the monitor was run, the current data was compared to the SMOV BD+28D4211 data at the same wavelength. A ratio and errors were calculated every 10 Å from ~1100 Å to ~1630 Å. While the sensitivity below Lyman-α decreased, an apparent increase occurred in sensitivity from ~1200 to 1350 Å, before it declined again. We do not understand this behavior, but it has remained fairly constant with time.

In addition to rederiving the baseline post-COSTAR sensitivity, we have also created time-dependent curves for the date of each sensitivity monitor based on the ratio of the counts from the monitor to the SMOV baseline data. Observers will need to interpolate between sensitivity curves to get a correction appropriate for the date of their observations.

37.2.3 Sensitivity Monitoring

Sensitivity monitoring was done for Side 1 and Side 2 separately. The Side 1 post-COSTAR monitor contained a series of visits of the ultraviolet standard BD+28D4211, done with identical instrumental configuration each time, except that the exposure times were increased at later dates to achieve better signal to noise. The target was acquired into the Large Science Aperture with a 5 x 5 spiral search using mirror N1, followed by a peak-up. The science observations were done with grating G140L in the ACCUM mode at two central wavelengths: 1200 Å and 1500 Å. For the Side 2 observations, BD+28D4211 was acquired into the LSA with a 3 x 3 spiral search using mirror N2, followed by a peak-up. Centering was confirmed by taking an image with the LSA. A series of spectra in the ACCUM mode were taken with gratings G160M (centered at 1200 and 1500 Å), G200M (2000 Å), and G270M (2500 and 3000 Å). This sequence was repeated approximately every three months.

These monitoring programs have shown that prior to COSTAR and the 1993 Servicing Mission, the GHRS was stable in sensitivity, with no perceptible changes. However, after the Servicing Mission we could see distinct declines in sensitivity, especially on Side 1 below Lyman-α. These changes were suspected to be due to contamination on the COSTAR mirrors for the GHRS, and a special measurement was planned to occur just before the second Servicing Mission to verify this. Unfortunately, the GHRS experienced a catastrophic failure one week before SM2 so that these measurements were never done.
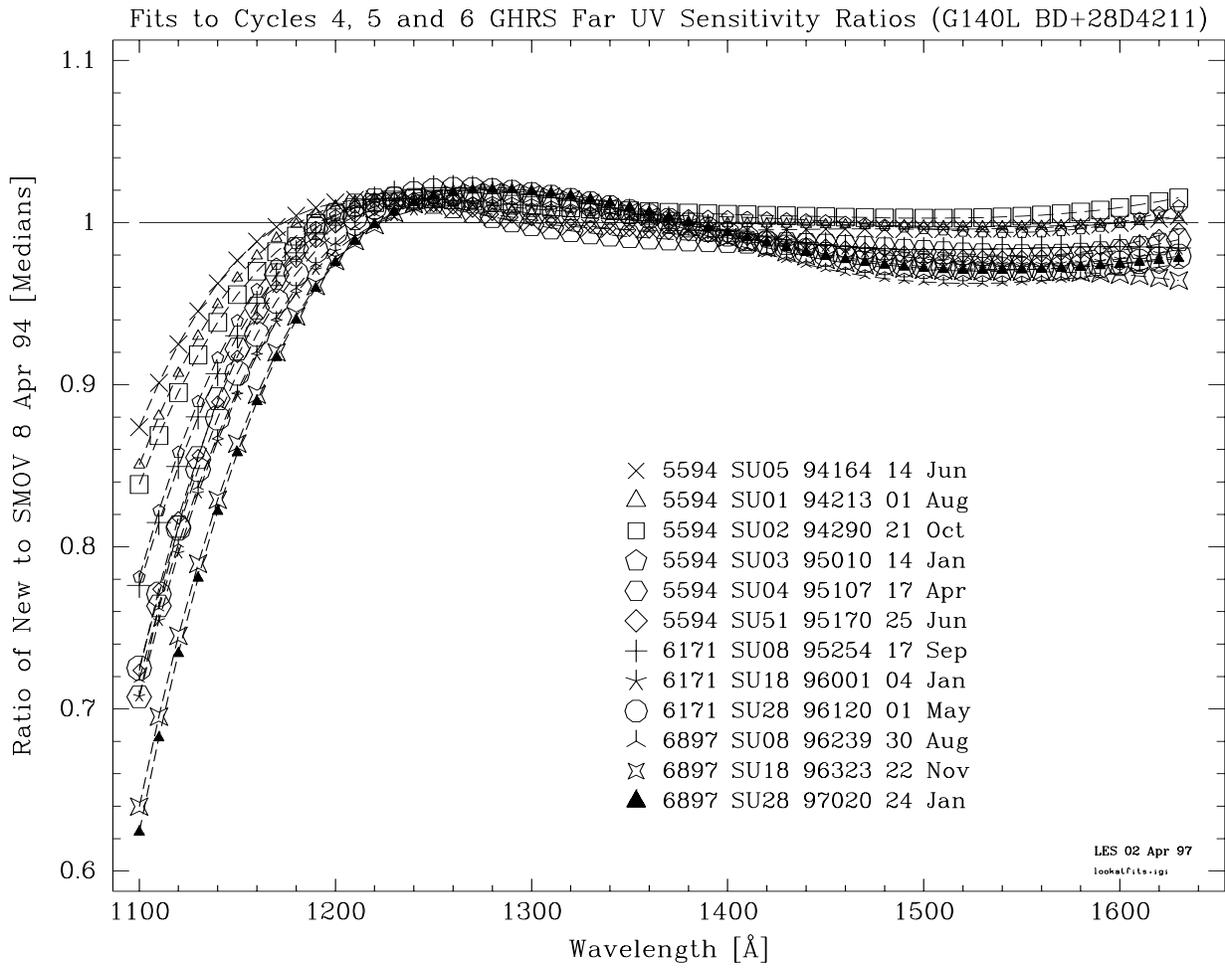
In any case, the declines in the post-COSTAR sensitivity of the GHRS are well-characterized. Typical errors in the ratios are less than 1% for wavelengths above 1200 Å and around 1 to 2% for wavelengths below 1200 Å (up to 3 to 4% on the 1100 Å point at the earliest dates with the least exposure time). Provision has been made for the decline by providing calibration reference files that apply to specific time periods. These time periods are three months in length, which is short enough that significant changes did not occur on shorter time scales. The difference between successive sensitivity files is listed in Table 37.2 below.

Table 37.2: Differences between Successive G140L Time Dependent
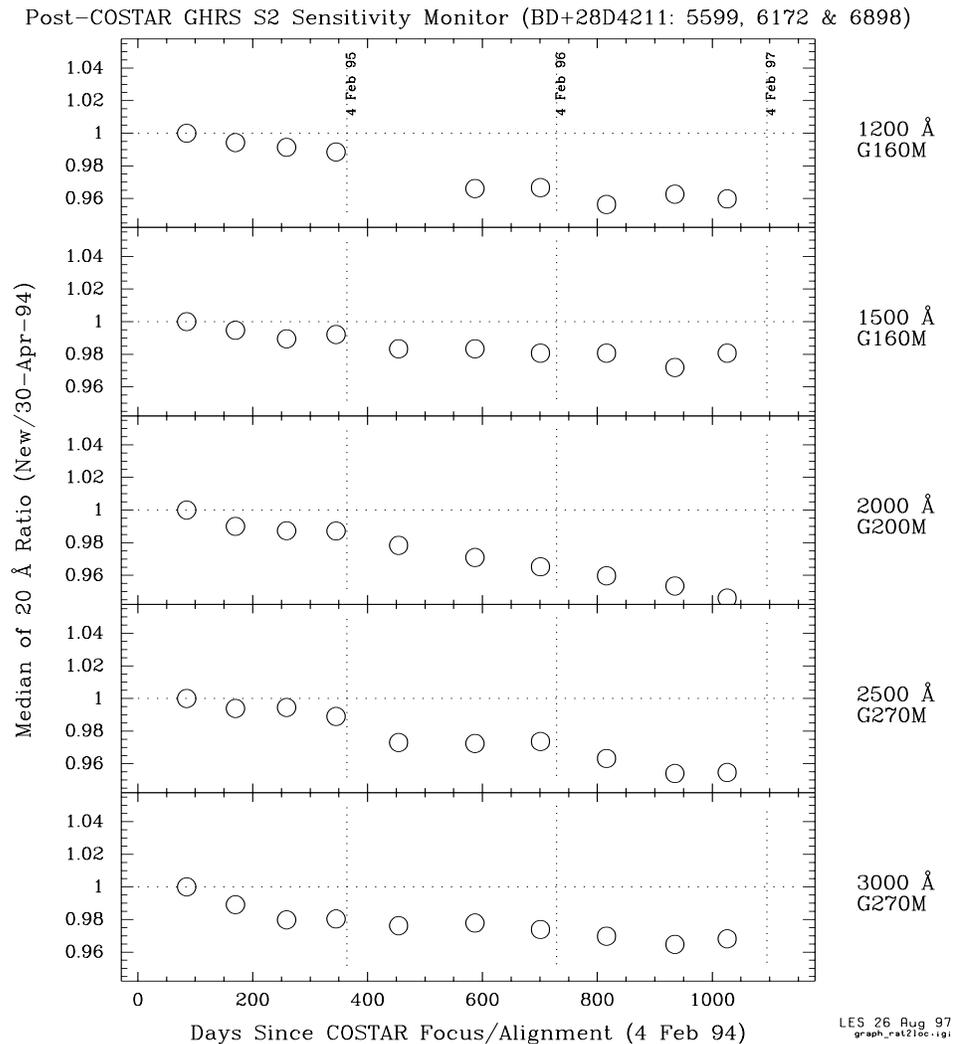Sensitivities

USEAFTER	MEAN	STDDEV	100x(1-MIN)	100x(1-MAX)
June 14, 1994	1.0133	0.0414573	1.41860	-14.449
August 1, 1994	1.00233	0.0087619	0.5979	-2.727
October 21, 1994	0.995793	0.0086304	1.2088	-1.443
January 14, 1995	1.01144	0.019553	0.0589	-7.321
April 17, 1995	1.02364	0.0254328	0.1453	-10.448
June 25, 1995	0.995898	0.0068702	2.2658	-0.814
September 17, 1995	0.994218	0.0213934	6.7518	-1.19
January 4, 1996	1.01534	0.0274196	-0.0120	-9.668
May 2, 1996	0.997726	0.0093042	2.40010	-0.524
August 30, 1996	1.00581	0.00362	0.23299	-1.263
November 22, 1996	1.01707	0.0345412	0.80189	-12.303
January 24, 1997	0.996619	0.0109268	1.40099	-2.483

Figure 37.2 shows the Side 1 sensitivity decline and Figure 37.3 shows the decline for Side 2. The Side 1 figure represents fits to the sensitivity monitor ratios for grating G140L. Illustrated are cubic-spline fits to the ratios of an observed spectrum to the one observed during SMOV. These fits are the basis for the time-variable G140L sensitivity files. Figure 37.4 and Figure 37.5 show details of the time variability for the two worst wavelength regions.

**Figure 37.2:** Side 1 Sensitivity Decline

Fits to Cycles 4, 5 and 6 GHRS Far UV Sensitivity Ratios (G140L BD+28D4211)

Legend:
- ✕ 5594 SU05 94164 14 Jun
- △ 5594 SU01 94213 01 Aug
- □ 5594 SU02 94290 21 Oct
- ⬠ 5594 SU03 95010 14 Jan
- ⬡ 5594 SU04 95107 17 Apr
- ◇ 5594 SU51 95170 25 Jun
- + 6171 SU08 95254 17 Sep
- ✶ 6171 SU18 96001 04 Jan
- ◯ 6171 SU28 96120 01 May
- ⅄ 6897 SU08 96239 30 Aug
- ✩ 6897 SU18 96323 22 Nov
- ▲ 6897 SU28 97020 24 Jan

LES 02 Apr 97
lookatfits.igi

Figure 37.3: Side 2 Sensitivity Since COSTAR

Post—COSTAR GHRS S2 Sensitivity Monitor (BD+28D4211: 5599, 6172 & 6898)

In Figure 37.3, the five panels are for central wavelengths of 1200 Å, 1500 Å, 2000 Å, 2500 Å, and 3000 Å. Each point represents the ratio of the median counts measured over 20 Å relative to the counts measured on 30 April 1994 over the same 20 Å (the first data point). The error on individual data points is 1%. Time is represented in days using the date we consider COSTAR to have aligned and focussed for GHRS (February 4, 1994) as the zero-point. The vertical dashed lines represent one-year intervals.

An example of the improvement possible from using the time-dependent files is shown in Figure 37.6. In this figure, the top plot is flux-corrected with an appropriate time-variable sensitivity file; the bottom plot is the same data calibrated by the pipeline (PODPS).

Figure 37.4: Time Variability for GHRS G140L Below Ly-α

GHRS G140L Change in Sensitivity Monitor Ratio Below Lyman α Since SMOV1
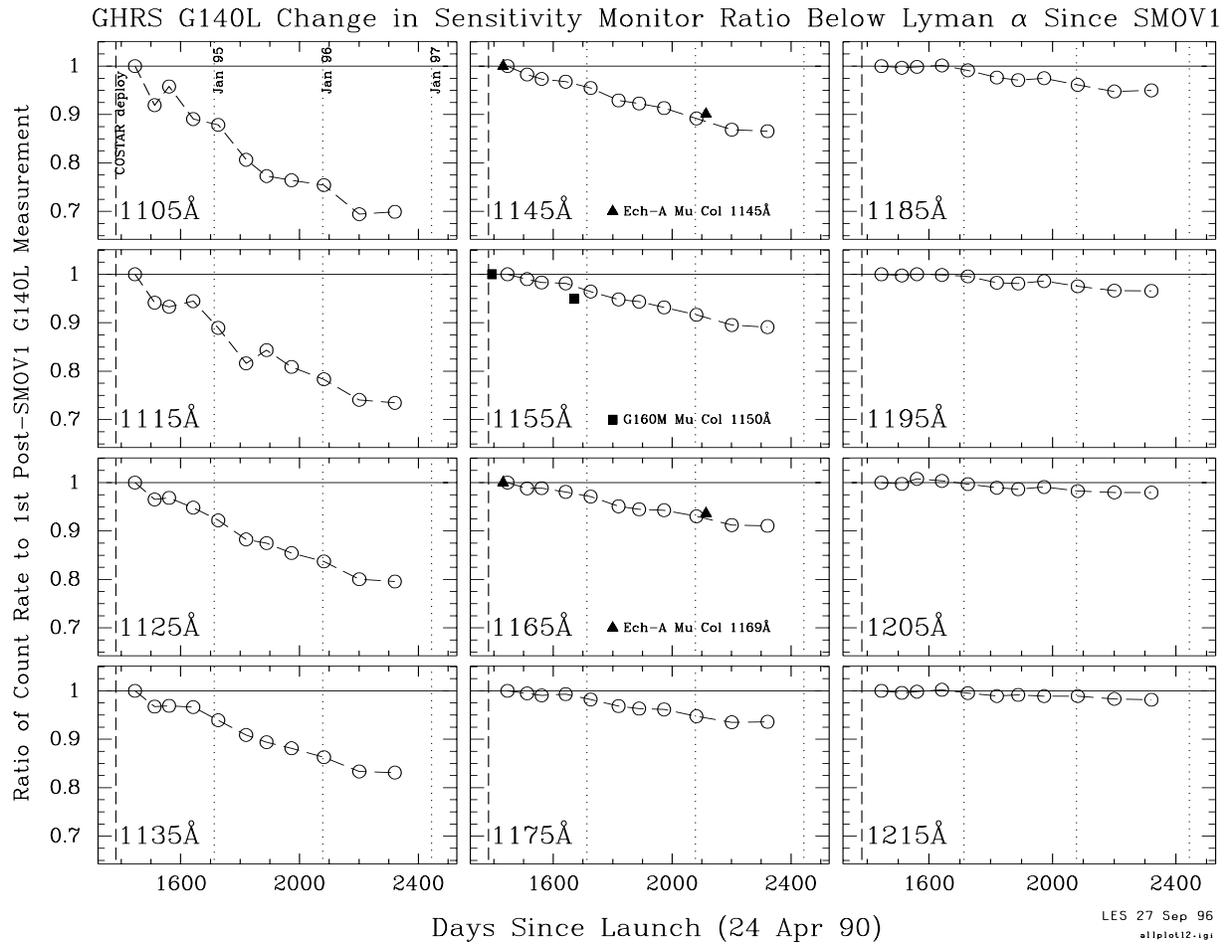
Figure 37.5: GHRS G140L Change in Sensitivity Monitor Ratio

GHRS G140L Change in Sensitivity Monitor Ratio Since SMOV1

Days Since Launch (24 Apr 90)

LES 28 Feb 97
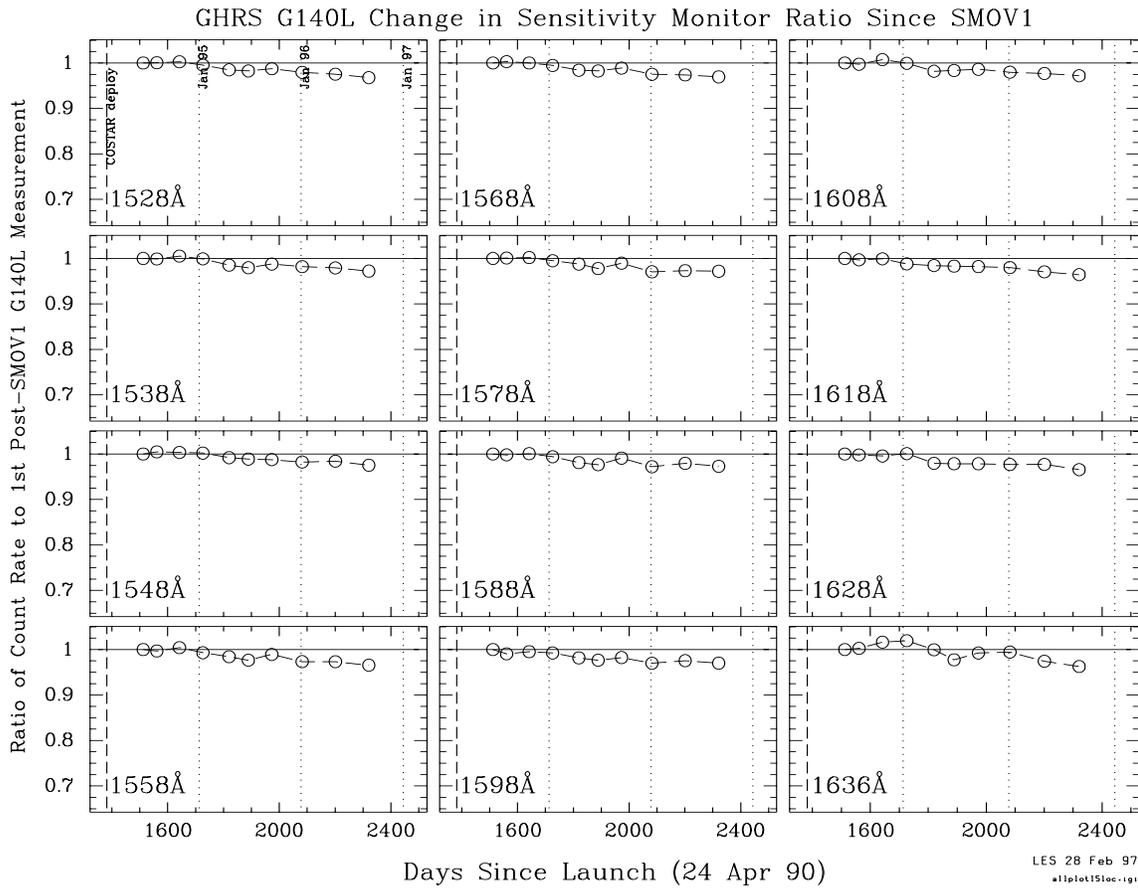
Figure 37.6: Ratio of Monitor Data to Reference Star

Flux-corrected with time-variable sensitivity file

Calibrated by pipeline

Comparison of Default to Time Variable Sensitivity File

Wavelength (Å)
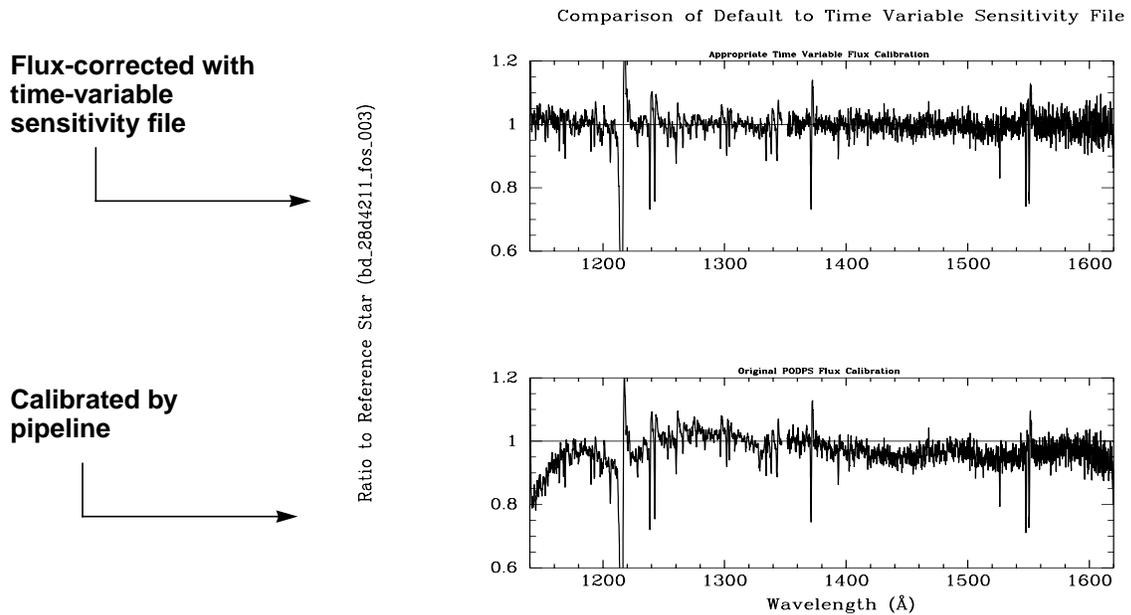
37.2.4 Calibrated Flux Quality

Absolute and Relative Fluxes

The foregoing discussion of the process used to create the components of the flux calibration illustrates some of the factors that influence the quality and reproducibility of flux calibrations in GHRS observations. You want to know how precise and accurate the flux values are, and that varies by situation.

For example, if the same point-source object was observed repeatedly at the same wavelength with the same grating, then many variables are removed. This situation is essentially that for BD+28 in the monitoring program. Figure 37.3, for example, shows that once the long-term trends are removed, Side 2 LSA fluxes for this best-case scenario are reproducible to within about 1%. The primary source of this uncertainty is error in positioning a star in the LSA. The uncertainty with the SSA will be significantly larger because the throughput of the SSA depends critically on centering the star, while the LSA is much less sensitive to that.

Now suppose that the same instrumental setup is used throughout (grating and wavelength do not change) but that different stars are being compared. If the stars have similar spectra, then the previous situation pertains. If the spectra differ significantly, then the convolution of that spectrum with the sensitivity and vignetting functions will introduce additional uncertainty. Near the center of the spectrum these effects will be minimal and the intercomparability should be to within 1 to 2%.

The same kind of additional uncertainty arises if the same or different objects are being compared but in a situation where the grating used or central wavelength are different. For example, one star may have been observed with G140L and the other with G140M, or perhaps G140L was used for both, but at different settings. In this instance some of the shape effects we described will apply—in the worst cases there can be uncertainty of about 4%, but 2 to 3% is more typical.

In other cases, you might want to know the quality of the flux on an absolute basis, perhaps to compare to models. This uncertainty is impossible to measure fully, but a comparison of observations from different instruments at different times indicates that fluxes on an absolute scale are reliable to about 5%. The absolute flux scale used by the GHRS is tied to the system of STScI observatory standards. In May 1994, we switched over to the new, revised absolute flux scale established from observations of the white dwarf G191-B2B (see *GHRS ISR* 062). The new scale differs from the old by up to 10%, depending on wavelength. Archived data obtained prior to May 1994 have not been recalibrated with the new flux scale. Therefore, spectra of the same star *calibrated* before and after May 1994 are on fundamentally different flux scales; recalibrating pre-May 1994 data with the latest GHRS reference files will produce calibrated data on the white dwarf flux scale. Bohlin et al. have compared FOS observations of white dwarfs to models and find consistency to within 2%. They also estimate that various systematic effects may lead to an overall error in absolute fluxes of about 5%, as we noted, but these errors are common to all the systems, meaning that the uncertainty with which HST fluxes can be compared to, say, IUE fluxes, is much lower and is comparable to comparing just HST fluxes.

GHRS / 37

The absolute throughput of the LSA is not well known. We estimate, based on models of the point spread function, that approximately 90 to 95% of the light of a point source that reaches the GHRS focal plane is encompassed by the LSA.

The relative throughput of the SSA with respect to the LSA was determined before and after the installation of COSTAR (see *GHRS ISR* 062). Post-COSTAR values are shown in Figure 37.7. LSA throughput is assumed to be 100% in this figure. The relative throughput of the SSA is wavelength dependent, with higher values measured at longer wavelengths. The pipeline automatically corrects for the point source differential aperture throughput.

In Figure 37.7, the circles are observations of μ Col—all five data points are based on a single SSA ACQ/PEAKUP. The crosses are for χ Lup; the first and last points are from a single ACQ/PEAKUP and the cluster of three points near 1950 Å is from another. The diamonds are for AGK+81D266; each point is based on an individual ACQ/PEAKUP. The solid line is a straight line fit to the μ Col and χ Lup data.

Figure 37.7: Ratio of Count Rates for Post-COSTAR SSA to LSA
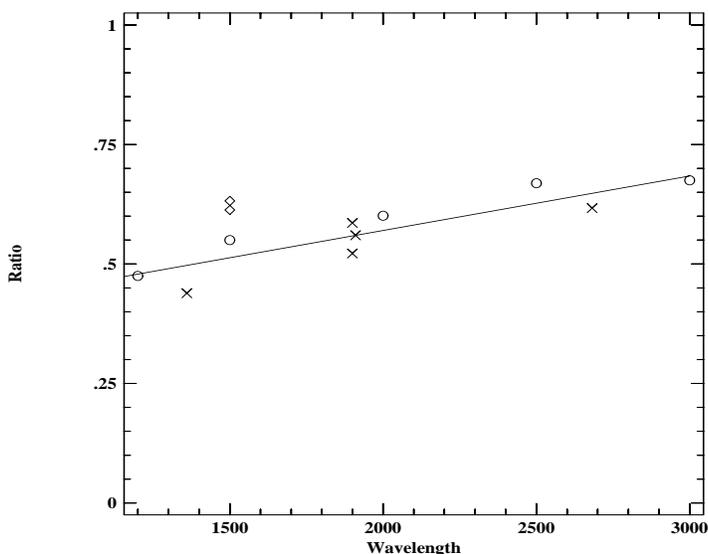
Sensitivity Changes Over Time-Scales of Months to Years

We noted earlier the evidence for changes in GHRS sensitivity with time since the first servicing mission. Corrections for the effects of these changes have been incorporated into CDBS so that you should get back the appropriate sensitivity reference file for the time an individual observation was taken.

Side 1

The largest effects are seen for grating G140L, especially below Lyman-α. From the monitoring data, a ratio and errors were calculated every 10 Å from ~1100 Å to ~1630 Å. While the sensitivity below Lyman-α decreased, an apparent increase occurred in sensitivity from ~1200 to 1350 Å, before it declined again. We do not understand this behavior, but it has remained fairly constant with

time. In addition to rederiving the baseline post-COSTAR G140L sensitivity, we have also created time-dependent G140L curves for the date of each sensitivity monitor based on the ratio of the counts from the monitor to the SMOV baseline data. Observers will need to interpolate between sensitivity curves to get a correction appropriate for the date of their observations. The derivation of these Side 1 changes is described in *GHRS ISR* 085.

Side 2

The results of the Side 2 GHRS medium-resolution sensitivity monitor suggest that since COSTAR was installed, the GHRS sensitivity changes between 1200 Å and 3000 Å do not exceed about 5%. We find evidence for a time-dependence of the sensitivity with a decline rate of about 2% per year. As an example we showed in Figure. 37.3 count rate ratios of BD+28D4211 obtained since COSTAR installation, focus, and alignment and referenced to the beginning of Cycle 4. (Details for the Cycle 4 observations are in *GHRS ISR* 071). *The sensitivity files used by calhrs reflect the state at the beginning of Cycle 4. The changes seen for Side 2 are described in GHRS ISR 089.*

Note that the calibrated science data in the .clh file take into account the different throughput for point sources of the LSA and SSA before and after the installation of COSTAR. Therefore a star observed before and after the installation of COSTAR will have the same flux although its count rate will be lower before COSTAR.

Decreasing Counts During an Orbit

A series of short-exposure spectra of a star over many orbits in ACCUM mode appeared to show a regular decline of the observed counts of roughly 10% over the course of each orbit. This is described in *GHRS ISR* 073, together with some possible explanations. The best guess is that this phenomenon is due to telescope "breathing." This effect can contribute to flux uncertainty, obviously.

Correction for Extended Sources

When **calhrs** photometrically calibrates your observations, it assumes you have observed a point source, and adjusts the flux in your spectrum to account for light loss due to the PSF outside of the aperture, i.e., it returns the flux you would have seen if all of the flux from your point source fell within the aperture. Therefore, the absolute fluxes of point sources measured through the LSA and SSA should be the same. Of course, the count rates will be lower for the SSA observation but **calhrs** will automatically apply a different sensitivity function to the SSA observation to account for the light loss. The properties of the GHRS apertures are presented in Table 37.3.

calhrs always assumes a point source is observed and it effectively applies a correction factor for the light lost outside the aperture. If you observed an extended source, then your source does not fill the aperture as does a point source and the flux calibration from **calhrs** will be inappropriate. To obtain a rough estimate of the specific intensity multiply the observed flux by 0.95±0.02 for observations taken through the LSA and divide by the area of the aperture in square arcseconds. This assumes that the extended source completely and evenly fills the

GHRS / 37

aperture. For pre-COSTAR observations, the correction factor is 0.725 (see *GHRS ISR* 061 for details).

■ The absolute fluxes for extended sources obtained with **calhrs** are incorrect.

Table 37.3: Properties of GHRS Apertures

Name	Clear Aperture (mm)	Pre-COSTAR	Post-COSTAR	Shape
LSA	0.559	2.0 arcsec	1.74 arcsec	square
SSA	0.067	0.25 arcsec	0.22 arcsec	square

Correction for Background Counts

The background level, or dark current for both GHRS detectors was very low: typically about 0.01 counts per second per diode when well away from the South Atlantic Anomaly. However, for very faint objects the dark level could dominate the signal, and accurate correction for the background is vital.

Because of this, some provision was made in the GHRS commanding software for features that would allow for lower net noise rates compared to standard observing modes. One of these modes used the CENSOR option, and the other used a parameter called FLYLIM. These will not be detailed here as they were rarely used. They are described in the *GHRS Instrument Handbook*.

For archival data there are several options for correcting for background. These were described in the previous chapter (see "Calibration Steps Explained" on page 36-2). Investigate this issue carefully before choosing the method, especially if your target was faint. You may wish to consider how many counts were collected in the background spectra that were obtained as part of the stepping pattern, for example, and to see if your object was observed in the vicinity of the SAA. *GHRS ISR* 070 discusses measurements of the background for Side 2 in detail, and *GHRS ISR* 085 describes the model used for estimating background counts.

37.3 Spectrum Shape

The shape of the spectrum and its overall level are closely tied, which is why both sensitivity and vignetting were discussed in the previous section. Here we go into vignetting and related effects a little further.

Shape Effects from the Sensitivity Function: G140L

For most GHRS observations, the observed bandpass samples only a small portion of the spectrum produced by a grating. Therefore, undulations in the sen-

sitivity function, which have length scales of many Ångstroms, at most have a small linear effect across a given spectrum.

G140L is an exception to this rule because it produces spectra nearly 300 Å long. Spectra from grating G140L may have modest shape effects that have their origin in the sensitivity function. These can be especially pernicious near Lyman-α because the breadth of that feature in the standard stars we observed prevented a good determination of the shape of the underlying sensitivity function at those wavelengths.

Light Falling Off the Diode Array

Thermal drifts caused a spectrum to move on the photocathode, so the GHRS routinely performed a SPYBAL (spectrum Y-balance) to properly center the spectrum on the diode array. A SPYBAL was performed every time a new spectrum element was used (i.e., the first use of a different grating) and approximately every two orbits thereafter. This centering can be important because a given spectrum is tilted across the diode array, and lack of proper centering could result in the ends of the spectrum falling off the array. Again, this is routinely corrected for and only becomes a problem if SPYBALs were suppressed for long exposures (i.e., several orbits).

A simple calculation can give us some idea of how large this effect can be. For example, the G140L spectrum of a point source may fall off the diode array due to drift as the temperature changes. Ignoring the width of the spectrum (something on the order of the size of the SSA or about 8 deflection units) the ends of the spectrum will differ by about 45 defection units and will be within about 9 deflection units of the edge of the diode array. If we assume a worst case drift of about 25 deflection units (seen over 10 hours), we find that at the end of this time about 25% of the spectrum will have fallen off the edge of the diode array!

In the case of an extended object uniformly filling the LSA, the effect is much more pronounced. In this case the width of the spectrum cannot be ignored. The width is equal to the size of the aperture or about 64 deflection units. For the case of a G140L observation of an extended object in the LSA, we start out with a loss of light. The spectrum is already falling off the array with the ends experiencing about 30% light loss. In the time it takes to drift 25 deflection units, some part or all of the spectrum may fall off the array, resulting in a significant reduction in signal.

G270M Vignetting Errors

The pre-COSTAR, in-flight sensitivity calibration for this grating is wrong shortward of 2300Å for the period November 11, 1991 through April 1, 1994. The pre-COSTAR vignetting correction for grating G270M is inadequate shortward of 2300 Å, and the post-COSTAR vignetting correction shortward of about 2150 Å is not handled properly by **calhrs** because the Y-deflection has not been measured below 2300 Å. The program which was to correct this failed. Please see *GHRS ISR* 077 if you wish to analyze data taken during this time period with this vignetting.

The Echelle Blaze Function

The echelle blaze function relates relative fluxes to those observed at the center of a given spectral order. This function was determined by observing the standard star μ Col at a number of different wavelengths in different orders, and relating those observations to others made with first-order gratings. It was impossible to cover fully a free spectra range or to sample every echelle order, so the blaze function is meant to be a reasonable approximation to the true function. An underlying, but unstated, assumption, is that observers used the echelles to measure the strengths or positions of weak spectrum features and were therefore not primarily concerned about the absolute flux level in the final, reduced spectrum.

Inappropriate Background Subtraction

In some cases the shape of a spectrum can be distorted if the background is improperly calculated and subtracted. This was seen in the first couple of years of GHRS operation because the background subtraction software fitted a polynomial to the background before subtracting it from the source spectrum. This was done to preserve shape in the background spectrum, but often the background had very few counts so that the fit was spurious. Modification of the procedure to fit a flat line removed the problem.

37.4 Spectrum Noise and Structure

Dead or Noisy Diodes

Each diode of the linear array (containing 512 diodes, diodes 7–506 are science diodes) was independently monitored via its own electronics chain. Diodes could exhibit anomalous behavior or fail. These diodes were grouped together as *dead* or *noisy* diodes. Diodes that showed anomalous behavior over an extended time were turned off for science observations. In practice, the threshold voltage for anomalous diode was set to a high value so that it did not detect electrons from the photocathode. The GHRS calibration software corrects for known anomalous diodes. If anomalous absorption features are present in the calibrated data, new noisy or dead diodes may be at fault. The non-standard thresholds for detector diodes are listed in Table 37.4.

Table 37.4: Problematic or Otherwise Important GHRS Diodes

Science Diode #[a]	Diode # 1-512[b]	AMP/CH[c]	Threshold[d]	Comments
Detector (Side) 1				
	1	24/07	46	Large background diode (50% peak +3)
	2	24/08	44	Large background diode (50% +3)
	3	27/07	120	Gold coat radiation diode
	4	00/08	255	Diode not connected by design

Table 37.4: Problematic or Otherwise Important GHRS Diodes (Continued)

Science Diode #[a]	Diode # 1-512[b]	AMP/CH[c]	Threshold[d]	Comments
85	91	30/00		Dead—BDT[e] r0h, r5h change May 29, 1995 (95149 SMS)
123	129	22/05	50	Threshold 60% stops noise
262	268	15/12	255	Dead electronics—in BDT
273	279	11/04	255	Bad contact—crosstalk when contact made. In crosstalk table
436	442	00/15	52	Threshold 60% stops noise
445	451	00/03	44	Bad 4096 bit—in bad diode table (BDT)
487	493	08/07	255	Very noisy—in BDT
	510	04/08	120	Gold coat radiation diode—not functional
	511	04/07	42	Large background diode (50% peak +3)
	512	08/08	47	Large background diode (50% +3)
Detector (Side) 2				
	1	24/07	46	Large background diode (50% +2)
	2	24/08	44	Large background diode (50% +2)
	3	27/07	120	Gold coat radiation diode
	4	00/08	255	Diode not connected by design
51	57	25/05	255	Bad diode—added to BDT 26 Feb 96.
80	86	30/14		Threshold 60% stops noise April 20, 1992, r0h
104	110	27/11	255	Bad diode—in BDT
140	146	24/13	40	Threshold 80%, crosstalk noise
144	150	25/12	255	Bad diode in BDT
146	152	16/09	49	Threshold 50%, occasionally noisy
168	174	24/10	43	Threshold 50%
237	243	16/00	44	Threshold 50% April 20, 1992; threshold 100% May 15, 1995
263	269			Flaky: intermittently strong (see *GHRS ISR* 080).
273	279	11/04	255	Bad contact—crosstalk April 20, 1992
293	299			Flaky: intermittently weak (see *GHRS ISR* 080).
313	319			Flaky: intermittently strong (see *GHRS ISR* 080).
339	345			Flaky: intermittently weak (see *GHRS ISR* 080).
342	348	11/10		Threshold 100% April 20, 1992
355	361			Flaky: intermittently weak (see *GHRS ISR* 080).
423	429			Flaky: intermittently weak (see *GHRS ISR* 080).

Table 37.4: Problematic or Otherwise Important GHRS Diodes (Continued)

Science Diode #[a]	Diode # 1-512[b]	AMP/CH[c]	Threshold[d]	Comments
426	432			Flaky: intermittently weak (see *GHRS ISR* 080).
440	446	00/14	41	Threshold 50%
441	447	01/02		Threshold 70% April 20, 1992
442	448	02/13	44	Bad 16384 bit—in bad diode table
	510	04/08	120	Gold coat radiation diode
	511	04/07	43	Large background diode (50% peak +2)
	512	08/08	41	Large background diode (50% peak +2)

a. Science Diode: diodes 7–506 used for science observations.
b. Diode: the entire (1–512) diode array.
c. AMP/CH: Amplifier/channel, onboard electronic location of diode.
d. Threshold: Discriminator threshold voltage setting for channel.
e. BDT: Bad diode table.

The easiest way to tell a bad diode from an absorption line or blemish is by the width, flat profile, and location. The width will depend on your comb addition, sub-stepping strategy (see "File Sizes" on page 35-5), and which file you are in. Dead diodes in data taken with the default comb addition will be 4-pixels wide in raw data and 16-pixels wide in default (quarter-stepped, merged) calibrated data. Dead or flaky diodes will be generally flatter than an absorption line. A dead diode, in raw data, is illustrated in Figure 37.9.

Flaky Diodes

In 1996 we noticed, first in some Side 2 CVZ RAPID mode data, that there were anomalous absorptions (so-called *flaky diodes*) in the data. Eventually we determined that increases in the GHRS pre-amp temperature resulted in non-linear amplification of input charge from diodes, effectively resulting in the occasional appearance of flaky diodes in spectra, as if a change in the threshold voltage had changed the response of a few Side 2 diodes. This phenomenon, also apparent in non-CVZ data as GHRS usage become heavier, is discussed in more detail in *GHRS ISR* 78. The same effect was *not* noticed in Side 1 spectra. Table 37.4 lists diodes that are occasionally seen as flaky in data after 1996. If you think you have seen flaky diodes, check the width of the features and which pixels are affected. The first low raw pixel in each feature should agree with the science diode value in Table 37.4 above.

Blemishes

Scratches, pits, and other microscopic imperfections in the detector window and on the photocathode surface are referred to as *blemishes*. The magnitude of blemishes upon spectra depends on how the spectrum illuminates the photocathode near a blemish. Many blemishes have spatial structures and depths that would make them difficult to distinguish from real stellar or interstellar features, see Figure 37.9. Therefore, it is difficult to automatically correct data for the effect of

Figure 37.8: Side 2 Diodes that Become Flaky at High Temperatures
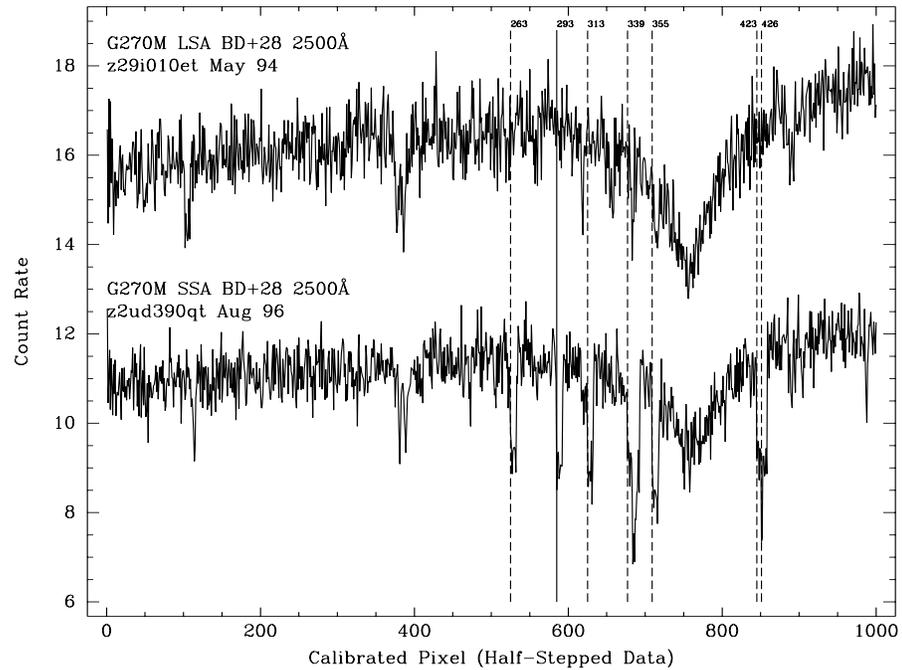
blemishes. In the absence of independent information, individual subexposures can be displayed in diode space to identify non-real spectral features. The calibration code does not correct for blemishes. However, the data quality file (.cqh) contains data quality values marking which pixels are affected by known blemishes. See Table 37.10 for information about data quality flags.

Spikes

Large spikes and unrealistic flux levels were found in a subset of Fall 1995 calibrated GHRS data. The affected observations were all made using the Ech-A grating in orders 35 and 36. Fortunately, this problem only affects a handful of observations in a few proposals. The solution to the problem is to recalibrate with a vignetting file with the groups in ascending line position order (e.g., fc11607fz.r2h, or more recent).

Also the stuck bit at Side 2 science diode position 442 will look like a spike as shown in Figure 37.9.

Granularity

As we noted in the previous chapter, the first-order diode-to-diode response variations are removed in **calhrs**. There are also granularity effects produced in the photocathode faceplates of the detectors. No calibration is provided for these because determining them is impractical. However, grating G140L has been so characterized because its bandpass is large (see *GHRS ISR* 076 for details on how this was derived). For the other gratings, features such as FP-SPLIT and COMB addition were provided to allow for improved signal to noise in the final spectrum.

Figure 37.9: Sample Blemish, Dead Diode, and Stuck Bit
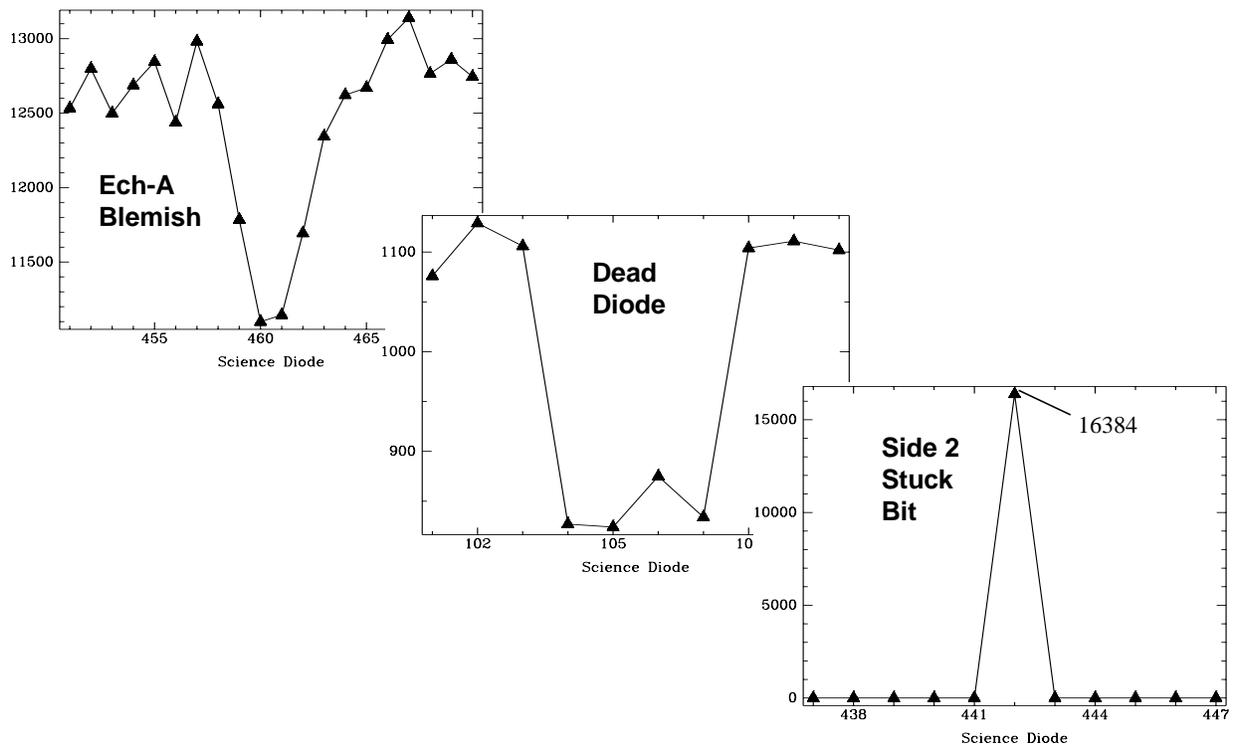
37.5 Calibration Quality Files

calhrs reads the raw data quality files, operates on the data using the quality flags as a discriminate, and flags the appropriate data values in the output quality files. Fill data are ignored. Reed-Solomon flagged data are calibrated, but is flagged as suspect in the output quality files.

The initial error in the data is assumed to be Poisson-limited. The error is propagated mathematically through the calibration process. The propagated statistical error file (.c2h) contains a measure of the statistical errors of the original data values; this file is calibrated in lock-step with the science data files.

The flux data quality file (.cqh) flags bad pixel values in the calibrated flux and propagated statistical error files.

Special diodes data quality files (.c4h) flags bad pixel values in the calibrated special diodes file (.c3h). Good pixel values are identified by a zero value.

Table 37.5: Calibrated Data Quality Flags

Flag Value	Description
Category 1: Data not useful —data values set to zero	
800	Data filled
400	Dead or disabled channel
300	Severe saturation (uncertainty >50%)
Category 2: Data uncertain—uncertainty not indicated in error computation	
190	Large saturation correction (uncertainty > 20%)
180	Photocathode blemish (deep)
150	Photocathode blemish (medium)
140	Photocathode blemish (small)
130	Moderate saturation correction (uncertainty >5%)
100	Reed-Solomon decoding error
Category 3: Data uncertain—uncertainty indicated in propagated error file	
30	Dead diode contributed to comb-added data point

37.6 About Wavelength Calibrations

37.6.1 Aperture Offsets

By convention all GHRS wavelengths are referred to the SSA. Corrections to apparent wavelengths from sources in other apertures is necessary because light from those other apertures enters the GHRS at angles slightly different from that of the SSA. These corrections are called *aperture offsets*.

During calibration, the zero-points of the wavelength scale are adjusted for the difference in incidence angle of apertures LSA, SC1, and SC2 from the SSA. Incident angle correction (IAC_CORR) coefficients are found in the CCR8 table. Currently, an average value for the zero-point wavelength correction is applied to all first order grating LSA observations regardless of the carrousel position. The recently-calculated and old offsets for GHRS gratings are listed in Table 37.6, which is taken from *GHRS ISR* 080. These coefficients are used to compute the offset using the following formula:

$$\lambda = \lambda + (A + Bs)/m$$

where:

- λ is the wavelength.

- *A* and *B* are coefficients from `ccr8`.

- *s* is the photocathode sample position.

- *m* is the spectral order.

Table 37.6: Incident Angle Correction for GHRS Gratings

Grating	A	B	Previous A
G140L[a]	0.0	0.0	0.0
G140M	–0.0065	0.0	0.0
G160M	–0.0448	0.0	–0.022±0.023
G200M	–0.057	0.0	–0.037±0.012
G270M	–0.060	0.0	–0.036±0.007
Ech-A	$-0.0076 \times m$	0.0	0.0
Ech-B	$-0.0078 \times m$	0.0	0.0

a. The entries for G140L are not based on measurements. They are set to 0.0 since the incident angle correction for the G140L grating is expected to be insignificant.

37.6.2 Doppler Compensation

Since HST orbits the Earth with a velocity of 7.5 km s^{-1}, spectra obtained with GHRS could see a Doppler shift of up to 15 km s^{-1}. The effect of the spacecraft velocity was corrected for in real time for ACCUM mode observations by deflecting the image of the spectrum an amount equal to the Doppler shift so that the spectrum appears fixed with respect to the diode array which is recording the spectrum. RAPID mode observations are not corrected for this effect. Unfortunately, it was discovered that GHRS spectra obtained prior to the end of March 1993 suffered from incorrect Doppler compensation.

The problem became visible in a set of high dispersion spectra obtained with short exposure times, where one could actually see a doubling of spectral features corresponding to the different Doppler shifts applied. At the maximum required correction, the flight software was mistakenly applying zero correction. Affected data will be obvious only in extreme cases, but the problem may degrade your data even when the effect is not obvious.

An on-board fix to the first problem was implemented in the flight software as of April 1993. Observations made after the update should not suffer from the Doppler compensation error. However a cumulative error in the onboard Doppler compensation still existed, which caused the accuracy of the Doppler compensation to be reduced for long exposures.

The **obsum** task in the STSDAS **calhrs** package can be used to identify GHRS spectra which were potentially corrupted by the first Doppler compensation problem. This task identifies periods when the Doppler compensation should have been maximal and provides information to allow you to estimate the fraction of the data in each group that is contaminated by incorrect Doppler compensation. If a substantial fraction of the data are corrupted for a given period of time, the only recourse is to discard the affected groups and reduce the remaining good data. See the help file of **obsum** for a detailed description of its use.

Also, all observations of moving targets made before July, 1994, were compensated incorrectly. The fix to this problem was implemented in July 1994 and moving target observations since then do not exhibit that problem. For help identifying and correcting moving target observations, please contact the STScI Help Desk via E-mail to `help@stsci.edu`.

37.6.3 Geomagnetically Induced Motion

The displacement of the image relative to the diodes due to the earth's magnetic field, Geomagnetic Image Motion (GIM) problem, may affect a GHRS observation depending upon the length of the exposure and the orbit during the observation. The rate of drift of an image across the diodes was small enough that there is no significant smearing of data on time scales of five minutes or less. Very long exposures may exhibit GIM related symptoms and should be investigated by the user. No correction for GIM has been incorporated into either the operations of the GHRS or in the data reduction procedures.

37.6.4 Carrousel Properties

The carrousel was rotated to engage the desired dispersive element or mirror and to place the requested wavelength at the center of the diode array. In the spring of 1991, the Side 1 carrousel control electronics developed an intermittent failure and the carrousel function was modified to operate the Side 1 carrousel from the Side 2 electronics. Any Side 1 observation obtained after April 1991 will have different carrousel function coefficients for specific wavelengths.

During normal operation, the carrousel was commanded to rotate to a pre-selected position depending upon the carrousel function. The carrousel could oscillate before achieving the desired position and take an appreciable amount of time to lock at that position. This may take longer than the normal amount of allocated time and thereby, following observations are affected. Before Spring 1995, if the carrousel took a significant time to lock, the following observations would not occur and be lost. After spring 1995, the flight software was updated to *time out* a set of GHRS observations if the end time of the observations was reached. The time-out was not enforced for GHRS target acquisitions. The header keyword FINCODE (see Table 37.7) will be set to 106 to indicate to the observer that a time-out occurred. The affected GHRS observation may be several observations down stream of the observation for which the carrousel took too long to lock into

GHRS / 37

position. The STSDAS task **obsum** in the **calhrs** package can be used to display to the screen the carrousel position and the FINCODE values.

```
st> obsum z2bd010c
```

Table 37.7: GHRS FINCODE Values

FINCODE	Explanation	Action
15	X-null balance failure during coarse locate	Usually benign
16	X-null balance failure during fine locate	Usually benign
20	Number of slews to center exceeded max	Usually benign
101	Normal beginning of observation	-
102	Normal end of observation	-
104	Observation ended, over-exposure	Exposure may have been shortened
105	Observation ended, too many bad data	Exposure may have been shortened
106	Observation ended, time out	Exposure may have been shortened

37.6.5 Wavelength Data Quality

The pipeline data reduction system (PODPS) automatically assigns a wavelength scale to your GHRS ACCUMs[3] and RAPIDs when they are reduced. Note that this default wavelength scale is the one appearing in the .c0h file that goes with the .c1h file containing fluxes, *even if there is a wavelength calibration exposure (wavecal) available for that program.* If you have a wavecal, you must analyze it and apply the results yourself; this is explained in the section "Recalibrating GHRS Data" on page 36-13.

This default wavelength scale is calculated using terms that depend primarily on the carrousel position (i.e., the orientation of the grating that was used), but there are also terms for the temperature within the GHRS (recorded in the engineering data stream). There is also a weak time-dependent term.

The default wavelength scale is good to approximately one diode rms, with contributions from various effects as enumerated in Table 37.8 (which is taken from Heap et al., 1995, *PASP*, 107, 871). Not listed is the error in wavelength that occurs for observations made in the Large Science Aperture (LSA), which was discussed in "Aperture Offsets" on page 37-23.

---

3. Here and elsewhere in this chapter we will consider OSCANs and WSCANs as equivalent to ACCUMs. Both OSCANs and WSCANs are macros that generate a series of ACCUMs when the program is executed on the telescope.

Table 37.8: Wavelength Error Sources

Source of Error	Maximum Error (diodes)
Quality of dispersion coefficients	0.1
Incident angle correction, SC2 to SSA	0.1
Uncertainty in thermal and time models	1.0
Short-term thermal motions	0.4 hour^{-1}
Carrousel repeatability	0.5 (0.17 typical)
Onboard Doppler compensation effects	0.15 typical
Geomagnetic image motion	0.25
Uncertainty in centering target in SSA	0.21

The largest sources of uncertainty in wavelength are obviously due to the geomagnetic image motion (GIM) and the model used to correct for thermal and time effects. We cautioned observers to break down long exposures into units lasting no more than five to ten minutes, in order to reduce the effects of GIM below significant levels. Thus you should not ordinarily find GIM leading to loss of resolution in the final spectrum.

Thermal effects, however, include a significant component that appears to be unpredictable. These thermal effects are best removed through use of a wavecal or SPYBAL. Thermal motions are just that: a motion of the overall image of the spectrum. The changes in image scale—dispersion—that occur are very small and can safely be ignored in most instances. For example, for grating G270M, the centers of our calibration spectra deviate from the default wavelength scale by no more than 100 mÅ (and typically about 70). The slope of a fit through the measured positions for the comparison lines relative to the default wavelength scale deviates in the center by no more than 100 mÅ (and typically about 70 mÅ), and has a slope of about 3×10^{-4} (in dimensionless units of Å per Å), so that the ends deviate from the center by, typically, about 3 mÅ across a 40 Å wide spectrum. The rms scatter of the fit is typically about 0.2 km s^{-1}. Not all the gratings are this good, and some other values for the quality of fit are provided in Table 37.9. The data in that table are taken from *GHRS ISR* 081, which summarizes wavelength calibrations for the first-order gratings in Cycles 4, 5, and 6 (i.e., post-COSTAR). Other ISRs with wavelength analyses include:

- *GHRS ISR* 035: An analysis of Side 2 data in 1990 and 1991.

- *GHRS ISR* 039: A check on the accuracy and repeatability for the pipeline wavelength calibrations after dispersions tables were corrected in 1992.

- *GHRS ISR* 052: An assessment of pipeline calibrations for the first-order gratings on Side 2 in Cycle 2.

- *GHRS ISR* 058: An assessment of pipeline calibrations for Echelle-B in Cycles 2 and 3.

GHRS / 37

Table 37.9: Quality of Default Wavelength Scale for Side 2 First-Order Gratings

Grating	rms deviation of fit(mÅ)	Deviation at center (mÅ)	Slope of fit (times 10^4)
G160M	7 to 11	60	0.2
G200M	30 to 50	20 to 80	0.2
G270M	7 to 16	50 to 100	0.3 to 0.5

37.7 Spatial Uncertainty: Target Acquisition Problems

Most of this topic was discussed in the chapter on data assessment and in *GHRS ISR* 079, "Interpreting GHRS Target Positioning". An onboard target Acquisition performed a spiral search followed by returning to the dwell point with the most counts. The end phase of the onboard acquisition was the locate phase (coarse *y* and *x* centering with a fine *x* balance at the end of the locate phase).

GHRS target acquisitions of very bright stellar targets could fail during the locate phase. This resulted from low contrast between the central four diodes of the eight diodes used for acquisitions. The high count rate in the central four diodes flattened the point spread function (PSF) leading to wrong centering in the aperture. The SSA science observations in this case may contain just noise.

The header keyword FINCODE value indicates the success or failure of the GHRS observation. FINCODE=102 indicates the observation completed successfully as planned, but does not indicate whether the target was centered in the aperture. Any other value for FINCODE indicates a possible problem. During RSDP pipeline calibration, if a FINCODE value is encountered other than 102, a warning message is written to the trailer file (.trl).

From April 1989 through August 1994, OSS (now part of OPUS) created an Observation Comment file (extension .ocx) for every HST observation. After that time through January 1995, OSS created an .ocx file for degraded observations. If an .ocx file exists for an observation, it should be checked for anomalies. (See Chapter 38 for more information.)

If OMS observation logs were created for an observation, they should be checked to verify that no anomalies occurred during the target acquisition.

Low Count Rate

Observations with low count rates, containing mostly noise, may contain few detected or no counts from the target. Calibrated data may have a bell or U-shaped appearance, quantized data values, or extremely low flux values. These data indicate a missed target, a target too faint for the GHRS, or inappropriate use of the GHRS.

GHRS / 37

37.8 Observation Timing

Knowledge of the exact time that observational activities take place onboard GHRS is not directly available. Instead, we only get timing information when data are dumped to the ground from the onboard computer from which we may infer when things happened. When data are dumped they are given time tags from the NSSC-1 computer; the spacecraft clock has a time resolution of approximately 0.125 seconds. While GHRS can operate on shorter time scales (0.050 seconds), information about these activities does not make it into the telemetry stream.

Nevertheless, as an observer, you may want answers to the timing questions posed in this section. You may find the **hst_calib.obsum** task helpful in determining timing questions.

37.8.1 When Did the Observation Start?

The closest time tag to the start of most exposures (excepting RAPIDs) is the packet time (PKTTIME) on the first group of the Unique Data Log (UDL), which is the data file with the `.ulh` extension (see the discussion on data structure in "Contents of Delivered Data" on page 35-1). A UDL is always dumped from the spacecraft prior to the start of a science exposure, effectively flagging the start of the observation. The PKTTIME keyword holds an MJD value good to a spacecraft clock tick (~0.125 sec). This MJD value (for ACCUM mode observations) is stored in the EXPSTART keyword in the science data headers (`*.d0h`, `*.c1h`). The accuracy of the start time is limited to the accuracy of the spacecraft clock—about 0.125 seconds.

For RAPID mode observations, the data are dumped as soon as they are taken. The PKTTIMEs represent the time the data left GHRS; calibrated data inherit the PKTTIMEs of the raw science data. The first two and last raw science packets (`*.d0h`) contain hysteresis information and are thrown away. This is why the calibrated data (`*.c1h`) will have three fewer groups than the raw science data. The best estimate of when a RAPID observation started is the PKTTIME of the first calibrated science packed (`*.c1h[1]`) *minus* the sample time of the observation, which, in this instance, can be found in the STEPTIME keyword. The accuracy in this case is half of a spacecraft clock tick (~0.0625 seconds). Unfortunately, the EXPSTART keyword in RAPID mode data appears to be incorrect.

37.8.2 When Did the Observation End?

For ACCUM mode observations, a second UDL is dumped at the end of the exposure and prior to reading out any science data. Therefore, the PKTTIME of the second group of the UDL can be used to mark the end of the exposure. For observations generating multiple readouts (e.g., FP-SPLITs and repeats) the UDLs come in pairs bracketing the science exposures. The MJD value of the second UDL in a pair should be used as the approximation of the ending of ACCUM mode observations. The accuracy is the same as the start time: about 0.125 sec-

GHRS / 37

onds. Misleadingly, the MJD value of the final `*.d0h` PKTTIME is placed in the EXPEND keyword.

For RAPID mode observations, a second UDL is not dumped until the last spectrum, which is a hysteresis measurement, has been dumped. In this case, the end of the observation is merely the time that the last spectrum has been read out and is contained in the PKTTIME for last group of the calibrated spectrum. Note that the PKTTIME for the science data is the tag when the science data are dumped and this must wait until the end of the exposure. Unfortunately, the EXPEND keyword for RAPID mode data is close to being the time-tag of the second UDL packet.

37.8.3 How Long Did the Observation Last?

The extent of an observation is reported in the EXPTIME keyword. This time may not be the same as the simple difference between the EXPEND and EXP-START. (See "Was the Observation Interrupted?" on page 37-31.) The exposure time in the header is simply the exposure time you requested in your proposal times the number of exposures. To verify that you got the exposure time you expected you can calculate the EXPTIME using available header keywords as shown below.

ACCUM mode

EXPTIME = (RPTOBS + 1) x (*fpsplits*) x MAXGSS x INFOB x STEPTIME

where,

- RPTOBS = Number of exposures – 1 (i.e., the number of repeats).

- *fpsplits* = 1 (FP_SPLIT=DEF) or 2 (FP_SPLIT=TWO or DSTWO) or 4 (FP_SPLIT=FOUR or DSFOUR).

- MAXGSS and INFOB contain information concerning the STEPPATT and COMB used. If you want more details about these contact a GHRS instrument scientist via the STScI Help Desk (`help@stsci.edu`).

- STEPTIME = the step time used (by default = 0.2 seconds).

RAPID mode

EXPTIME = (*groups*) x STEPTIME

where:

- *groups* – is the number of spectra read out (i.e., the number of groups in the calibrated multi-group image, GCOUNT).

- *STEPTIME* – is the integration time for each spectrum (specified as SAM-PLE-TIME in the proposal).

37.8.4 What was the Exposure Time Per Pixel?

The exposure per pixel is found in the EXPOSURE keyword in the calibrated flux header. This number is not equal to the EXPTIME because of the multiplicity of step pattern, FP-SPLITs and repeated observations.

This value is calculated by **calhrs** during pipeline calibration. To double check you may calculate EXPOSURE as follows:

EXPOSURE = INFOC x MAXGSS x (STEPTIME – 0.002)

where:

- INFOC and MAXGSS contain information about the STEPPATT and COMB used. (Note: INFOB and INFOC are different keywords containing similar information.)

- STEPTIME = the step time specified.

- 0.002 = the time in seconds of the internal overhead for integrating a single STEPTIME.

If you are interested in the exposure per diode, you must rebin the data from substep pixels to diodes.

37.8.5 Was the Observation Interrupted?

By design, the GHRS was interruptible: a given exposure may begin, be interrupted, and then resume. Observations were routinely interrupted for SAA passages and Earth occultations. The interruption could last anywhere from a few minutes, when skirting the SAA, to about half the orbit for an Earth occultation. In general, this is of no concern. Still, there may be times when you want to know the details of a given observation. Unfortunately, it is nearly impossible to determine when an observation was actually stopped and restarted—this information is just not available in the telemetry stream.

Additional details are available in the OMS observation log files as discussed in Appendix C of Volume I. It is also possible that a given observation may end prematurely. This information is encoded in the FINCODE keyword. We routinely see observations time out due to carrousel resets. If you have additional questions about interruptions, contact the STScI Help Desk via E-mail to `help@stsci.edu`.

37.9 Instrument and Spacecraft Errors

All HST science observations are first received on the ground at White Sands, New Mexico, and are then relayed by satellite to the DCF (Data Capture Facility, after January 1996, PACCOR), Goddard Space Flight Center, Maryland. The DCF staff perform a check of the transmission using a Reed-Solomon error checking routine. When Reed-Solomon is used, the data are encrypted into a cyclic pattern.

GHRS / 37

The down-linked data are then decrypted and the Reed-Solomon code will verify the pattern and corrects, if possible, those words that are not as expected. If any packets are missing, DCF will wait for the next STR (space tape recorder) dump to verify no more data packets are forthcoming. Missing data packets and the results of the Reed-Solomon check are written to the data quality accounting capsule (QAC). The data packets and QAC are transmitted to the pipeline.

Each GHRS observation set was processed through the pipeline as far as generic conversion. The output of generic conversion is what users refers to as the *raw* uncalibrated dataset. Furthermore, the pipeline automatically ran the **calhrs** software to calibrate science files, such as ACCUMs, RAPIDs, and SPYBALs. Any ACQuisition files, IMAGEs, and DEFCALs are not calibrated.

Each science data file (.d0h), extracted data file (.x0h), and target acquisition (.d1h) have a corresponding data quality file containing flags or fill values for bad data. These quality files (.q0h,.xqh,.q1h) were created during pipeline processing and contain information extracted from the QAC or were filled during the data evaluation process. For each data point in the .d0h, .x0h, or .d1h file, there is a corresponding data point in the quality file. For each good data value, the corresponding point in the quality file is zero. If there are missing data (data-dropout), due to tape recorder flips, down link problems, or data loss due to unforeseen problems, the pipeline will pad the corresponding data file with fill data; the corresponding data point in the quality file was set to 16. If the data failed the Reed-Solomon error check, the corresponding data point in the quality file was set to one. Data that fails the Reed-Solomon check were classified as suspect, and may not be bad data.

Table 37.10: Pipeline Data Quality Values

Quality Value	Description
0	Good data point
1	Reed-Solomon error
16	Fill data

GHRS Data Analysis

38.1 The Post-COSTAR Point Spread Function

The post-COSTAR point spread function (PSF) has a sharp core and weak wings. Observations through the SSA show a Gaussian core with a FWHM of 0.975 diodes and wings that fall off (in intensity) as r^{-3} at radii larger than 1 arcsec. When this measured profile is deconvolved from the square SSA aperture, we find a sharp core with a FWHM of about 0.375 diodes—this amounts to about 0.08 arcsec. For a detailed description of the analysis of the PSF please see, Robinson, R. "Investigating the Post-COSTAR Point Spread Function for the GHRS" in *Calibrating Hubble Space Telescope: Post Servicing Mission*, 1995.

During preflight testing of COSTAR, the GHRS mirrors were contaminated by fine dust particles. Light scattering was expected to be a problem at the radial distance of 2 to 3 arcsec. The first Servicing Mission Orbital Verification (SMOV) observations agreed moderately with the light scattering theoretical expectations. Special observations were obtained in Cycle 4 and 5 to measure this scattered light.

The observing plan for the special observations was to center up on the target star, back off 0.2 arcsec, and scan across the star out to a radial distance of 3.0 arcseconds. The first dwell position at radial distance of –0.2 arcsec from the SSA acquisition position was chosen so the scan would sample both sides of the PSF. A scan with nine dwell positions was defined. The target was centered in the SSA with an ACQ/PEAKUP before the start of each SCAN. Three SCANs were obtained, two were in the –x direction at a wavelengths of 1400 Å and 2700 Å and one was in the +y direction at 2700 Å. A previous scan in y at 1400 Å already existed.

The light entering the FOC (OTA+COSTAR) is a close match to the light entering the GHRS. Model FOC PSF images were created using TinyTim. Models were created to match the GHRS 1400 Å (FOC F140M filter) and the 2700 Å (FOC F278M filter) observations, see Figure 38.1 in which model profiles are offset by one pixel. The FOC model PSF pixel scale is 0.0143 arcsec/pixel (*f*/96). A square aperture (15 pixels on a side) was walked across the model PSF images to match the scan positions of the GHRS observations. A plot of the sum of the counts in this aperture at each position should represent the measured PSF envelope extracted from the GHRS observations. The model points were scaled to match the GHRS second dwell position points.

A good match was found between the FOC model scan points and the first four GHRS dwell positions in each scan. Beyond dwell position #4 (1.0 arcsec), the counts in the model scan continue to fall off in intensity while the counts in the GHRS scan level off. The GHRS profile beyond 1.0 arcsec suggests higher scattered light than is predicted by the FOC PSF model. It is unlikely that these profile wings are due to detector noise because the counts detected are significant and well above normal background levels.

The FOC model fit, of course, is not intended to represent the actual GHRS PSF, but instead to determine the position of the star relative to the GHRS scan. However, comparisons of the FOC model scans with the actual GHRS scans do show some similarities as well as some discrepancies that are worth noting.

First, the –*x*-axis scans indicate the GHRS PSF within the region <1.0 arcsec is slightly broader at 1400 Å than at 2700 Å. This broadening of the profile may be due to a halo effect at 1400 Å that is not present at 2700 Å. This broadening appears to be in both the actual GHRS scans and the FOC model scans which suggests it is possibly related to the COSTAR optics. The 1400 Å scan starts to diverge from the FOC model at ~1.0 arcsec, while the 2700 Å scan tracks the FOC model scan out to a distance of ~1.4 arcsec before diverging from the model scan. This would indicate the onset of scattering is more pronounced at 1400 Å than at 2700 Å.

Second, the +*y*-axis scan at 2700 Å shows a narrower inner core to the profile compared to the –*x*-axis scan profiles. This result is possibly due to the inferred large offset (~0.050 arcsec) introduced in the positioning of the +*y*-axis spatial scan. This only indicates the target star was more centered in the aperture at dwell position #2 for the +*y*-axis scan than for the –*x*-axis scans. If the +*y*-axis and –*x*-axis scans at 2700 Å are overlaid and moved vertically so as to match the counts at dwell position #4, the fall off in the profiles are nearly identical. This suggests the far wings of the PSF are symmetrical at 2700 Å. The –*x*-axis scan, which has better positioning to measure the wings of the PSF, is a good indicator of the fall off in the wings of the GHRS PSF.

The observations at both 1400 and 2700 Å demonstrate that the GHRS PSF has extended wings. These do not rise above the expected (FOC) level until one is at about 1% of the peak intensity for a star, therefore these wings are unlikely to contaminate the spectrum of a nearby star in a significant way except when there is a large (~5 magnitude) difference in brightness. The information provided in the figures and tables should allow a first-order correction to be made in such cases if spectra of both objects exist.

GHRS / 38
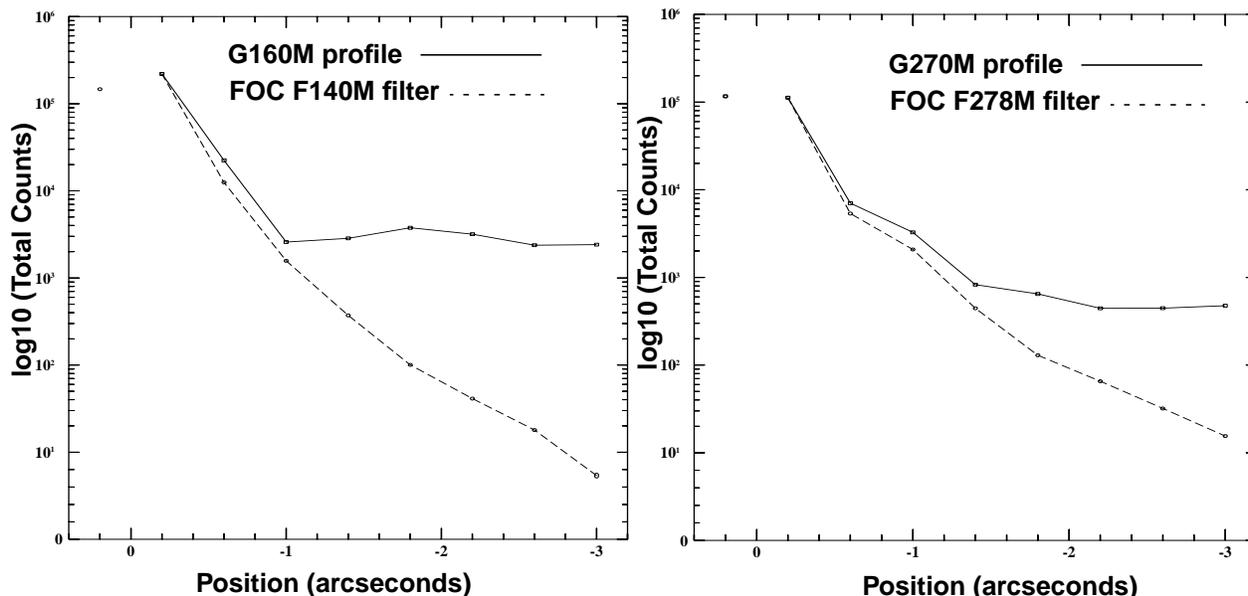
38.2 The GHRS Line Spread Function

The line spread functions (LSFs) for the GHRS gratings describe the instrumental broadening for a delta-function spectral feature. Knowledge of such a blurring function is necessary for quantitative studies of GHRS spectral line profiles. The resolution element (one diode) for GHRS was matched to the width of the SSA. By using substepping strategies, it is possible to get properly sampled spectra, obtaining the minimum of two sample points per resolution element. A delta-function spectra line observed through the SSA can be described by a Gaussian with a FWHM of about 0.925 diodes which is about 3.7 quarter-stepped pixels. (See Gilliland 1992, *PASP*, 104, 367).

Since an SSA spectrum is the best resolution we can obtain with GHRS, it is useful to describe the LSA LSF in terms of the SSA PSF. Consequently, we have measured the LSA-SSA differential LSF for a number of gratings and at a sample of wavelengths. This differential LSF satisfies the relationship: LSF * SSA = LSA; i.e., the differential LSF is the LSF that when convolved with an observed SSA spectrum produces the best match to an identical spectrum obtained through the LSA. By combining the intrinsic LSF for the SSA with the empirical differential LSF we can obtain the intrinsic LSF for the LSA. Since the SSA and differential LSF are Gaussians, we obtain an LSA LSF that is also a Gaussian with a FWHM that is slightly greater than that of the SSA.

The pre-COSTAR LSF of the GHRS was characterized by a Gaussian core nearly twice as broad as that provided by the instrumental resolution limit, provided by the SSA, with extended non-Gaussian wings. The post-COSTAR

LSF for the LSA is only 19–51% broader in a Gaussian core than spectra from the SSA and the extended wings are absent. The LSF results are presented in *GHRS ISR* 063. The differential degradation of the LSF due to the LSA with respect to the LSF of the SSA was derived. A spectral line of a point source with an infinitesimal line width (delta function) measured with the SSA has an LSF with a full width at half maximum (FWHM) of 0.925 diodes. This is independent of wavelength and grating. Measurements of the differential LSF of the LSA were performed for the five wavelength/grating combinations listed in Table 38.1. Column 3 of this table gives the measured FWHM of the differential LSF. Adding this value in quadrature to the FWHM of the SSA LSF (=0.925 diodes) leads to the FWHM of the LSA LSF, given in column 4 of the table. Plots showing the differential LSFs are in *GHRS ISR* 063. No reliable measurements of the LSF for the G140L grating are available. It is very likely that the G140L LSF is similar to those of other gratings.

Table 38.1: GHRS Post-COSTAR Differential LSF

Grating	Wavelength (Å)	Differential LSF of the LSA (diodes)	Relative FWHM (LSA/SSA)
G160M	1360	0.60	1.10
G160M	1900	0.72	1.18
G200M	1900	0.60	1.10
ECH-B	1900	0.82	1.24
ECH-B	2680	0.60	1.10

Deconvolution of GHRS spectra was investigated after the spherical aberration was found in the primary mirror. With COSTAR, the need for deconvolution has become less pressing, however, for the best spectral resolution, it is possible to deconvolve LSA spectra to the level of SSA spectra. See, *The Restoration of HST Images and Spectra*, (proceedings of the HST Calibration Workshop at STScI), STScI, 1990. The STSDAS task, **lucy**, can be used to deconvolve GHRS spectra.